

**PRODUCTION OF HIGH PURITY OF D-(-)-LACTIC ACID
FROM FERMENTATION BROTH:
PROCESS MODELING**



**A Thesis Submitted in Partial Fulfillment of the Requirements for the
Degree of Master of Science in Biotechnology
Suranaree University of Technology
Academic Year 2017**

การผลิตกรดดีแลคติกความบริสุทธิ์สูง
จากน้ำหมัก: การจำลองกระบวนการ



วิทยานิพนธ์นี้เป็นส่วนหนึ่งของการศึกษาตามหลักสูตรปริญญาวิทยาศาสตรมหาบัณฑิต
สาขาวิชาเทคโนโลยีชีวภาพ
มหาวิทยาลัยเทคโนโลยีสุรนารี
ปีการศึกษา 2560

**PRODUCTION OF HIGH PURITY OF D-(-)-LACTIC ACID FROM
FERMENTATION BROTH: PROCESS MODELING**

Suranaree University of Technology has approved this thesis submitted in partial fulfillment of the requirements for a Master's Degree.

Thesis Examining Committee



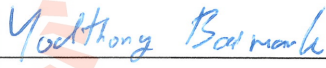
(Prof. Dr. Montarop Yamabhai)

Chairperson



(Assoc. Prof. Dr. Apichat Boontawan)

Member (Thesis Advisor)



(Assoc. Prof. Dr. Yodthong Baimark)

Member



(Prof. Dr. Santi Maensiri)

Acting Vice Rector for Academic Affairs
and Internationalization



(Prof. Dr. Neung Teaumroong)

Dean of Institute of Agricultural Technology

ใหม่ คัน ทัง : การผลิตกรดดีแลคติกความบริสุทธิ์สูงจากน้ำหมัก: การจำลองกระบวนการ (PRODUCTION OF HIGH PURITY D(-)-LACTIC ACID FROM FERMENTATION BROTH: PROCESS MODELING) อาจารย์ที่ปรึกษา : รองศาสตราจารย์.ดร.อภิชาติ บุญทาวัน, 106 หน้า.

กรดดีแลคติกเป็นสารเคมีที่มีความสำคัญ สามารถนำมาใช้ในอุตสาหกรรมยาอุตสาหกรรม เครื่องสำอาง อุตสาหกรรมอาหาร รวมถึงใช้ในการผลิตพอลิเมอร์ย่อยสลายทางชีวภาพ เช่นเดียวกับพอลิเมอร์ที่ผลิตโดยปิโตรเคมีทั่วไป กรดดีแลคติกส่วนใหญ่สามารถผลิตได้โดย กระบวนการหมักจากแหล่งอาหารชีวภาพ อย่างไรก็ตามกรดแลคติกที่ได้จากการหมักจะต้องผ่าน ขั้นตอนการทำบริสุทธิ์ เนื่องจากหลังจากกระบวนการหมักจะมีความบริสุทธิ์ของผลิตภัณฑ์ต่ำ ใน การศึกษานี้มีการใช้เทคนิคการทำบริสุทธิ์โดยใช้เมมเบรนชนิดนาโนฟิลเตรชัน และเทคนิค เพอร์เวปอเรชันร่วมกับปฏิกิริยาเอสเทอริฟิเคชันในการทำบริสุทธิ์กรดดีแลคติกจากน้ำหมัก ทั้งนี้ มีการใช้เมมเบรนนาโนฟิลเตรชันที่มีลักษณะแบบเกลียว ซึ่งเป็นเทคนิคที่ใช้สำหรับการปรับสภาพ น้ำหมักที่ช่วยในการกำจัดโปรตีนและสารสีต่าง ๆ โดยทำให้มีความบริสุทธิ์ของกรดดีแลคติกสูงขึ้น (93.4 เปอร์เซ็นต์) จากน้ำหมัก สำหรับเทคนิคเพอร์เวปอเรชันร่วมกับปฏิกิริยาเอสเทอริฟิเคชันใน การทำบริสุทธิ์กรดดีแลคติกนั้น มีการใช้เอทานอล พบว่าทำให้กรดแลคติกเปลี่ยนเป็นเอทิลแลคเตท ประมาณ 94.96 เปอร์เซ็นต์ โดยที่น้ำถูกกำจัดออกจากกระบวนระหว่างปฏิกิริยาเอสเทอริฟิเคชัน ทำให้ มีอัตราการเปลี่ยนเป็นกรดแลคติกสูงขึ้น (0.928) เมื่อเปรียบเทียบกับอัตราการเปลี่ยนเป็นกรด แลคติกในปฏิกิริยาเอสเทอริฟิเคชันแบบกะ ที่ อุณหภูมิ 75 องศาเซลเซียส เป็นเวลา 92 ชั่วโมง

นอกจากนี้การจำลองกระบวนการนั้นมีการใช้แบบจำลองทางคณิตศาสตร์เป็นพื้นฐานใน การวิเคราะห์ การคาดการณ์ การทดสอบการตรวจสอบพฤติกรรมกระบวนการซึ่งเป็นส่วนหนึ่งของการ ศึกษาด้วย แบบจำลองทางคณิตศาสตร์โดยการใช้แบบจำลอง Spiegler-Kedem ในการจำลอง การคายซับ และการจำลองการแพร่ซึ่งใช้ทฤษฎี NRTL ที่เป็นแบบ โมเดลค่าสัมประสิทธิ์ของ กิจกรรม เพื่อเปรียบเทียบกับความสัมพันธ์กับข้อมูลที่ได้จากการทดลอง จากรูปแบบการกรองชนิด นาโนฟิลเตรชัน พบว่าค่าสัมประสิทธิ์การสะท้อน (σ) และความสามารถในการซึมผ่านตัวทำละลาย (P_s) ตรงตามแบบจำลองดีที่สุด และแสดงการคาดการณ์สารละลายแลคเตทในส่วนที่เก็บไว้ หรือ ส่วนรีเทนชันและอัตราการซึมผ่านของเพอร์มิเอท เทคนิคเพอร์เวปอเรชันร่วมกับปฏิกิริยา เอสเทอริฟิเคชันนั้น พบว่าไคเนติกของปฏิกิริยา ค่าการแยก ค่าฟลักซ์แฟคเตอร์เบื้องต้น (Q_{memb}) และ พลังงานกระตุ้น (E_{perm}) ของเพอร์เวปอเรชันจากการจำลองด้วยโมเดล แสดงให้เห็นว่ามี ข้อผิดพลาดจากข้อมูลที่ได้จากการทดลอง 8.763 เปอร์เซ็นต์ ผลลัพธ์นี้เป็นประโยชน์สำหรับในทุก

TRANG KHANH MAI : PRODUCTION OF HIGH PURITY D-(-)-LACTIC
ACID FROM FERMENTATION BROTH: PROCESS MODELING.

THESIS ADVISOR : ASSOC. PROF. APICHAT BOONTAWAN, Ph.D., 106 PP.

D-(-)-LACTIC ACID/NANOFILTRATION/ESTERIFICATION ASSISTED
PERVAPORATION/MODELING

D-(-)-lactic acid is an important chemical that can be used in the pharmaceutical and cosmetic industries, the food industry, as well as in the manufacture of biodegradable polymers for conventional petrochemical polymers. D-(-)-lactic acid can be produced mainly by fermentation from biosource, however, fermentation-derived lactic acid requires extensive purification operations because of low purity of the product. In this study, membrane-assisted purification, consisting of nanofiltration (NF) membrane and pervaporation, was used to obtain purified D-(-)-lactic acid from fermentation broth. The spiral wound nanofiltration was determined to be a good pretreatment technique candidate for removing protein, and color with high recovery (93.4%) of lactic acid from fermentation broth. The pervaporation-assisted esterification of lactic acid with ethanol investigated the enhancement of the lactic acid conversion to form ethyl lactate. 94.96% of water was separated from the system during the esterification time, led to the higher lactic acid conversion (0.928) compared to the conversion of lactic acid (0.306) in the batch esterification at 75 °C after 92h.

Additionally, the process simulation as a key discipline, using mathematical models as the basis for analysis, prediction, testing, and detection of a process behavior, was also presented in the following parts of this work. Mathematical modeling such as

the Spiegler–Kedem model, the solution desorption model and the solution-diffusion model using NRTL theories as activity coefficient models were explored, which resulted in a very high agreement compared to the experimental data. In the nanofiltration model, the reflection coefficient (σ) and the solute permeability (P_s) were obtained using the best-fit method and showed the prediction of lactate retention and permeate flux. In the pervaporation-assisted esterification, the kinetic of reaction as well as the separation factor, the pre-exponential factor (Q_{memb}) and the activation energy (E_{perm}) of pervaporation were found and showed the model result with 8.763% error in the experimental data. These results are useful in all phases of chemical engineering from research and development to plant operations and the support in scale-up calculations.

After obtaining ethyl lactate from esterification, the fractionation, hydrolysis, and evaporation were used and achieved purity D-(-)-lactic acid.

มหาวิทยาลัยเทคโนโลยีสุรนารี

School of Biotechnology

Academic Year 2017

Student's Signature

Advisor's Signature

ACKNOWLEDGEMENTS

Firstly, I would like to express sincere thanks to my thesis advisor, Assoc. Prof. Dr. Apichat Boontawan for his consistent supervision and thoughtfully comment on several drafts and advice towards the completion of this study. I would like to thank Prof. Dr. Montarop Yamabhai and Assoc. Prof. Dr. Yodthong Baimark for their valuable suggestions, advice, and guidance given as committee members.

My thank also goes to Prof. Dr. Jürgen Rarey who provided me an opportunity to join his “Chemical process development” course. Without his valuable suggestion and guidance given, it would not be possible to conduct this research.

I wish to thank Assist. Prof. Dr. Sureelak Rodtong for providing D-(-)-lactic acid fermentation broth.

Furthermore, I am grateful to thank Asst. Prof. Dr Lakkana Rujanakraikarn and Dr. Long Thanh Le for their introduction and encouragement for my study. I also would like to thank all the faculty and staff members of the School of Biotechnology and labmates for their help and assistance throughout the period of this work.

Finally, I would also like to express my deep sense of gratitude to my parents for their support and encouragement me throughout the course of this study at the Suranaree University of Technology.

Trang Khanh Mai

CONTENTS

	Page
ABSTRACT IN THAI	I
ABSTRACT IN ENGLISH	III
ACKNOWLEDGEMENTS	V
CONTENTS	VI
LIST OF TABLES	X
LIST OF FIGURES	XI
LIST OF ABBRVIATIONS	XIV
CHAPTER	
I INTRODUCTION	1
1.1 General introduction	1
1.2 Research objectives	3
1.3 Research hypothesis and its significance.....	4
1.4 Scope and limitation of the study	4
II LITERATURE REVIEW	5
2.1 Lactic acid.....	5
2.1.1 Lactic acid properties	5
2.1.2 Lactic acid application	6
2.1.3 Lactic acid market	9
2.1.4 D-(-)-lactic acid production.....	9
2.1.5 Downstream process	12

CONTENTS (Continued)

	Page
2.1.5.1 Membrane separation	13
2.1.5.2 Acidification of salt	18
2.1.5.3 Esterification.....	19
2.1.5.4 Membrane – assisted esterification.....	21
2.1.5.5 Distillation	23
2.1.5.6 Hydrolysis.....	23
2.2 Transport and separation mechanism: modeling of NF membrane.....	24
2.2.1 Hydraulic/ water permeability, L_p	27
2.2.2 Membrane pore size	28
2.2.3 The reflection coefficient (σ) and the solute permeability (P_s).....	29
2.3 Modeling of pervaporation-assisted esterification	30
2.3.1 Process model – Simulation.....	30
2.3.2 Esterification of lactate salt.....	32
2.3.3 Kinetic equation of esterification reaction	33
2.3.4 Pervaporation performance	37
2.3.5 Kinetic of esterification-pervaporation coupled.....	40
III MATERIALS AND METHODS.....	42
3.1 Materials	42
3.2 Methods	43
3.2.1 Nanofiltration operation.....	43
3.2.2 Preparation of sodium lactate from fermentation broth	44

CONTENTS (Continued)

	Page
3.2.3 Kinetic Study of Esterification.....	45
3.2.4 Modeling of pervaporation-assisted esterification	45
3.3 Analysis	46
3.3.1 Cell dry weight.....	46
3.3.2 Protein concentration	47
3.3.3 Ion concentration.....	47
3.3.4 Gas Chromatography (GC).....	47
3.3.5 High Pressure Liquid Chromatography (HPLC).....	47
3.3.6 Kinetic calculation	48
IV RESULTS AND DISCUSSION.....	49
4.1 Modeling of nanofiltration membrane for sodium lactate from fermentation broth.....	49
4.1.1 Hydraulic/ water permeability, $L_{p,w}$	49
4.1.2 Mean reflection coefficient (σ) and solute permeability (P_s)	50
4.1.3 Model validation and results	54
4.1.4 The performance of nanofiltration experiment	57
4.2 Kinetic analysis of ethyl lactate (ELA) production via pervaporation- assisted esterification technique: mathematical model.....	59
4.2.1 Preliminary kinetic study of esterification reaction in batch mode.....	59
4.2.2 The model for pervaporation-assisted esterification.....	66

CONTENTS (Continued)

	Page
4.2.2.1 Performance of pervaporation in quaternary mixture	66
4.2.2.2 Pervaporation parameter estimation	68
4.2.2.3 The performance of pervaporation-assisted esterification ion	71
4.3 Membrane-assisted purification of optically pure D-(-)-lactic acid from fermentation broth process	75
V CONCLUSIONS	81
REFERENCES	83
APPENDICES	96
APPENDIX A THERMODYNAMIC PROPERTIES	97
APPENDIX B BINARY PARAMETERS OF THE RELATED COMPONENTS FOR ACTIVITY COEFFICIENT CALCULATION USING NRTL MODEL	100
APPENDIX C LACTATE PERFORMANCE IN NANOFILTRATION BY SPIELER AND KEMEN MODEL	102
APPENDIX D KINETIC OF ESTERIFICATION AND PERVAPORATION- ASSISTED ESTERIFICATION BY NRTL MODEL IN MATHCAD	103
BIOGRAPHY	106

LIST OF TABLES

Table	Page
2.1	Characteristics of selected bacteria, substrates for fermentation broth 11
2.2	Composition of the reaction mixture of batch esterification34
2.3	Composition of the reaction mixture of pervaporation-assisted esterification41
4.1	Mean reflection coefficient (σ) and solute permeability (P_s) for the studied membranes at the different sodium lactate concentration.....52
4.2	Kinetic parameters of sodium lactate esterification with ethanol using 1.5 wt% of H ₂ SO ₄ as catalyst.....61
4.3	The kinetic parameters of lactic acid, magnesium lactate, ammonium lactate and sodium lactate with ethanol.....63
4.4	Pervaporation parameters (the pre-exponential factor and the activation energy)70
4.5	Comparison of membrane performance parameters of different pervaporation systems74
4.6	The summary characteristic of fermentation broth, nanofiltration permeate and final product78

LIST OF FIGURES

Figure		Page
2.1	Production of lactic acid and poly(lactic acid) using starch as a substrate.....	5
2.2	Filtration principle: dead-end filtration and cross-flow filtration.....	13
2.3	Spiral wound membrane	18
2.4	Solubility of sodium sulfate in ethanol/ water mixtures at different temperature. (+) 25 °C, (▲) 40 °C, (□) 60 °C	19
2.5	Modeling transport across a NF membrane.....	26
2.6	Schematic representation of a NF membrane.....	29
3.1	Flow diagram of nanofiltration operation.....	43
3.2	Pervaporation-assisted esterification set-up	45
4.1	Pure water permeability experiment for NF under different TMP, bar	49
4.2	Lactate rejection as a function of solution flux at different lactate concentrations (118 – 1245 mM) at TMP = 16.2 bar, T = 30 °C, the experimental data were fitted by using the SK mode	51
4.3	Reflection coefficient (σ) and solute permeability (P_s) as the function of lactate concentration; the curves were fitted by using a Freundlich adsorption isotherm	53
4.4	Nonlinear regression volume of R_{obs} as the function of lactate concentration at a constant operation pressure TMP = 10.3 bar	54

LIST OF FIGURES (Continued)

Figure	Page
4.5 Experimental and modeling results for permeate flux as the function of lactate rejection of model solution (A) and permeate flux plus lactate rejection as function of volumetric concentration ratio (B). T = 30 °C, TMP = 10.3 bar	56
4.6 Histograms showing the compositions of the feed and the NF permeate solutions (A). Evidence of the decolouration induced by the NF process (B)	58
4.7 The concentration of lactic acid, ethanol, ethyl lactate and water from fermentation broth during esterification at A. 45 °C; B. 55 °C; C. 65 °C, D. 75 °C, (E). LA conversion of esterification reaction of the experiments with 1.5 wt% H ₂ SO ₄ , ratio of E:L is 3:1, W:L is 5:1 at 45 °C, 55 °C, 65 °C, and 75 °C	60
4.8 Arrhenius plot between ln(k) and (1/T), K ⁻¹ for esterification reaction of the experiments with 1.5 wt% H ₂ SO ₄ , ratio of E:L is 3:1, W:L is 5:1 at 45 °C, 55 °C, 65 °C, and 75 °C	62
4.9 The comparison between experimental mole fraction profile and predicted mole fraction profile of lactic acid esterification of the experiments with 1.5wt% H ₂ SO ₄ , ratio of E:L is 3:1, W:L is 5:1 at 45 °C, 55 °C, 65 °C and 75 oC (● : LA, □ : ETOH, ◆: ELA, ○: W, — — : LA model, — ETOH model, - - - : ELA model, : W model).....	65

LIST OF FIGURES (Continued)

Figure	Page
4.10	Influence of feed water mole fraction on total permeation flux, J_{tot} (kg.m ⁻² .h ⁻¹) at various operating temperatures.....66
4.11	Influence of the temperature on the separation factor for the fermentation mixture at 55 °C, 65 °C and 75 °C68
4.12	Temperature dependence of species permeances, $Q_{memb,w}$ and $Q_{memb,ETOH}$ (mol.m ⁻² .h ⁻¹ .bar ⁻¹) and linear fitting.....69
4.13	Calculated total permeation flux versus experimental total permeation flux at different temperature 55 °C; 65 °C; 75 °C71
4.14	Mole fraction of lactic acid, ethyl lactate, ethyl lactate, and water as the function of time obtained from experimental data and the model data by using pervaporation-assisted esterification at 75 °C, A/V = 23.8 m ⁻¹ 72
4.15	Lactic acid conversion profile for esterification reaction with and without pervaporation at 75 °C, E:L=7:1, W:L=5.5:1, A/V = 23.8 m ⁻¹ 72
4.16	Process of lactic acid purification.....76
4.17	HPLC chromatogram of sample taken during purification processes of lactic acid and final D-(-)-lactic acid fermentation broth (A) and chiral separation of optical purity of purified D-(-)-lactic acid (B).....79
4.18	Image of samples taken during purification processes of lactic acid and final D-(-)-lactic acid80

LIST OF ABBREVIATIONS

L_p	=	hydraulic permeability
P_s	=	solute permeability
σ	=	reflection coefficient
J_v	=	solvent flux, $L.m^{-2}.h^{-1}$
J_s	=	solute flux, $L.m^{-2}.h^{-1}$
TMP	=	transmembrane pressure, bar
ΔP_e	=	the effective pressure driving force, bar
$\Delta \pi$	=	osmotic pressure difference, bar
v	=	Van't Hoff factor, dimensionless
R	=	Universal gas constant, $J.mol^{-1}.K^{-1}$
T	=	absolute temperature, K
ΔC	=	the difference of the concentration of solute i in the feed solution and in the permeate solution, M
C	=	solute concentration, M
C_p	=	permeate concentration, M
C_f	=	feed concentration, M
V	=	volume, L
r_p	=	average membrane pore radius, m
μ	=	water viscosity, Pas
Δx	=	membrane thickness, m

LIST OF ABBREVIATIONS (Continued)

A_k	=	porosity, dimensionless
R_{obs}	=	observed rejection
γ	=	activity coefficient
g_{ij}	=	energy interaction between I and j molecules
α_{ij}	=	non-randomness factor in the mixture
r	=	reaction rate, s^{-1}
C_i	=	concentration of component i at time t, $mol.L^{-1}$
$C_{i,e}$	=	concentration of component i at equilibrium, $mol.L^{-1}$
$C_{i,0}$	=	initial concentration of component i, $mol.L^{-1}$
k	=	reaction rate constant, s^{-1}
k_0	=	pre-exponential constant, s^{-1}
K_e	=	equilibrium constant
a_i	=	activity of component i
x_i	=	mole fraction of component i
X_{LA}	=	conversion of lactic acid
E_A	=	activation energy, $J.mol^{-1}$
J_i	=	flux across the membrane, $kg.m^{-2}.s^{-1}$
$Q_{ov,i}$	=	overall mass transfer coefficient of i in vapor pressure term
$K_{ov,i}$	=	overall mass transfer coefficient of i in liquid term
A	=	membrane area, m^2
$p_{l,i}$	=	partial vapor pressure of i in liquid side, bar

LIST OF ABBREVIATIONS (Continued)

$p_{g,i}$	=	partial vapor pressure of i in vapor side, bar
$C_{l,i}$	=	concentration of i in the liquid, g.L ⁻¹
$C_{g,i}^*$	=	concentration of i in the liquid which would be in equilibrium with vapor, g.L ⁻¹
$Q_{memb,i}$	=	mass transfer coefficient, mole.m ² .h ⁻¹ .bar ⁻¹
VCR	=	volume concentration ratio
p_i^0	=	saturation vapor pressure of I at the feed temperature, bar
ρ	=	molar density of liquid, kg.m ⁻³
P_p	=	total pressure on the permeate side, bar
y_i	=	liquid mole fraction in permeate side
α	=	membrane selectivity

CHAPTER I

INTRODUCTION

1.1 General introduction

By virtue of presence of both hydroxyl and carboxylic acid groups, lactic acid can participate in a wide variety of chemical reactions producing a host of high value and large volume products ranging from food preservatives, green solvent and oxygenated chemicals to biodegradable poly-lactic acid thermoplastics (Dey et al., 2012). Be an important industrial chemical as L-(+)-lactic acid, D-(-)-lactic acid is an intermediate product during the synthesis process of many chiral materials (Wang et al., 2017). In particular, D-(-)-lactic acid not only becomes a significant feed stock monomer material for chemical conversion into poly-lactic acid and plays a key role in improving the quality and performance of poly-lactic acid which serves as biodegradable commodity plastic and biocompatible polymer, but also has a great potential to be applied in the fields of food, environmental protection, medicine etc. (Boonpan et al., 2013; Hama et al., 2015; Li et al., 2012). Nowadays, through using the main method, microbial fermentation, LA can be produced with the high yield around 90-95wt%, based on bacterial and initial feed-stocks. In many studies, cassava was interested as a starting natural raw and low cost material for fermentation with high concentration of sucrose (12%), rapid rate of fermentation, low amount of contaminant, high yield of lactic acid production (Chookietwattana, 2014; Wang et al., 2010).

Normally, alkalis like NaOH, Ca(OH)₂ or NH₄OH were used for pH adjustment during fermentation. It results that the fermentation broth contaminated lactate salts instead of lactic acid and high impurities compounds such as cell biomass, impurities, protein, color and other organic therefore necessitating further processing like filtration, evaporation, acidified with sulfuric acid membrane, solvent extraction, absorption, distillation, electrodialysis and esterification (Dey et al., 2012).

Being an environmentally friendly and economic processes generating no secondary waste (Khunnonkwaoa et al., 2012) as well as a high effective for protein and color removal with the low rejection of organic acid compound in general, and of lactic acid in particular from fermentation broth (Lubsungneon, 2014), nanofiltration was used as a single membrane pretreatment in this study before applying further purification technique. Nevertheless, such purification procedures, for example, distillation, filtration do not perform satisfactorily due to the low volatility of LA, its affinity to water, and tendency to self-polymerize action that causes the main limiting boundaries of the necessary energy and material requirements as well as waste generation. Therefore, due to the selectivity and reactivity of LA with alcohol, esterification technique can be used as an effective downstream method to obtain highly purified lactic acid from fermentation broths (Delgado et al., 2007) by altering the boiling point of their respective ester compound (Lubsungneon, 2014). To rise the conversion of esterification, in recent years, there are the efforts to combine downstream/upstream separation with reaction to reduce the thermodynamic limitation via selective removal of one or more product species from the reaction mixture technique, especially water. In this regard, membrane technology which can help to get high rate of dehydrate from reaction, has emerged as one of the viable separation

processes. Among these membrane technique, pervaporation which special suits for organic-water and organic-organic separations, is an ideal candidate for enhancing conversion in reversible condensation reactions which is generated water as a product (Benedict, 2003). A ceramic pervaporation module which was known as a good candidate to decrease the acidic effect on membrane and increase the using time of membrane was be used in this study. Additionally, even though nanofiltration and esterification are the well-known techniques that were used in many industrial sectors with advantage side by reducing processing costs, the performance of the operation for organic acid compounds was not controlled clearly. So, in order to get more detailed data that can be used in building the full process for producing lactic acid in industry, mathematical modeling such as Spiegler–Kedem model, solution desorption model and solution-diffusion model used NRTL theories as activity coefficient models for nanofiltration and pervaporation-assisted esterification were explored as a necessary step.

Finally, the completed conceptual process of LA purification from fermentation broth will be presented for obtaining the high purity of D-(-)-lactic acid.

1.2 Research objectives

- To study and model the performance of pretreatment techniques, nanofiltration in lactate broth based on the Irreversible thermodynamics (IT) equation.
- To study the mathematic study of the esterification of lactic acid with ethanol, catalyzed by sulfuric acid, coupled to a ceramic membrane pervaporation unit. Using non-random two liquid (NRTL) model as the thermodynamic activity coefficient models.

- To complete the conceptual process of LA purification from fermentation broth and obtain the high purity of D-(-)-lactic acid.

1.3 Research hypothesis and its significance

High purity D-(-)-lactic acid can be produced by membrane filtration and esterification techniques from fermentation broth. From the experimental results, a NF model and pervaporation assisted esterification can be developed with a small error that will allow to obtain membrane characteristics, predict process performance. Therefore, this study will be helpful for understanding more about D-(-)-LA separation technique with the high yield as well as for the design and scale-up the LA purification process.

1.4 Scope and limitation of the study

This work involves the purification of the D-(-)-lactic acid using nanofiltration and pervaporation assisted esterification. The model parameters of nanofiltration were studied based on experimental data and using Spiegler–Kedem model and then obtained the reflection coefficient (σ) and the solute permeability (P_s). The mathematic model for batch esterification and esterification of lactic acid with ethanol to product ethyl lactate in pervaporation assisted esterification with sulfuric acid as catalyst was studied based on the kinetic (the activation energy, reaction rate constant) and the performance of pervaporation (pre-exponential factor, $Q_{memb,0}$ and the activation energy, E_{perm}) for esterification reaction.

CHAPTER II

LITERATURE REVIEW

2.1 Lactic acid

2.1.1 Lactic acid properties

Lactic acid (IUPAC systematic name: 2-hydroxy propanoic acid) is a propionic acid with formula $\text{CH}_3\text{CH}(\text{OH})\text{COOH}$. Because having a hydroxyl group adjacent to the carboxyl group, it is an alpha-hydroxyl acid (AHA). L-(+)-lactic acid

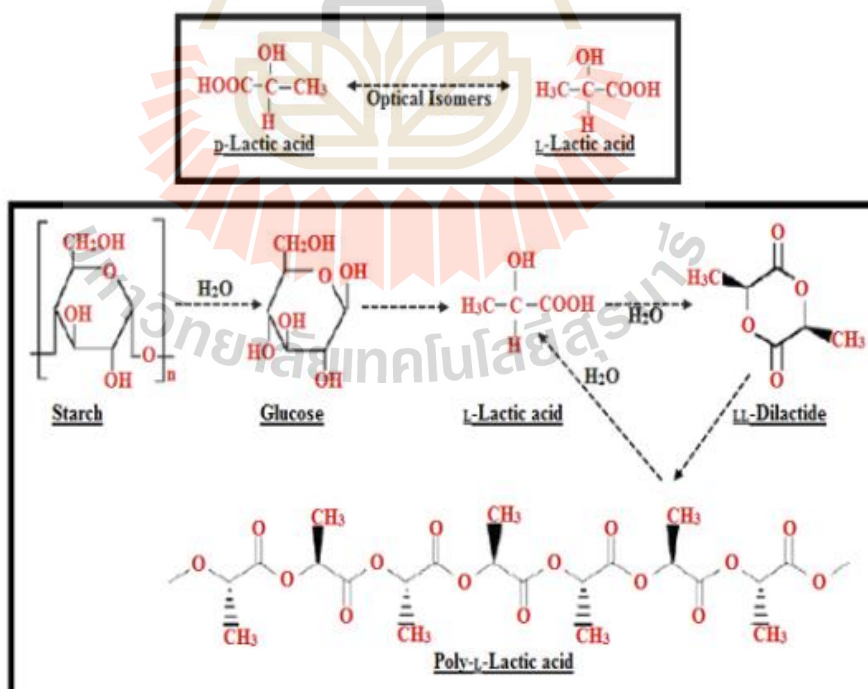


Figure 2.1 Production of lactic acid and poly(lactic acid) using starch as a substrate (Ghaffar et al., 2014).

and D-(-)-lactic acid, as well as racemic lactic acid (a mixture of D- and L- form of lactic acid) was known as three types of lactic acid.

Lactic acid is both an alcohol and an acid, therefore, its molecules can form esters with one another. In a solution containing less than 20% of lactic acid, the acid is in the simple monomeric form, but solutions of greater concentration contain some esters. Pure 100% lactic acid is a colorless, viscous liquid. It is water-soluble and most of the organic solvents that are hygroscopic and corrosive. Lactic acid produced both by naturally and synthetically (Chow, 1962). The physicochemical properties of lactic acid were shown in Table A1 (Appendix A).

The chemical behavior of lactic acid is determined by its physicochemical properties, among which are a) acidic character in a aqueous medium; b) bifunctional reactivity associated with the presence of a carboxyl and a hydroxyl group, which gives it great reaction versatility; and c) asymmetric optical activity of C2.

2.1.2 Lactic acid application

Lactic acid is a valuable industrial chemical used in the food industry and in numerous other applications in the pharmaceutical, leather and textile industries, and also for the production of biodegradable and biocompatible polylactide polymers, such as poly(L-lactic acid) (PLLA) and poly(D-lactic acid) (PLDA), an environmentally friendly alternative to biodegradable plastics (Vijayakumar, 2008).

- Biodegradable plastics

Biodegradable PLLA is a biodegradable polymer approved for the use in food packaging in several countries, particularly U.S.A., European Union countries, and Japan (Narayanan, 2004) because it is a highly versatile, biodegradable derived from

renewable resources. It has extensive applications in industrial packaging, fibers, clothes, and biocompatible materials for medical application (Zhang, 2015). PLLA has gained great attention because of its excellent biocompatibility and mechanical properties. However, its long degradation times coupled with the high crystallinity of its fragments can cause inflammatory reactions in the body. In order to overcome this, D-(-)-lactic acid as a material combination of L-(+)-lactic acid, is the important compound in poly(DL-lactic acid) (PDLLA) which is the latter rapidly degraded without formation of crystalline fragments during this process (Lopes et al., 2012).

PDLA which obtained by polymerization of D-(-)-lactic acid, is important agent to be blended with PLLA in biopolymer production and lead to the widen PLLA applications as an alternative of commercial polymers and drug delivery systems (Xu et al., 2006). With PDLA, PLLA could form stereocomplex crystallites which could enhance the mechanical performance, thermal stability, and hydrolysis-resistance of PLLA-based materials. Tsuji and co-workers reported that the melting temperature of stereocomplex which is produced by 1:1 blend of PLLA and PDLA was 50 °C higher than of PLLA (Tsuji & Fukui, 2003). The difference in hydrolysis behaviors between the well-stereo-complexed 1:1 blend and non-blended films was investigated by Tsuji (Tsuji, 2002). From this work, the hydrolysis which is indicated through the rate of reduction in molecular weight, tensile strength, Young's modulus, melting temperature, and mass remaining of the 1:1 blend was found at a lower rate than of the non-blended films. These findings strongly suggest that the well-stereo-complexed 1:1 blend film is more hydrolysis resistant than the non-blended (Pramkaew, 2010). This is probably due to the peculiar strong interaction between L- and D-lactyl unit sequences in the amorphous state, resulting in the future decreased

interaction of PLLA or PDLA chains and water molecules. However, the peculiar strong interaction between PLLA and PDLA chains may have caused the retarded proteinase K-catalyzed hydrolysis of the PLLA/PDLA blend film compared with that expected from the hydrolysis rates of non-blended PLLA and PDLA films. PDLA acted as a nucleating agent of PLLA, thereby increasing the crystallization rate (Yamane & Sasai, 2003).

- Other industries

In other applications, lactic acid and its salt are used increasingly in various types of chemical products and processes. Lactic acid is widely used in most part of the food industry especially in the production of beer, wine, beverages, pickles, cheese, yogurt, meat, and bakery products. Lactic acid is also one of the most effective alpha hydroxy acids (AHAs) that is found in the skin thus, it is used in many applications in cosmetics. Because of having the lowest irritation potential, it is a common ingredient in moisturizers, skin whiteners, and anti-acne preparations. Lactic acid is used as an anti-aging chemical demanded to soften lines, decrease the damage from the sun's UV radiation, recover skin texture and tone and being as a pH-regulator in many types of hair care product. In the pharmaceutical industry, lactic acid as an electrolyte in many parenteral/I.V. (intravenous) solutions that are intended to replenish the bodily fluids or electrolytes. Lactic acid is used in a wide variety of mineral preparations, which include tablets, prostheses, surgical sutures, and controlled drug delivery systems (Wee et al., 2006). However, the food and pharmaceutical industries have a preference for the isomer L(+)-, the only one that can be metabolized by the human body (Martinez et al., 2013). Moreover, Lactic acid functions as a descaling agent, pH regulator, neutralizer, chiral intermediate, solvent, cleaning agent, slow acid-release agent, metal complexing agent, an antimicrobial agent, and humectant (Wee et al., 2006).

2.1.3 Lactic acid market

According to the business report published by Grand View Research, Inc., the global market of LA market was estimated to be a very high amount (714.2 kilotons) in 2013 and is growing 12 - 15% every year. The level of this production is expected to reach 1960.1 kilotons which are anticipated to reach 4,312.2 million USD by 2020 (Grand.View.Research, 2015). Major driving forces of the lactic acid market are PLA and lactate solvents as well as personal care products. The demand for sustainable packaging products as well as the rising crude oil prices are expected to drive demand for the PLA. Although the demand for PLA is increasing, its current production capacity is only 496 kilotons per year, which results from the high manufacturing cost of its monomer-lactic acid (Zhang, 2015).

Currently as a building block for a further range of performance PLA grades, D-(-)-lactic acid has attracted intensive attention. Nature works LLC (the United States) which has been the dominant leader in PLA business, has announced their efforts for the production of D-lactic acid in June 2017. However, while small volumes of D-lactic acid have previously been available from producers in Europe and Asia, there is the expectation for the more availability of D-lactic acid as a monomer for the rapid growth of PLA industry.

2.1.4 D-(-)-lactic acid production

Lactic acid is a naturally occurring organic acid that can be produced by chemical synthesis or fermentation. Chemical synthesis of lactic acid is mainly based on the hydrolysis of lactonitrile by strong acids, which provide only the racemic mixture of D-(-)-and L-(+)-lactic acid. However, fermentation using modified or optimized LAB

strains such as *Lactobacilli* is the most common and efficient method for high yield of a desired optically pure L-(+)- or D-(-)-lactic acid (Martinez et al., 2013). The interest in the fermentative production of lactic acid has increased due to the prospects of environmental friendliness and of using low cost, renewable resources instead of petrochemicals. The substrates that can be used for synthesizing LA are glucose, sucrose, lactose derived from cassava, beet sugar, molasses, whey, barley malt and etc. The summarizes of the key characteristics of selected bacteria, substrates for lactic acid fermentation was shown in Table 2.1.

During the fermentation by the time, it is necessary to neutralize the lactic acid being formed otherwise, the fermentation would decrease in rate and eventually stop. In this case, sodium hydroxide (NaOH) is normally used as the neutralizing agent. The reasons are not only a cheap material to use for the neutralization of the acid during its fermentation but also soluble lactate or lactic acid can easily be prepared in a relatively pure condition from sodium lactate by reaction with sulfuric acid, since sodium sulfate is practically insoluble in ethanol and hence can readily be separated from the product by filtration. Hydrated lime, Ca(OH)_2 , also can be used in this case but NaOH has the advantage that the sodium sulfate produced in equation forms soft sludge. However, if Ca(OH)_2 is used the calcium sulfate formed might set into hard masses of gypsum wherever there was insufficient water for the hydration reaction. After fermentation, lactic acid broth contains a number of impurities such as residual sugars, color, nutrients and other organic acids, as part of cell mass that results in the low quality desirable product. These impurities must be removed from the broth in order to obtain the high purity of LA. The broth will be neutralized to approximately pH 7.0 that leads to all lactic acid being present in the salt form, kills bacteria, coagulates protein of the medium

and helps to decompose any residual sugar in the medium (Vijayakumar, 2008). The supernatant liquid can be decanted to a storage vat and the sludge filtered in a filter press before doing the further purification steps.

Table 2.1 Characteristics of selected bacteria, substrates for fermentation broth (Litchfield, 2009).

Microorganism	LA isomer	Fermentation pattern	Raw material
<i>Lactococcus lactis</i>	L(+)	Homofermentative	Glucose, lactose
<i>L. casei subsp. rhamnosus</i>	L(+)	Homofermentative	Glucose, sucrose, molasses
<i>Lactobacillus amylophilus</i>	L(+)	Homofermentative	Starch
<i>Enterococcus faecalis</i>	L(+)	Homofermentative	Sugar cane molasses
<i>Bacillus sp.</i>	L(+)	Homofermentative	Sugar cane bagasse
<i>L. coyneformis subsp. torquens</i>	D(-)	Homofermentative	Enzyme-converted cardboard
<i>L. delbrueckii subsp. bulgaricus</i>	D(-)	Homofermentative	Cheese whey and permeate, lactose
<i>L. helveticus</i>	DL	Homofermentative	Cheese whey and permeate, lactose
<i>L. amylovorus</i>	DL	Homofermentative	Starch

2.1.5 Downstream process

After the fermentation, purification or product recovery is an essential step in LA production process in order to reduce LA losses and to increase the purity. In the early 1980's, a comprehensive review covered the major technologies and principles governing recovery of carboxylic acids from fermentative media using solvents, amines, phosphates, or their mixtures (Kertes & King, 1986). Since then, several patented processes for LA recovery have been developed which can be classified as those that use direct precipitation (as salt or acid), extraction (solvents, amines), ion exchange, membranes, or esterification of the free acid followed by hydrolysis.

With the optimized participation of distillation, centrifugation, or membrane modules such as microfiltration and nanofiltration membrane in a steady production system, a high yield of 95% pure lactic acid can be achieved (Pal & Dey, 2012). Normally, microfiltration or centrifugation are the techniques that can be used for separating the cell and some suspended particles, while magnesium, calcium phosphate, as well as sulfate ions are efficiently removed by nanofiltration from a sodium lactate fermentation. Factors such as pH, mixing time, initial concentration of LA, pressure of trans-membrane and volume ratio between the organic and the aqueous phase affect the extraction of LA. However, these purification methods have some technical problems for example azeotropic point of distillation, low separation degrees, the high concentration of water in the fermentation broth, therefore, the technique named esterification and hydrolysis, were be interested and were used for getting more purify LA from fermentation broth.

2.1.5.1 Membrane separation

Membrane filtration is the process of removing undesirable chemicals, biological contaminants, suspended solids and gasses from a contaminated feed that is based on the presence of semi permeable membranes. The goal is to produce permeate for a specific purpose. The advantage of membrane filtration technique is the ability to separate define compounds at low temperatures with no phase change. Moreover, this technique requires the lower overall energy cost per unit, the fewer expenses on supervision, operation and maintenance than conventional methods, for instance, filter presses, centrifuge.

There are two filtration modes: dead-end filtration, where the entire solution is directed normal to the membrane area under applied gaseous pressure and cross-flow filtration, where the direction of flow is parallel to the surface of the membrane. However, the tangential flow in the cross-flow mode creates better conditions for reduced fouling and reasonable permeate flux, particularly important with concentrated or viscous solutions that generate significant concentration polarization layers, and successfully used for microfiltration and nanofiltration of some natural extracts (Tsibranska, 2013). Therefore, cross-flow filtration is used by the majority of membrane processes and consistent with the industrial scale.

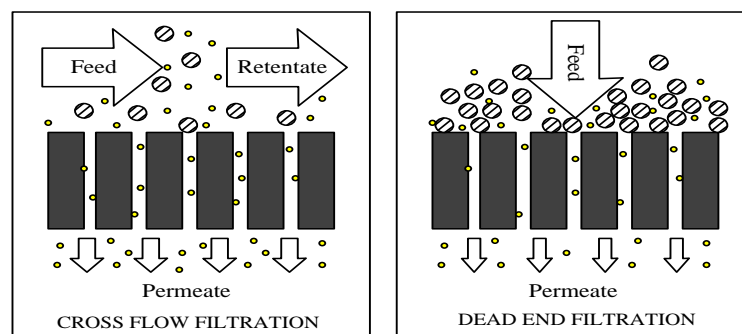


Figure 2.2 Filtration principle: dead-end filtration and cross-flow filtration.

Cross-flow membrane filtration technology is accepted as an effective step in many of the separation process in the food, dairy, pharmaceutical, biotechnological, chemical and industries. The most important part of any membrane filtration process is the membrane, and choosing the suitable membrane for a given process is a complex task. Cross-flow microfiltration is an efficient operation for clarifying such complex fermentation media and it requires no adjuvant. Clarifying fermentation broth by cross-flow filtration is thus becoming more and more attractive in the present context of industrial waste reduction. If batch plants are involved, microfiltration is generally operated under constant transmembrane pressure, which is the simplest operating mode, or under constant permeate flux. The latter mode is very convenient when the plant is operated at a constant permeate flux below the critical flux. It is thus possible to run the filtration plant during a very long period of time with no fouling in the case cross-flow filtration (Carrère & Blaszkow, 2001).

There are several types of membrane with different pore size ranging from 100 molecular weight to 10 μm : reverse osmosis, ultrafiltration, microfiltration, and nanofiltration.

- Reverse Osmosis (RO)

RO which has a pore size range of 0.0001 – 0.001 μm , is a high pressure, energy-efficient means of the desalination and purification of water, concentration of low molecular weight compounds.

- Ultrafiltration (UF)

UF has a pore size range of 0.1 to 0.01 μm . It is a selective separation step that is used for concentrating and purifying medium to high molecular weight components, for example, dairy proteins, carbohydrates, and enzymes.

- Microfiltration (MF)

Microfiltration refers to filtration processes that use the porous membrane with a diameter between 0.1 and 10 μm to separate large molecular weight suspended particle or colloidal compounds, for example, cells. It usually serves as a pre-treatment for other separation processes such as ultrafiltration, nanofiltration and a post-treatment for granular media filtration at a low pressure (1 – 5 bar).

- Nanofiltration (NF)

Nanofiltration is a type of membrane separation in which the pores are very small (0.5 – 2.0 nm) and lies in the range between truly fine porous and dense polymeric membrane. It works in a high pressure-driven process (10 – 20 bar) that is used to treat solution for achieving very small compounds without any phase change. Through NF, the macro impurities such as sugar, other organic molecules, multivalent salts, proteins can be separated from one hand and monovalent salts and water on the others. Due to many researches, NF was shown as an ideal candidate as it separates without the use of additional chemicals simply by the molecular weight differences of LA and protein. With the high permeability for monovalent salts (for example sodium chloride, potassium chloride), organic compounds with low molecular weights range 300 – 1000 Da (Ericksson, 1988) and a very low permeability for organic compounds of molecular weight greater than 300 Da (such as protein), NF membranes are successfully applied in the removal of protein and mineralization out of organic acid fermentation broths (Chandrapala et al., 2016; Lubsungneon, 2014).

- Membrane materials

Typically, membrane filtration is designed with polymer- or ceramic-based. The natural properties and, the condition of the incoming process stream

as well as the purpose application will direct the engineer towards making the final decision for the proper membrane such as membrane configurations and materials. Polymeric spiral membranes are generally used when a high throughput is required, while polymeric tubular membranes, which can often be mechanically cleaned, are more suited for low-maintenance operations, highly viscous products, or fluids with a suspended material. However, for the incompatible environments process fluid with the high levels of solvents and wide pH ranges, ceramic membranes are more frequently becoming the first choice module. An alumina or zirconia coating that contains a uniform system of channels is normally applied to the inside surface of a ceramic support (Gitis & Rothenberg, 2016). The capital cost of ceramic membranes is much higher than with conventional polymeric membranes, but in some applications, they are the only viable proposition. Offsetting the high initial cost, though, is the fact that ceramic membranes are not only mechanically, thermally and chemically stable but also often provide a longer operational lifetime (the average 15 – 20 years lifespan of ceramic membranes is roughly double than the 7 – 10 years of current polymeric membranes) because of not being abrasion (Gitis & Rothenberg, 2016).

- Membrane shape and module

Industrial membrane plants often require hundreds to thousands of square meters of membrane to perform the separation required on a useful scale. Therefore, the problem is how one can pack the most area of membranes into the least volume, to minimize the cost of the containment vessel consistent with providing acceptable flow hydrodynamics in the vessel. These packages are called membrane modules and there are four main types of module: plate and frame, tubular, hollow fiber, and spiral wound. The plate-and-frame module is the simplest types, consisting of two

end plates, the flat sheet membrane, and spacers. Normally, plate-and-frame modules can be used in electrodialysis and pervaporation systems and in a limited number of reverse osmosis, ultrafiltration, microfiltration, and nanofiltration. Tubular modules are the type of module that is known the membrane inside of a tube and the feed solution is pumped through the tube. Tubular polymeric membranes are typically housed in modules of stainless steel or plastic. Even though, having the high resistance and the high cost, tubular modules have several great advantages in industry. They can use for the separation of viscous liquids with high levels of suspended solids such as organic fermentation broth with long-term life cycles and can be cleaned easily by chemical and mechanical methods. Hollow fiber modules consist of bundles of hollow fibers in a pressure vessel and present a very large membrane area. They can have a shell-side feed configuration where the feed stream passes along the outside of the fibers and exits the fiber ends. They are used in ultrafiltration, pervaporation, and some low to medium pressure gas applications. Spiral wound modules are the most popular modules in industry for nanofiltration or reverse osmosis membranes. The components of each module are the flat sheet membrane combine with mesh spacer that was wound around a perforated central collecting tube to form the spiral wound membrane (SWM) module. The SWM module is the basic component for building a very broad range of filtration facilities, for purification of an organic acid. A typical SWM module is schematically shown in Fig. 2.3. A membrane envelope is made of two sheets, glued at the three edges, with a fabric filling the permeate channel. The open permeate-side of this envelope is fixed on a perforated inner tube where the permeate is collected. Several envelopes, separated by relatively thin net-type spacers, are tightly wrapped around the perforated inner tube (Karabelas, 2015).

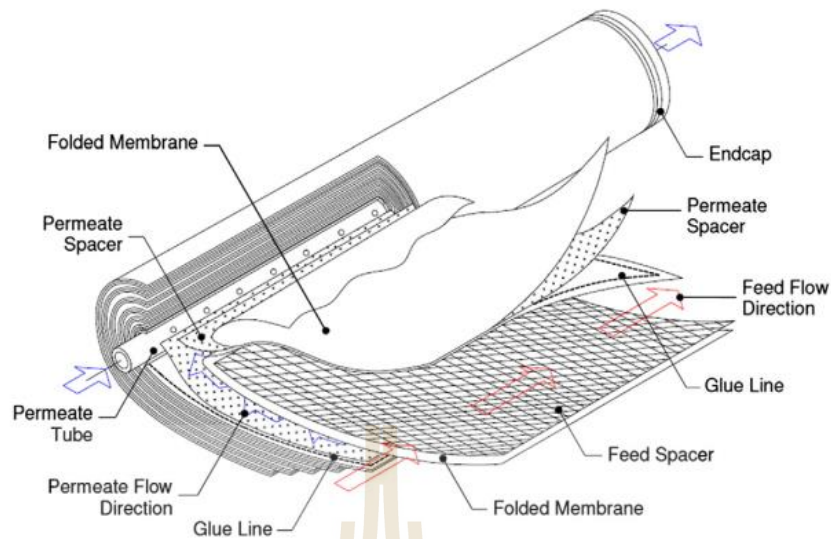


Figure 2.3 Spiral wound membrane (Karabelas, 2015).

2.1.5.2 Acidification of salt

This recovery process is used for sodium salts (sodium lactate). First of all, sodium lactate reacts with H_2SO_4 to form lactic acid. After that, the excess of H_2SO_4 performs like a catalyst for esterification of free lactic acid with ethanol. The chemistry of this process is presented as follow:



These reactions occur simultaneously during acidification at rates and extents that depend on temperature, H_2SO_4 concentration, and time. (Londono, 2010). As soon as acidification is complete, the lactate species dissolved in ethanol are subject to further esterification via reactive distillation to form the desired product, ethyl lactate. During this processing, the large quantity of sodium sulfate sludge can be produced. The sodium sulfate is insoluble in ethanol and precipitates so it can be

removed out of the system by using filtration. The solubility of sodium sulfate in ethanol and water is shown in Fig. 2.4.

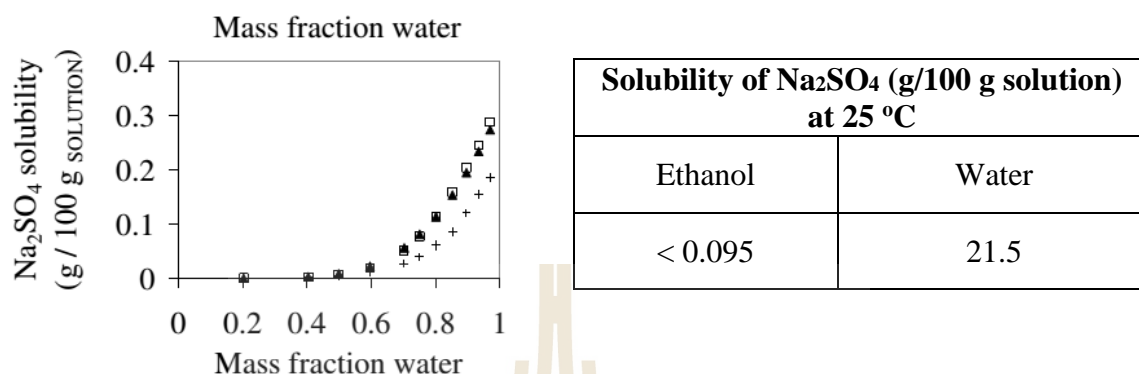


Figure 2.4 Solubility of sodium sulfate in ethanol/ water mixtures at different temperature. (+) 25 °C, (▲) 40 °C, (□) 60 °C.

Sodium sulfate as solid waste from this process would be harmed to environment. However, nowadays sulfate sodium salt Na₂SO₄ is also a material that is used to generate H₂SO₄ and NaOH by the electro-electrodialysis process (EED) which is the useful way not only to reduce the waste of process (Na₂SO₄) but also to reuse the products (H₂SO₄ and NaOH) for the lactic acid purification process.

2.1.5.3 Esterification

Esterification is the method that is used for forming esters by the reaction of carboxylic acid and an alcohol with the elimination of water. It is the only downstream process that can remove contaminating compounds by altering the boiling points of their respective ester compounds. The esterification of LA involves the chemical reaction with alcohols, such as ethanol, to produce the corresponding lactate esters (Khunnonwao, 2010). This reaction will be carried out until equilibrium is reached

and after that, the next step is recovery desired purity ethyl lactate by using separation unit such as distillation, filtration, membrane (Komesu et al., 2015).

For the recovery of LA, two main steps can be used of esterification technique was performed (Benedict, 2003; Delgado et al., 2010). First, LA will be reacted with ethanol to get ethyl lactate before distillate purification. The second step is hydrolysis reaction using water in the presence of acid catalyst to produce ethanol and LA. Following reactions are involved in this process (Delgado et al., 2008).



Actually, the esterification reactions will happen in a liquid phase until it reaches the equilibrium point and a reverse reaction happened then. For making sure the high yield of ethyl lactate and the reaction keeps continuously, one of the reactants (ethanol and LA) should be redundant or the draw out of the products (ethyl lactate and water) from the reaction phase, for example, water dehydration. The concentrations present at equilibrium depends on the characteristics of the alcohols and esters involved, but in most practical uses of the reaction, one or both of the devices mentioned are used to force the reaction toward completion (Aslam et al., 2000).

- Catalysts

The esterification reaction requires a catalyst to combine the molecules of LA and an alcohol to produce esters as well as to increase the rate of the esterification reaction. Generally, the catalysts are acid, alkaline depending on the reactants. In the alkaline catalysts group, alkali metal alkoxides are the most common effects such as the sodium or potassium alkoxide. For the acid catalysts, sulfuric acid, sulfonic acids, and hydrochloric acid are most used.

- Temperature

The temperature that is optimal for esterification reaction depending on the kinds of catalyst using for the reaction. Alkaline is the good catalyst for esterification, the reaction often takes place at room temperature or even lower temperatures, however, the alkaline is highly corrosive and difficult to control and use in industry. With acid catalysts, around 50 – 100 °C is the temperature that is used. Although the reaction is lower, acid is the commonly used because of the high yield. If without using catalyst, the temperature that is required for the reaction may be 250 °C.

- Alcohols

In general, the primary alcohols are most reactive for esterification. Under the same conditions, the secondary and the tertiary alcohols react more slowly and form lower conversions to ester products (Aslam et al., 2000). Normally, almost esterification process currently produced worldwide come from the reaction of organic acid and methanol, however, the use of ethanol instead of methanol is the logical step and it will be emphasized for this studied. The reasons are ethanol can be produced from agricultural renewable resources and has lower human toxicity than methanol, therefore it is safer to handle and store. In addition, ethanol also is a simple alcohol and it reacts very fast as they are relatively small and contain no carbon atom side chains which would hinder their reaction (Pisarello et al., 2010).

2.1.5.4 Membrane – assisted esterification

Because the extent of esterification is thermodynamically limited, removal of reaction products is required to achieve complete conversion. To overcome such thermodynamic limitations, reactive distillation (RD) can be

implemented as a scalable industrial process to continuously remove either water or ester from the reactive media as it is formed (Londono, 2010). This is usually not the case in many processes and in addition formations of azeotropes were noted. However, the mismatching of the reaction and distillation temperature is an additional complication and in many cases, the process performance and energy consumption in reactive distillation are the major cost factor in the manufacturing of esters (Jyoti et al., 2015). Therefore, membrane can be integrated with either distillation or a chemical production step to provide intensification and energy integration. Among separation methods, pervaporation is a process which is suitable for almost the separation of special liquid mixtures.

The integration of esterification reactor with a pervaporation pilot plant via hybrid reactor permits the selective permeation of the component (water) from the mixture. Pervaporation (PV) is a rate controlled separation process and the separation efficiency is not limited by relative volatility. In pervaporation process, only water is permeated by membrane and accomplishes phase change. Hence, the energy required is comparatively lower. In addition to this, the temperature of operation of pervaporation setup matches with the temperature of reaction and hence could be advantageously used for enzymatic esterification due to temperature constraints normally imposed by enzyme stability. The combination of pervaporation with the chemical reaction is very attractive system nowadays. The coupling of pervaporation separation process into conventional esterification processes with suitable membranes enhances the yield of the esters and conversion of acid. PV enhanced the conversion and it was higher for the PV-assisted esterification than for the reaction without PV. Water content for the reaction without PV was higher than that for the PV-assisted reaction due to water removal by PV. It summarizes the results of pervaporation

esterification integrated system in terms of conversion when compared to a nonintegrated system (Jyoti et al., 2015).

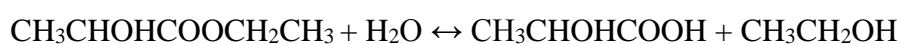
2.1.5.5 Distillation

Distillation is a separation process in which the certain quantity of a mixture (gas, solid, liquid, enzymes, suspension, or isotope) are divided during a phase transition, into a number of smaller quantities (fractions) according to a gradient. For example, due to the difference in boiling point of the individual components, the desired product will be separated in a reactive column. There are several recent studies that were used distillation for removing ethanol out of the organic acids such as acetic, succinic, citric, and lactic acids or organic ester, for example ethyl lactate and methyl succinate mixture (Matsuda et al., 2016).

2.1.5.6 Hydrolysis

After the volatile lactate ester is separated from the reactive mixture, it will be hydrolyzed back to pure lactic acid and the corresponding alcohol in excess pure water with an acidic ion-exchange resin (such as Amberlyst 15) as a catalyst. This process is called hydrolysis.

Hydrolysis is the technique that esters are cleaved (hydrolyzed) into an acid and an alcohol through the action of water via presenting acids or bases catalysts. The mechanistic aspects of ester hydrolysis have received considerable attention and have been reviewed and presented in the following reaction (Asthana et al., 2006).



The catalyst that can be used for hydrolysis reaction are acids, bases, and enzymes. The acid ion exchange resin, Amberlyst 15 brings new possibilities of simplification to the ethyl lactate technology, making the process more environmentally friendly compared with common homogeneous processes (Gao et al., 2007). However, esters have poor solubility in water, the reaction rate in dilute acids is fairly low (Asthana et al., 2006). The complete reaction can only be achieved by removal of alcohol or acid from the equilibrium by using RD. In general, RD seems to be a simple, energy-saving process with lower investment and operation costs. At the last step, the excessive water was removed by vacuum evaporation to produce concentrated lactic acid (Khunnonkwaoa et al., 2012).

2.2 Transport and separation mechanism: modeling of NF membrane

NF membranes are ones of the mainly utilized for the process of organic compound recovery. It can be used as an effective macromolecule, protein and multivalent ionic compounds removing method, therefore, NF membranes are a good choice for the pretreatment of organic compound production. Therefore, in this study, NF is an ideal candidate as it separates without the use of additional chemicals simply by the molecular weight differences of LA and protein. Uniquely, this process allows separation of organics and monovalent salts in the molecular weight range 300 – 1000 Da (Ericksson, 1988). NF membranes classically have a high permeability for monovalent salts (such as NaCl and KCl) and organic compounds with low molecular weights. However, it has a very low permeability for organic compounds of molecular weight greater than 300 Da such as proteins. NF membranes are already applied in the

separation of protein and LA in fermentation broths, while demineralization is also a useful effect (Chandrapala et al., 2016).

Additionally, the factors affecting NF separation that can also play an important role in membrane fouling and cleaning are as follow membrane properties such as surface roughness pore size distribution, membrane thickness, membrane charge type and charge density. The chemistry of the treated solution such as solute composition, the size, geometry and the charge of the components, the concentration of ions, the pH and the fouling potential of the solution and its interaction with membranes. The operation design of the NF systems, their capacity, dimensions, and flow. The processes environment temperature and pressure (Ahmed & Lovitt, 2007).

Generally, the fundamentals of NF separation and selectivity NF are the combination of the uncharged components removing at nano-size with the charge compounds that have effects between solution, and the surface of the membrane. The removal of uncharged components results from size exclusion or may be a result of differences in diffusion rates in a non-porous structure, which depends also on molecular size. The charge effect, on the other hand, results in the removal of (mainly multivalent) ions; the former effect results in the removal of uncharged organic species (Hilal et al., 2004). The performance of NF process can be analyzed and predicted by using a mathematical model. Unfortunately, NF separation of multi-ionic solutions is often difficult to predict given the complex nature of the interactions that occur among the ions themselves, and the ions and the membrane. A rigorous model becomes essential to understand what governs the separation process and what transport and membrane properties dictate the performance of organic salts before extending our NF pretreatment in a larger scale (Labban, 2017).

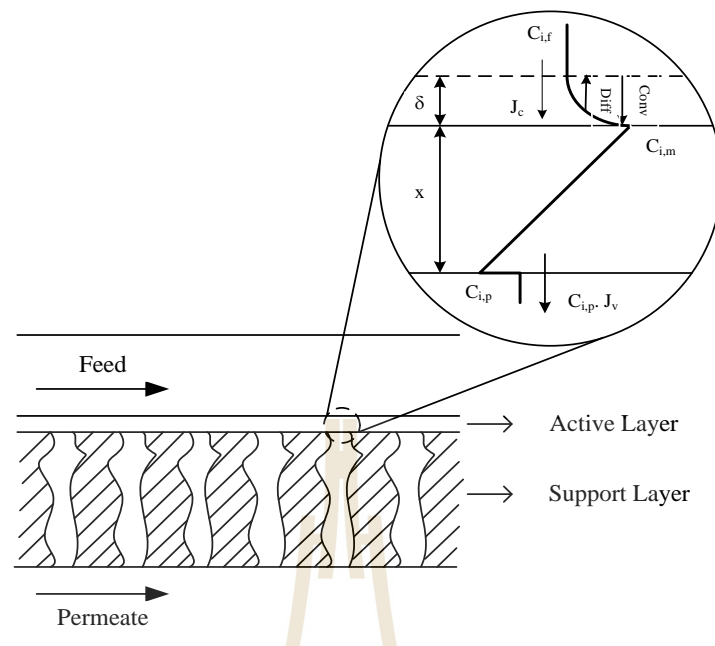


Figure 2.5 Modeling transport across a NF membrane.

Literature models for high-pressure membranes (NF & RO) are usually based either on a mechanism-independent approaches, such as irreversible thermodynamics (IT) or on the extended Nernst-Planck method. Initial descriptions of the NF process were based upon irreversible thermodynamics. These methods were originally employed as a black box description of dense reverse osmosis membranes (Dach, 2008; Kedem & Katchalsky, 1958; Spiegler & Kedem, 1966).

IT models is based Spiegler and Kedern model that is used to describe the transport phenomena in the NF system. This model is not only applied when the electrostatic interaction between membrane and solute is trivial as well as used this model in retention of electrolyte with a charged NF membrane (Kedem & Katchalsky, 1958; Kim et al., 2012; Spiegler & Kedem, 1966). In general, the transport equations for the components through a NF membrane consist of two components which are the

diffusion component and the convection component. For a system involving a single solute in aqueous solution, solute retention can be described by three transport coefficients: specific hydraulic permeability (L_p), solute permeability (P_s) and reflection coefficient (σ) (Hidalgo et al., 2013).

The solution flux (J_v) and solute flux (J_s) can be described as follow:

$$J_v = L_p(TMP - \sigma\Delta\pi) \quad (\text{Eq. 2.1})$$

$$J_s = P_s.\Delta C + (1 - \sigma)J_v C \quad (\text{Eq. 2.2})$$

Where J_v and J_s are the solvent flux and the solute flux, respectively ($\text{L.m}^{-2}.\text{h}^{-1}$).

TMP is the membrane transmembrane pressure, bar.

$\Delta\pi$ is the osmotic pressure differences between each side of the membrane, bar.

$\Delta\pi = \nu.R.T.\Delta C$ in which ν dimensionless Van't Hoff factor ($\nu=2$ for sodium lactate); R is universal gas constant, $\text{J.mol}^{-1}.\text{K}^{-1}$; T is absolute temperature, K;

ΔC is the difference of the concentration of solute i on the surface membrane (C_m) and the permeate solution (C_p), $\Delta C = C_m - C_p$, M,

C is solute concentration in feed, M.

L_p is the hydraulic permeability to pure water, $\text{L.m}^{-2}.\text{h}^{-1}.\text{bar}^{-1}$.

σ is the reflection coefficient, a measure of the degree of selectivity of the membrane.

2.2.1 Hydraulic/ water permeability, L_p

From the flux of water ($J_{v,w}$) is calculated by $J_{v,w} = L_p(TMP - \sigma\Delta\pi) = L_p\Delta P_e$ (Eq. 2.3) where $\Delta P_e = TMP - \sigma\Delta\pi$ is effective pressure driving force, N.m^{-2} and the flux of water due to the virgin NF membrane at the high pressure can be assumed

as same as the water volume of permeate, therefore, therefore, the hydraulic

$$\text{permeability } L_p \text{ is } L_p = \frac{J_{v,w}}{\Delta P_e} = \frac{V_w}{\Delta P_e} \quad (\text{Eq. 2.4})$$

2.2.2 Membrane pore size

Determination of an effective pore size is the significant step in the membrane characterization process. The rate pore size for nanofiltration is usually a molecular weight cut off (MWCO) in Dalton. MWCO is nominal ratings based on the ability to retain more than 90% of a solute of a known molecular weight. The pore size and MWCO are important parameters for membrane quality and membrane transport mechanisms. They allow an appropriate membrane process to be chosen to achieve specific separation and purification goals.

The relative between the radius (r_p) in nm and MWCO in kDa of membrane is as follow (Guo & Santschi, 2007):

$$r_p = 1.3(MWCO)^{0.341} \quad (\text{Eq. 2.5})$$

With fixed r_p , the value for $\Delta x/A_k$ can be calculated as following equation:

$$L_{p,w} = \frac{r_p^2}{8\mu_w(\Delta x/A_k)} \rightarrow \frac{\Delta x}{A_k} = \frac{r_p^2}{8\mu_w L_{p,w}} \quad (\text{Eq. 2.6})$$

Where r_p is the average membrane pore radius, m.

μ is water viscosity within pores, N.s.m⁻².

Δx is membrane thickness, m.

A_k is porosity, dimensionless.

The parameter of characterization of Desal-DK membranes manufactured by GE-Osmonics was be found by Y. Roy et al., the pore radius was obtained at 0.45 nm and the active layer thickness to porosity ratio ($\Delta x/A_k$) at 3 μ m when characterized by

glucose (Roy et al., 2015). In this study, these results from the characterization of Desal – DK membranes were used for further modeling step.

2.2.3 The reflection coefficient (σ) and the solute permeability (P_s) from Spiegler-Kedem model

Membrane is divided into parallel segments of perfectly semipermeable (A) and entirely non-selective areas (B) (Ahmed, 2013).

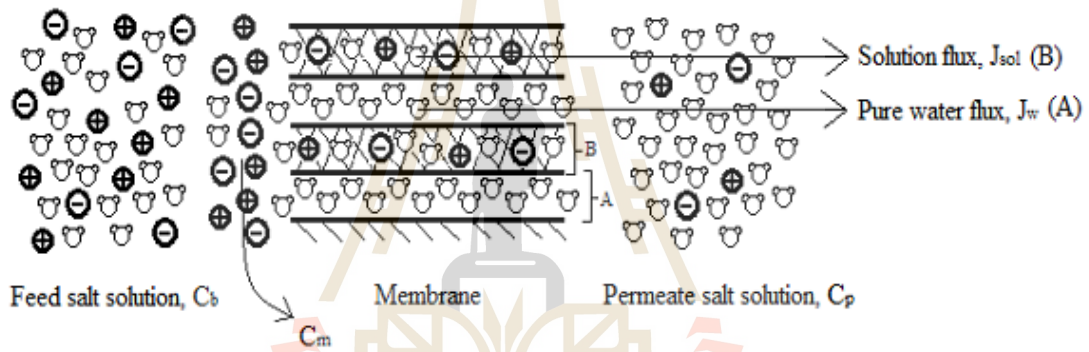


Figure 2.6 Schematic representation of a NF membrane.

Spiegler and Kedem proposed the relationship between the real rejection R_{real} and the solution flux, J_v . In the case of using a high crossflow velocity of feed flux, the concentration polarization effect is eliminated. The real rejection R_{real} is assumed to be equal to the observed rejection, R_{obs} (Kim et al., 2012):

$$R_{real} = R_{obs} = 1 - \frac{C_p}{C_f} = 1 - \frac{1-\sigma}{1-\sigma e^{-\frac{1-\sigma}{P_s} J_v}} = \frac{\sigma(1-F)}{1-\sigma F} \quad (\text{Eq. 2.7})$$

Where C_p is the permeate concentration of lactate, M.

C_f is the feed concentration of lactate, M.

With $F = e^{-\frac{1-\sigma}{P_s} J_v}$

From equation (Eq. 2.7), the follow equation can be obtained:

$$\frac{R_{obs}}{1-R_{obs}} = \frac{\sigma}{1-\sigma} (1 - F) = \frac{\sigma}{1-\sigma} \left(1 - e^{-\frac{1-\sigma}{P_s} J_v}\right) \quad (\text{Eq. 2.8})$$

With $A = \frac{\sigma}{1-\sigma}$ and $B = \frac{1-\sigma}{P_s}$, Eq. 2.8 can be rewritten as:

$$\frac{R_{obs}}{1-R_{obs}} = A(1 - e^{-B \cdot J_v}) \quad (\text{Eq. 2.9})$$

The two parameters, A and B from the previous equation can be obtained using the permeation/rejection data for the solvent and the solute. These values can then be used to calculate the reflection coefficient (σ) and the solute permeability (P_s), thus giving more insight into the convective and diffusive flux of transport mechanism. Obviously, the convective contributions will be dominant when the asymptotic solute rejection values are low. This has been also pointed out by Gilron and associates in their work and they suggested that the convective transport of the solute in such cases could not be neglected. Thus, the above treatment could be easily extended to non-aqueous systems. The P_s and σ values can be correlated with the different solute/solvent properties and can then be used as a predictive tool for extending it to different systems (Bhanushali, 2002).

2.3 Modeling of pervaporation-assisted esterification

2.3.1 Process model – Simulation

Process model is a relation between “outputs” and “inputs” (feed conditions, design parameters, and process adjustable parameters) in view of (i) scale-up from lab to industrial scale, (ii) prediction of process dynamics and (iii) optimization of operating conditions (Rodrigues & Minceva, 2005). There are several supported software that are helped to model and simulate for the comprehensive process as well

as for each unit operation, for instance, Aspen HYSYS, Aspen Plus, EMSO and Aspen Plus is arguably the most popular.

Aspen Plus, basically a sequential modular simulator, has grown considerably and has many advanced functionalities, such as links to a variety of specialized software, such as detailed heat exchanger design, dynamic simulation, batch process modeling, and many additional functions. It also has a facility for using an equation-based approach in some of its models, which permits convenient use of design specifications in process modeling (Schefflan, 2011).

When building a simulation, it is important to make certain that the properties of pure components and mixtures are being estimated appropriately. Consequently, selecting the proper method for estimating properties is one of the most important steps that will affect the rest of the simulation. In Aspen Plus, the estimation methods are stored in what is called a "Property Method". Among the available classes of property methods, phase equilibrium calculation is one of the key calculations performed for several unit operations such as flash tanks, distillation columns, extraction in process simulations. Generally, with the non-ideal liquid of organic acid mixture, the choice to calculate fugacity of phase equilibrium is activity coefficient models which include non-random two-liquid (NRTL), Wilson, Van Laar, UNIFAC, UNIQUAC, Flory Huggins, Electrolyte NRTL, and Scatchard Hildebrand models.

As the NRTL model was the most successful to describe the reaction constant, it was decided to use this model to calculate the activities in the remainder of this study (Schwarzer, 2006). NRTL is an activity coefficient model that bases on the local composition theory of Wilson and the two-liquid solution theory of Scott. The model provides the precise representation of highly non-ideal VLE and LLE systems.

The NRTL activity coefficient (γ) expression for a binary system is shown in the following equation:

$$\ln\gamma_i = \frac{\sum_{j=1}^n x_j \tau_{ji} G_{ji}}{\sum_{k=1}^n x_k G_{ki}} + \sum_{j=1}^n \frac{x_j G_{ij}}{\sum_{k=1}^n x_k G_{kj}} \left(\tau_{ij} - \frac{\sum_{m=1}^n x_m \tau_{mj} G_{mj}}{\sum_{k=1}^n x_k G_{kj}} \right) \quad (\text{Eq. 2.10})$$

With τ_{ij} and G_{ij} defined as follow: $G_{ij} = \exp(-\alpha_{ij} \tau_{ij})$; $\tau_{ij} = a_{ij} + \frac{b_{ij}}{T}$

Where a_{ij} and b_{ij} are the binary parameters of the related components for NRTL model (Appendix B), α is the non-randomness factor in the mixture, and T is the mixture temperature in K.

NRTL is not only the first choice for a multi-component organic-water system but also is a recommended method for highly non-ideal chemical systems with regressed vapor pressure. Especially, NRTL is suitable for polar mixtures with a pressure lower than 10 bars and when it has an interaction parameters data. Hence, NRTL is a suitable method for this process.

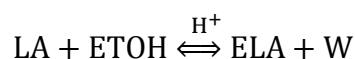
2.3.2 Esterification of lactate salt

There are several kinetics studies of esterification of lactic acid with alcohol. Troupe and Dimilla investigated the esterification reaction between lactic acid and ethanol using sulfuric acid as a homogeneous catalyst (Dimilla, 1957). Effect of reaction temperature, amount of catalyst loading and initial reactant molar ratio were examined. It was found that temperature and catalyst loading did not have a great effect on equilibrium constant of the reaction but the initial reactant molar ratio did (Dimilla, 1957; Zhang et al., 2015). However, the longer period was required to reach reaction equilibrium when the catalyst loading decreased. Besides that, the esterification of lactate salt that directly obtained from lactic acid production, such as ammonium

lactate, has been investigated. In 1952, Filachione and Costello studied the production of lactic esters by reaction of ammonium lactate with various alcohols (Filachione & Costello, 1952). In their study, primary alcohols were observed showing higher conversion to ester than secondary alcohols did. They also found that the reaction proceeded through dissociation of the lactate salts (ammonium lactate) to salts (ammonia) and lactic acid and that the latter undergoes esterification with primary alcohol (n-butanol). The increasing of alcohol to lactate salt ratio would enhance the formation of ester form. Catalyst, such as sulfuric acid, boric acid, basic aluminum acetate, as well as silica gel, helped to reduce the reaction time by approximately one-half but did not greatly affect the conversion.

2.3.3 Kinetic equation of esterification reaction

Esterification is a reaction between a carboxylic acid (R-COOH) and an alcohol (R-OH) to form an ester and water as the reaction products. This reaction is reversible and the reaction conversion is generally limited by chemical equilibrium. To enhance the equilibrium conversion of the reaction, Le Chatelier's principle was used. This is normally done by using an excess amount of one of the reactants or continuously removing one of the products from the reaction mixture (Kumar and Mahajani, 2007). In addition, catalysts are always used to enhance the reaction rate. The esterification of lactic acid (LA) with ethanol (ETOH) to produce ethyl lactate (ELA) and water (W) can be written as:



For that esterification reaction, when the excess of ethanol is used and the selectivity of the desired production is 100%, the yield of ethyl lactate is equal to the conversion of lactic acid, X_{LA} (Xuehui & Lefu, 2001).

$$X_{LA} = \frac{N_{ELA}}{N_{LA0}} = 1 - \frac{N_{LA}}{N_{LA0}} \quad (\text{Eq. 2.11})$$

The reaction composition in the feed, at the $t = t_1$ and at equilibrium was shown in the Table 2.2.

Table 2.2 Composition of the reaction mixture of batch esterification.

Time (h)		Molar quantity (mole)			
		LA	ETOH	ELA	W
Feed	$t = 0$	N_{LA0}	$R_1 N_{LA0}$	0	$R_2 N_{LA0}$
At time t_1	$t = t_1$	$N_{LA0}(1-X_{LA})$	$N_{LA0}(R_1-X_{LA})$	$N_{LA0}X_{LA}$	$N_{LA0}(R_2+X_{LA})$
Equilibrium	$t \rightarrow \infty$	$N_{LA0}(1-X_{LAe})$	$N_{LA0}(R_1-X_{LAe})$	$N_{LA0}X_{LAe}$	$N_{LA0}(R_2+X_{LAe})$

Where N_{LA0} is initial molar quantity of lactic acid in feed, mole.

N_{ELA} is molar quantity of ethyl lactate produced by esterification, mole.

R_1 and R_2 are ratio of the initial molar quantity of ethanol and water to lactic acid respectively.

X_{LA} is yield of the ester or lactic acid conversion, $X_{LA} = 1 - \frac{N_{LA}}{N_{LA0}}$

The lactic acid esterification with ethanol is a reversible second order reaction and the reaction rate of it can be expressed in equation

$$-r_{LA} = \frac{dX_{LA}}{dt} = k(C_{LA}C_{EtOH} - \frac{C_{ELACW}}{K_e}) \quad (\text{Eq. 2.12})$$

$$Ke = \frac{C_{ELA,e}C_{W,e}}{C_{LA,e}C_{EtOH,e}} \quad (\text{Eq. 2.13})$$

Where r_{LA} is reaction rate of lactic acid, s^{-1} .

C_i is concentration of component i at time t, mol.L^{-1} .

$C_{i,e}$ is concentration of component i at equilibrium, mol.L^{-1} .

k is reaction rate constant, s^{-1} ; $k = k_0 \exp\left(-\frac{E_A}{RT}\right)$.

k_0 is pre-exponential constant, s^{-1} .

R is the gas constant, $\text{J}\cdot\text{mol}^{-1}\cdot\text{K}^{-1}$.

T is temperature, K^{-1} .

E_A is activation energy, $\text{J}\cdot\text{mol}^{-1}$.

Ke is equilibrium constant.

X_{LA} is conversion of lactic acid, $X_{LA} = 1 - \frac{C_{LA}}{C_{LA,0}}$

C_{LA} is concentration of lactic acid at time t, mol.L^{-1} .

$C_{LA,0}$ is initial concentration of lactic acid, mol.L^{-1} .

In order to account for the non-ideality of the solution, the reaction rate can be expressed in term of activity instead of concentration as in following equations:

$$\begin{aligned} -r_{LA} &= \frac{dX_{LA}}{dt} = k \left(a_{LA} a_{EtOH} - \frac{a_{ELA} a_W}{Ke} \right) \\ &= k (\gamma_{LA} \gamma_{EtOH} x_{LA} x_{EtOH} - \gamma_{ETLA} \gamma_W \frac{x_{ELA} x_W}{Ke}) \end{aligned} \quad (\text{Eq. 2.14})$$

$$Ke = \frac{a_{ELA,e} a_{W,e}}{a_{LA,e} a_{EtOH,e}} = \left(\frac{x_{ELA,e} x_{W,e}}{x_{LA,e} x_{EtOH,e}} \right) \left(\frac{\gamma_{ELA,e} \gamma_{W,e}}{\gamma_{LA,e} \gamma_{EtOH,e}} \right) \quad (\text{Eq. 2.15})$$

Where a_i is the activity of component i.

$x_{i,e}$ is mole fraction of component i at equilibrium.

γ_i and $\gamma_{i,e}$ are activity coefficient and equilibrium activity coefficient of component i, respectively. The γ_i and $\gamma_{i,e}$ were determined by the general equation (Eq. 2.10)

in the mixture and the binary parameter of the LA, ELA, ETOH and W for NRTL that was shown in Appendix B.

The equilibrium is a word that means to a static condition in which absence of change. In thermodynamics, it means not only the absence of change but the absence of any tendency toward change on a macroscopic scale. Therefore, a system at equilibrium exists under conditions such that no change in state can occur. Because any tendency toward change is caused by a driving force of one kind or another, the absence of such a tendency indicates also the absence of any driving force. Hence for a system at equilibrium, all forces are in exact balance. Whether a change actually occurs in a system, not at equilibrium depends on resistance as well as one driving force. In many systems subject to appreciable driving forces change occurs at a negligible rate, because the resistance to change is very large (Smith et al., 2005).

When K_1 is equal to $k\gamma_{LA}\gamma_{ETOH}$, the rate of reaction can be written as

$$\frac{dX_{LA}}{dt} = \frac{K_1}{(1+R_1+R_2)^2} \left[(1 - X_{LA})(R_1 - X_{LA}) - \frac{X_{LA}}{Ke} (R_2 + X_{LA}) \right] \quad (\text{Eq. 2.16})$$

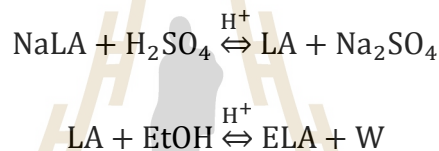
The reaction rate constant (k), equilibrium constant (Ke) and reaction rate were determined from the experiments by using program Mathcad (Appendix D). The fitting between the experimental and predicted profile was confirmed by using the mean relative deviation (MRD), defined by equation 2.21.

$$MRD = \frac{1}{n_{exp}} \left(\sum n_{exp} \left| \frac{x_{i,exp} - x_{i,cal}}{x_{i,exp}} \right| \right) \times 100\% \quad (\text{Eq. 2.17})$$

The flow chart of simulation and the computer program were shown in Appendix D. The relationship between the reaction rate constant and reaction temperature is expressed by Arrhenius equation

$$k = k_o \exp\left(-\frac{E_A}{RT}\right) \quad (\text{Eq. 2.18})$$

In our case, the process of lactic acid purification from fermentation broth was concerned esterification of the lactate salts in ethanol. After centrifugation (5000 rpm, 15 minutes) for separating the cell, nanofiltration for removing the low molecule compound, protein, impurities, and color. Excess water was evaporated from clear broth until it reached 50 Brix. The kinetic of the process was presented for sodium lactate (NaLA). The sodium lactate reacted with sulfuric acid to produce lactic acid (LA) and sodium sulfate. After that free lactic acid reacted with ethanol forming ethyl lactate with unreacted H_2SO_4 . The sodium sulfate was insoluble in ethanol, precipitates and was taken out by filtration.



2.3.4 Pervaporation performance

Generally, the permeation flux of pervaporation is a function of component concentration in feed and temperature of the system. The effectiveness of pervaporation or pervaporation performance of membrane is mainly evaluated in term of pervaporation flux and separation factor (membrane selectivity). For simplification, the water/organic selectivity in the quaternary mixture (LA, ETOH, ELA, W) through the pervaporation membrane was assumed that is equal to the selectivity observed in binary water/organic mixtures.

- The performance of pervaporation flux

The transport of component across the membrane in pervaporation is described by solution desorption model that results from these processes in series: (i) diffusion of the component through the liquid boundary layer to the membrane surface,

(ii) sorption/diffusion into the membrane, (iii) transport through the membrane and (iv) diffusion through the vapor phase boundary layer into the bulk of the permeance (Jyoti et al., 2015). In the mathematic modeling of pervaporation transport, the resistance offered by the boundary layer at the vapor phase is negligible can be assumed therefore, the concentration of the solute is nearly zero at the permeate at a low vacuum. However, at the higher pressure in permeance side, this resistance will be increase and cannot be ignored. The set of transport equation of pervaporation was identified in the review article of Ghoshna Jyoti and associates (Jyoti et al., 2015) in two term: the transport through the boundary layer on the liquid feed side of the membrane, $J_a^{bl} = k_l \rho (C_f - C_{i,l})$ and membrane transport, $J_o^m = k_i \rho (C_{m,l} - C_{m,g})$. Therefore, the overall organic flux can be described by the following equation:

$$J_i = K_{ov} \rho (C_f - C_p) \quad (\text{Eq. 2.19})$$

Where k_l is the boundary layer mass transfer coefficient on the liquid side.

ρ is molar density of liquid, kg.m^{-3} .

C_f and $C_{i,l}$ are the organic concentration at the liquid-membrane interface and feed side, respectively.

k_i is the membrane mass transfer coefficient.

$C_{m,l}$ and $C_{m,g}$ are the organic concentration at the membrane in liquid phase and vapor phase, respectively.

The subscripts f and p refer to feed and permeate.

It can be expressed in terms of partial vapor pressure, concentration of i or fugacity as:

$$J_i = Q_{ov,i} A (p_{l,i} - p_{g,i}) = K_{ov,i} A (C_{l,i} - C_{g,i}^*) \quad (\text{Eq. 2.20})$$

$$J_i = Q_{memb,i} (f_i^{feed} - f_i^{permeate}) \quad (\text{Eq. 2.21})$$

where J_i is the flux of across the membrane, $\text{kg}\cdot\text{m}^{-2}\cdot\text{s}^{-1}$.

$Q_{ov,i}$ and $K_{ov,i}$ are the overall mass transfer coefficient of i in terms of vapor pressure and liquid concentration, respectively.

A is the membrane area, m^2 .

$p_{l,i}$ and $p_{g,i}$ are partial vapor pressure of i in the liquid side and in vapor side, respectively, bar.

$C_{l,i}$ and $C_{g,i}^*$ are the concentration of i in the liquid and in the liquid which would be in equilibrium with vapor, $\text{g}\cdot\text{L}^{-1}$.

$Q_{memb,i}$ is the apparent mass transfer coefficient, $\text{mole}\cdot\text{m}^2\cdot\text{h}^{-1}\cdot\text{bar}^{-1}$.

$f_i^{feed} = \gamma_i x_i^{feed} p_i^o(T^{feed})$ (Eq. 2.22) and $f_i^{permeate} = y_i P_p$ (Eq. 2.23) are fugacity of component i in the feed side and permeate side.

p_i^o is the saturation vapor pressure of compound i at feed temperature T^{feed} which was estimate by the Antoine equation, bar and it is presented in Appendix A, bar.

γ_i is activity coefficient (calculated by using NRTL model).

P_p is total pressure on the permeate side, bar.

x_i and y_i are the liquid mole fraction of component i in the feed side and permeate side, respectively.

Substituting (Eq 2.22) and (Eq 2.23) to (Eq 2.21), the solution-diffusion model which provides the transport for the permeation molar flux of a component through the membrane can be derived.

$$J_i = Q_{memb,i} (\gamma_i x_i^{feed} p_i^o(T^{feed}) - y_i P_p) \quad (\text{Eq. 2. 24})$$

This model was successfully applied in the description of solvent dehydration using pervaporation membrane (Ma et al., 2009). The permeance of

component i through membrane, $Q_{memb,i}$, was determined by an Arrhenius-type equation (Pereira, 2009).

$$Q_{memb,i} = Q_{memb,0} \exp\left(\frac{-E_{perm,i}}{RT}\right) \quad (\text{Eq. 2.25})$$

where $Q_{memb,0}$ is the pre-exponential factor, $E_{perm,i}$, is the activation energy of permeation, which is a combination of activation energy of diffusion and the heat of adsorption on the membrane, T is the absolute temperature (K) and R is the ideal gas constant.

- Membrane selectivity

The value of separation factor shows the selectivity of membrane. The higher value of separation factor is determined, the higher effectively selectivity can be obtained. When describing the selectivity of a membrane for separation of a mixture, the separation factor is defined as:

$$\alpha = \frac{y_i/y_j}{x_i/x_j} = \frac{y_i/(1-y_i)}{x_i/(1-x_i)} \quad (\text{Eq. 2.26})$$

where x_i and x_j are the liquid mole fraction of component i and j on the feed side and y_i and y_j are the vapor mole fraction of component i and j on the permeate side.

The generalized parameter F_i is defined as: $F_i = \frac{J_i A/V}{r_i}$ (Eq. 2.27)

where F_i is a dimensionless parameter that represents the ratio of the removal rate of species i due to pervaporation to the overall reaction rate.

2.3.5 Kinetic of esterification-pervaporation coupled

The combination of pervaporation and reactor for esterification is caused the change of concentration of each component are different from the conversion of them in a batch reactor as the following table:

Table 2.3 Composition of the reaction mixture of pervaporation-assisted esterification.

Time (hr)		Molar quantity (mole)			
		LA	ETOH	ELA	W
Feed	$t = 0$	N_{LA0}	$R_1 N_{LA0}$	0	$R_2 N_{LA0}$
At time t_1	$t = t_1$	$N_{LA0}(1-X_{LA})$	$N_{LA0}(R_1-X_{LA})$	$N_{LA0}X_{LA}$	$N_{LA0}(R_2+Y)$
Equilibrium	$t \rightarrow \infty$	$N_{LA0}(1-X_{LAe})$	$N_{LA0}(R_1-X_{LAe})$	$N_{LA0}X_{LAe}$	$N_{LA0}(R_2+Y_e)$

where Y is molar the ratio of the molar quantity of water produced by esterification and remained in mixture after pervaporation, $\frac{N_w}{N_{LA0}}$.

J_i is component flux through pervaporation, which water flux J_w could be calculated as $J_w = N_{LA0}(X_{LA} + R_2) - N_{LA0}(Y + R_2)$ (Eq. 2.28), mole.

The material balance was also applied for expressing the mole fraction of components in mixture as follow: $\frac{dx_i}{dt} = r_i - \frac{J_i A}{\sum N}$ (Eq. 2.29)

where x_i is mole fraction of component i; J_i is the permeation flux, $\text{mol.m}^{-2}.\text{h}^{-1}$.

r_i is the reaction rate of each component, has a negative sign of reagent and positive of product species.

$\sum N$ equals total initial mole minus the mole that was removed by pervaporation, mole.

CHAPTER III

MATERIALS AND METHODS

3.1 Materials

A – 300L of lactic acid fermentation broth was prepared by Asst. Prof. Dr. Sureelak Rodtong (Suranaree University of Technology, Thailand) using *Lactobacillus* sp. SUT.W73 and cassava starch as the main substrate. Chemicals used for media preparation will be yeast extract 10 g.L⁻¹, tryptone 2.5 g.L⁻¹, soy protein 2.5 g.L⁻¹, ammonium sulfate 1 g.L⁻¹, potassium hydrogen phosphate 0.1 g.L⁻¹, magnesium sulfate 0.3 g.L⁻¹, manganese sulfate 0.3 g.L⁻¹, iron (II) sulfate 0.03 g.L⁻¹, calcium chloride 0.1 g.L⁻¹ and cassava starch 110 g.L⁻¹. During fermentation, pH was automatically maintained at 6.8 by the addition of 2 M NaOH solution.

Lactic acid (99 %w/w), sodium hydroxyl (99 %w/w), sulfuric acid (96 w/w%) were obtained from Sigma Aldrich (Singapore). Absolute ethanol (99.8 %w/w) was produced in our laboratory (Biofuel Production from Biomass Research Unit, School of Biotechnology, Suranaree University of Technology, Thailand). Amberlyst 15-E was supplied by Fluka (United Kingdom).

3.2 Methods

3.2.1 Nanofiltration operation

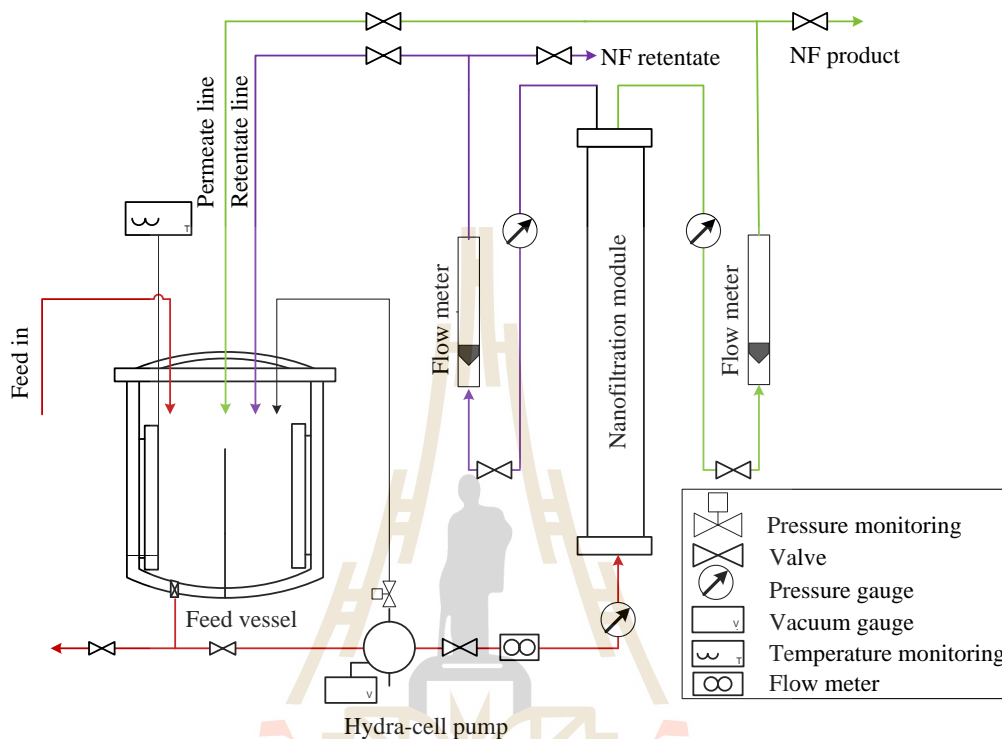


Figure 3.1 Flow diagram of nanofiltration operation.

NF experiments were conducted using the spiral wound membrane DK4040F1021 (GE Osmonics, DK series, USA) in the cross flow system depicted in Fig. 3.1. This module has an average MWCO of 300 Dalton and effective membrane area was 6.0 m^2 . The fermentation broth was centrifuged (Sorvall Legend XFR, Thermofisher, USA) at 5000 rpm within 15 minutes before being contained in the feed tank that was pumped from the tank into the membrane module system. The concentration of sodium lactate was 34 g.L^{-1} . The feed temperature was maintained approximately at $30 \text{ }^\circ\text{C}$ by using a thermostat and the feed flow rate was 1.28 m.s^{-1} . A high-pressure pump (G-20 Models with metallic pumping head, Hydra cell) was used

to circulate the feed solution in the cross-flow filtration batch mode with both permeate and retentate recycled to the feed tank to maintain constant feed conditions.

The flow rate of permeate was measured by collecting the accumulated volume against the time. During the NF process and for each pressure, one milliliter and a minimum volume (~10 mL) of the permeate collected respectively for analysis. All flux and rejection measurements were performed in duplicate as a minimum. The remaining volume of permeate was recycled to the feed vessel. To determine the reflection coefficient (σ) and the solute permeability (P_s), the NF experiment was operated with variable data of sodium lactate from 118 mM to 1245 mM at the constant TMP was 10.3 bar. Pure water flux (J_w) was then measured at various trans-membrane pressures (ranging from 1.65 to 4 bar) to evaluate the pure water hydraulic permeability ($L_{p,w}$). The volume concentration ratio (VCR) value was calculated as the ratio of the initial volume of feed and volume of retentate. The membrane used in the previous experiment was washed with water, NaOH, and H₃PO₄ solutions until the initial water flux was observed (Lubsungneon, 2014).

3.2.2 Preparation of sodium lactate from fermentation broth

After pretreatment step (centrifugation and nanofiltration), fermentation broth was removed excess water by using rotary evaporation (RV 10, IKA, Germany) at 65 °C and 1 mbar until it reached the concentration at 185.6 g.L⁻¹ and 385 g.L⁻¹ in order to decrease interference of water in the esterification reaction and acidified by using 1M of sulfuric acid until reaching pH = 2 (Daengpradab, 2014). Sulfuric acid was not only the reagent for dissolving sodium lactate but also the catalyst for esterification reaction. The solubility of sodium lactate in the solution was observed and lactic acid concentration in the solution was analyzed by HPLC.

3.2.3 Kinetic Study of Esterification

Experiment for measuring kinetic parameters of sodium lactate esterification (185.6 g.L^{-1} and 385 g.L^{-1}) was performed from fermentation-derived sodium lactate with ethanol at atmospheric pressure in 500 mL glass reactor using 1.5 v/v% sulfuric acid as homogeneous catalyst. The reaction was carried out at varied initial feed molar ratio of ethanol to lactic acid 3:1 at reaction temperature from 45, 55, 65 and 75 °C. The impeller was maintained at 350 rpm (Khunnonwao, 2010). The conversion of lactic acid, ethanol, the production of ethyl lactate and water were analyzed by HPLC, GC, and Fluka Hydranal®-Moisture Test Kit at regular interval time for 6 hours.

3.2.4 Modeling of pervaporation-assisted esterification

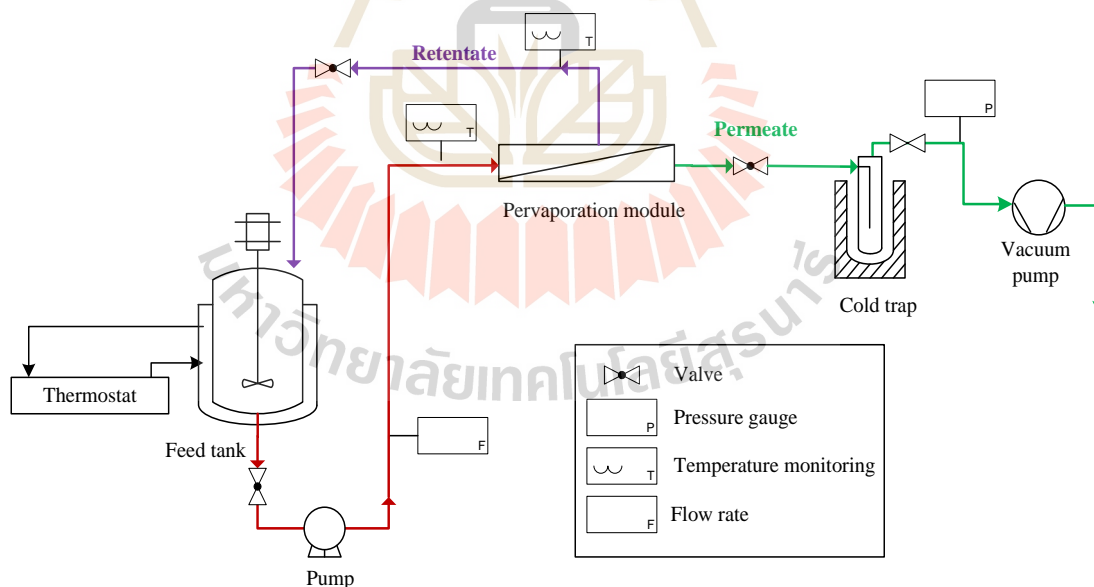


Figure 3.2 Pervaporation-assisted esterification set-up.

The set-up line used for this experiment was shown in Fig. 3.2. A – 500 mL stirred reactor was connected with a pervaporation module SS316 PVM-025-1

working under vacuum condition. The membrane was a ceramic mono channel tube 25 cm with dense Hybrid silica AR top layer which has 0.005 m² membrane surface (Pervaptech BV, Germany). The membrane area to initial reaction volume ratio (A/V) was kept at 23.8 m⁻¹. The temperature of the feed liquid mixture was kept constant by using a thermostat (Sartorius, Germany). After going through membrane, permeate was passed a cold trap filled with nitrogen liquid to ensure that all permeates were fully condensed and collected under vacuum pressure (was maintained at 10 mbar). In pervaporation processes, concentration polarization was generally assumed to be of minor importance. Hence, the feed flow rate across the membrane was chosen high enough to avoid mass transfer resistance from the bulk liquid phase to the feed membrane interface (35 L.h⁻¹), the impeller was maintained at 350 rpm (Khunnonwao, 2010). The system was first prepared to reach steady state by keeping the feed mixture in the membrane module overnight under a slight vacuum pressure. The product of reactor before going to pervaporation module was collected and measured each compound concentration and calculated of kinetic parameters.

3.3 Analysis

3.3.1 Cell dry weight

Cell dry weight (CDW) was analyzed by using a spectrophotometer (Bioespectro SP 220, China) at the wavelength of 600 nm (OD₆₀₀). CDW was calculated from the calibration curve between OD₆₀₀ against CDW (Boontawan, 2011).

3.3.2 Protein concentration

Protein concentrations were analyzed by Bradford method. 100 μ L sample was prepared with 5mL Bradford reagent and then measured by a spectrophotometer (Bioespectro SP 220, China) at 595 nm (OD_{595}) (Lubsungneon, 2014).

3.3.3 Ion concentration

Mineral ions were measured by a Dionex ion chromatograph system (ICS 5000, Thermo Scientific, USA) equipped with a CD20 conductivity detector.

3.3.4 Gas Chromatography (GC)

The quantities of ethyl lactate that was produced from esterification reaction, were analyzed by Gas chromatography using column DB-WAX UI, 30m \times 0.53mm \times 0.25 μ m (p/n 122-7032UI) with flame ionization detector (FID) using helium (99.999% purity, 35 $\text{cm}\cdot\text{s}^{-1}$) as a carrier gas. The inlet was controlled with split ratio 20:1. Initially, the temperature of the oven was held at 50 $^{\circ}\text{C}$ for 3 minutes, before it was increased to 240 $^{\circ}\text{C}$ at a rate of 10 $^{\circ}\text{C}\cdot\text{min}^{-1}$ and held for 1 minute. 1 μ m of each samples were injected automatically by CP-3800 auto-sampler.

3.3.5 High Pressure Liquid Chromatography (HPLC)

The concentration of organic acid was determined using a high performance liquid chromatography system (Agilent Technology, USA) equipped with an UV detector set to 210 nm. An ion exclusion column (Aminex HPX-87H, Biorad,

Hercules, CA) was employed with an oven temperature of 55 °C using 10 mN H₂SO₄ as a mobile phase at a flow rate of 0.4 mL.min⁻¹. The samples were diluted with water and injected in amount of 0.1 µL (Boontawan, 2011).

3.3.6 Kinetic calculation

The equilibrium constant (Ke) was calculated from the experiment results while the reaction rate constant (k) of reversible second order reaction between sodium lactate esterification, and ethanol in two cases, batch esterification and esterification pervaporation reaction, were calculated by using Mathcad program (Appendix D).



CHAPTER IV

RESULTS AND DISCUSSION

4.1 Modeling of nanofiltration membrane for sodium lactate from fermentation broth.

4.1.1 Hydraulic/ water permeability, $L_{p,w}$.

The results of the permeate and the effects of NF was depended to the property of membrane that was used in the process. Therefore, it is important to determine hydraulic permeability with DI water and then calculate the other parameter for NF model.

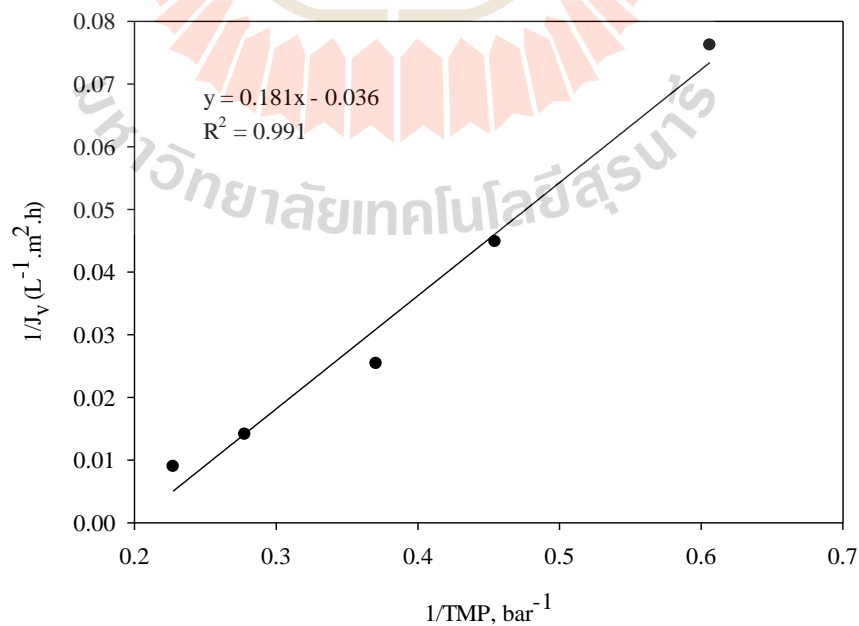


Figure 4.1 Pure water permeability experiment for NF under different TMP, bar.

As shown in figure 4.1, the hydraulic permeability which was obtained based on the effective pressure driving force and the flux of water due to the virgin NF membrane was shown. It was indicated by the cumulative permeate mass of DI water as a function of time at different pressures. With the transmembrane pressure increasing trend, permeate flux of water rose automatically (Markovic et al., 2006). Moreover, as expected, the flux of pure water has a linear relationship to transmembrane pressure with high regression $R^2 = 0.991$. Due to the given formula in section 2.2.1 (Eq. 2.3) and slope of the plot in Fig. 4.1, the water permeability of this NF module was equal to the inversion of slope and was $5.539 \text{ L.m}^{-2}.\text{h}^{-1}.\text{bar}$. This result felt in the range of permeability values for NF membranes found in the literature ($10 - 66 \text{ L. m}^{-2}.\text{h}^{-1}.\text{MPa}^{-1}$) (Oliveira, 2013) and ($1.5 - 30 \text{ L.m}^{-2}.\text{h}^{-1}.\text{bar}^{-1}$) (Dach, 2008). The pure water permeability reflects the porous structure of the membrane. A constant value of pure water permeability as well as the linear dependence of the reversible pure water flux $1/J_v$ on the reverse pressure data ($1/\text{TMP}$), points to unchangeable membrane porosity (Košutić et al., 2006).

4.1.2 Mean reflection coefficient (σ) and solute permeability (P_s)

In order to determine solution flux, the reflection coefficient and solute permeability are required. Therefore, the NF experiments at different sodium lactate concentrations were performed and the results of sodium lactate rejection data as a function of initial lactate concentration were obtained and shown in Fig. 4.2.

According to this figure, at the same operating conditions, the value of permeate flux, as well as rejection of sodium lactate, were obtained with the decreasing trend with an increase of lactate concentration in the feed side. At higher concentration

of lactate (844 – 1245 mM), the flow rate data were approximate 9.885 – 23.529 L.m⁻².h⁻¹ replaced for the value around 16.807 – 38.824 L.m⁻².h⁻¹ obtained at low feed concentration (118 – 452 mM).

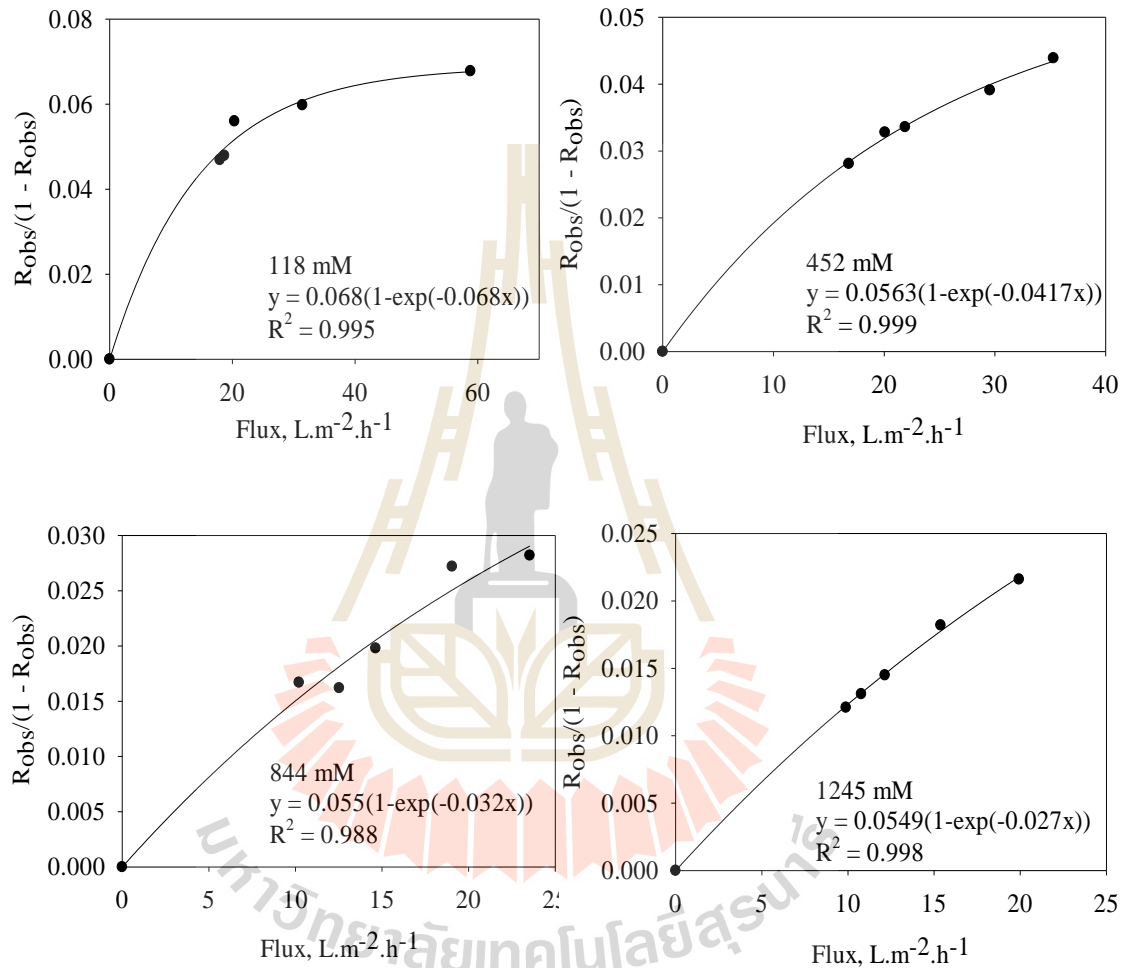


Figure 4.2 Lactate rejection as a function of solution flux at different lactate concentrations (118 – 1245 mM) at TMP = 10.3 bar, T = 30 °C, the experimental data were fitted by using the SK mode.

In addition, it can be seen in the figure is that lactate rejection reduced with the rise of feed concentration. The reason is that the increase in the osmotic pressure at the membrane surface as well as the shield effect of the cations on the membrane

charged groups becomes progressively stronger, a decrease on the membrane repulsion forces on the anions occurs, and then the water permeate flux and dissolved solids rejection decreases (Alsahy et al., 2013; Dach, 2008). Moreover, at low fluxes, the contribution of the diffusive transport of the ions through the membrane is relatively higher than the convective transport, resulting in a low rejection. With the increase in solvent flux with pressure, the convective transport dominates the ionic diffusion and rejection increases (Ahmed, 2013).

For the measurement of solution flux, the reflection coefficient (σ) and the solute permeability (P_s) need to be estimated. Therefore, the results of permeation experiments series that were performed in Fig. 4.2, were used to solve Eq. 2.9 in section 2.2.3. The corresponding estimated transport parameters were listed in Table 4.1.

Table 4.1 Mean reflection coefficient (σ) and solute permeability (P_s) for the studied membranes at the different sodium lactate concentration.

Concentration (mM)	A	B	σ	P_s (L.m ⁻² .h ⁻¹)
118	0.0690	0.0682	0.0645	4.121
452	0.0563	0.0417	0.0533	6.367
844	0.0549	0.0320	0.0520	8.196
1245	0.0533	0.0263	0.0506	9.866

According to the data in Table 4.1, the calculated σ declined whereas P_s increase when the lactate concentration in feed side was increased. These results were reasonably concordant with the changing trends that were reported in the studies of

Ahmed and Kim (Ahmed, 2013; Kim et al., 2012). The developing feed concentration led the depression of the permeate flux. At low fluxes, the contribution of the diffusive transport of the ions through the membrane was relatively higher than the convective transport, resulting in a low rejection, low solute permeability, and higher reflection coefficient. With the increase in solvent flux with pressure, the convective transport commands the ionic diffusion and rejection increases (Ahmed, 2013).

The reflection coefficient and solute permeability could be effectively related to the lactate concentration by using empirical power functions (Ahmed, 2013) and this relationship was determined as follow: $\sigma = 0.051C_f^{-0.107}$ ($R^2 = 0.954$) (Eq. 4.1) and $P_s = 32.394C_f^{0.421}$ ($R^2 = 0.998$) (Eq. 4.2).

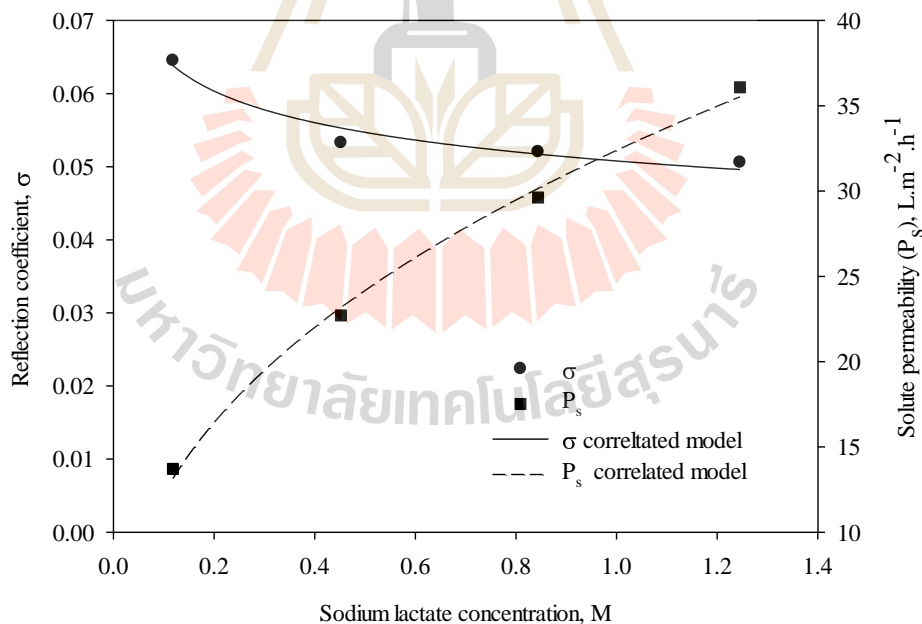


Figure 4.3 Reflection coefficient (σ) and solute permeability (P_s) as the function of lactate concentration; the curves were fitted by using a Freundlich adsorption isotherm.

In all the nanofiltration process, R_{obs} and J_v are required to be estimated from experimental data at different sodium lactate concentrations at a given operating pressure. The lactate rejection, R_{obs} was empirically represented as a function of its concentration by nonlinear regression (Kim et al., 2012) with an exponential function $R_{obs} = 0.014 + 0.061\exp(-1.739C_f)$ (Eq. 4.3) as following figure:

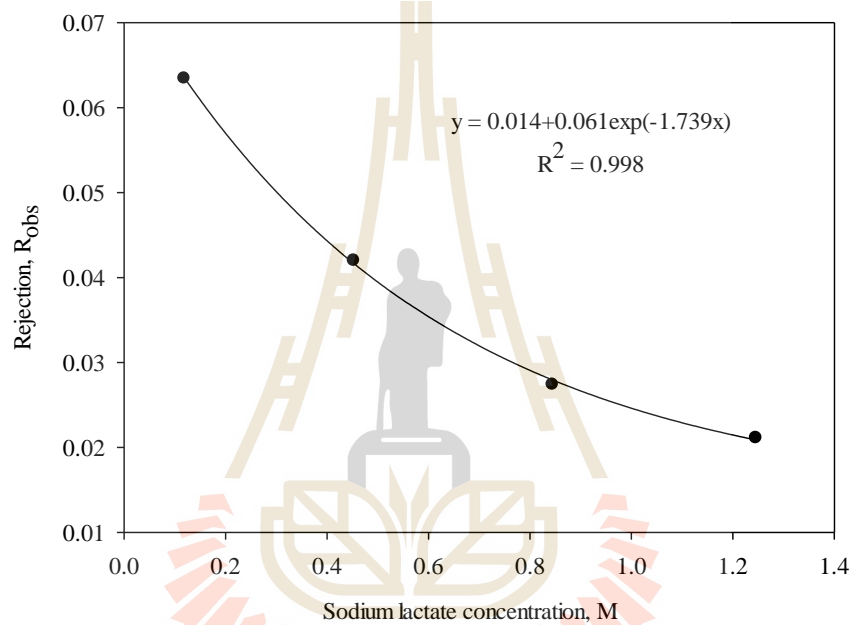


Figure 4.4 Nonlinear regression volume of R_{obs} as the function of lactate concentration at a constant operation pressure TMP = 10.3 bar.

4.1.3 Model validation and results

In this section, the IT model that was applied for simulating the nanofiltration performance was validated against the experimental results obtained with the free cell fermentation broth mentioned in section 3.2.1. Basing on the model parameters calculated from Eq (4.1), (4.2), (4.3) and (2.7), numerical calculations of solution permeate and sodium lactate rejection of single salt solution (A) and free-cell

lactic acid fermentation broth (B) were carried out. As the Fig. 4.5A, model prediction of sodium lactate profile as the function of solution permeate had the high agreement of the experiment performance with an average deviation of (MRD = 5.169%). Therefore, the success of the proposed model for NF process was confirmed.

The performance of lactate obtained from fermentation broth was also shown at Fig. 4.5B. This experiment was maintained at feed pressure TMP = 10.3 bar and temperature 30 °C to characterize the flux and lactate rejection during nanofiltration process. The permeate flux was dramatically reduced from 29.090 L.m⁻².h⁻¹ at initial time and then leveled off at 6.91 L.m⁻².h⁻¹ at VCR = 1.97. This significant downward trend was caused by the presence of the rapid deposition of macromolecules on the membrane surface (Lubsungneon, 2014) and the effect of the concentration polarization phenomenon (Matheswaran et al., 2007; Porter, 1990; Vela et al., 2008). Furthermore, the high selectivity of nanofiltration for organic salts was achieved which was induced the low retention of sodium lactate. The retention value was in the range of 0.043 and 0.099. The increasing of retention was obtained due to the decreasing of lactate concentrations in the feed side. Indeed, in such conditions, the retention of sodium lactate, which was negatively charged, results from the combination of steric effects and electrostatic interactions between the membrane and the solute. At low solute concentrations, electrostatic repulsions were predominant so that high retentions were obtained (Bouchoux et al., 2005). In contrast to the fermentation broth, the constant membrane flux and retention was indicated by proposed model at 30.411 and 0.047, respectively. These results were clearly explained due to the absence of macromolecules deposited on the membrane surface and the effect of the concentration polarization (Lubsungneon, 2014).

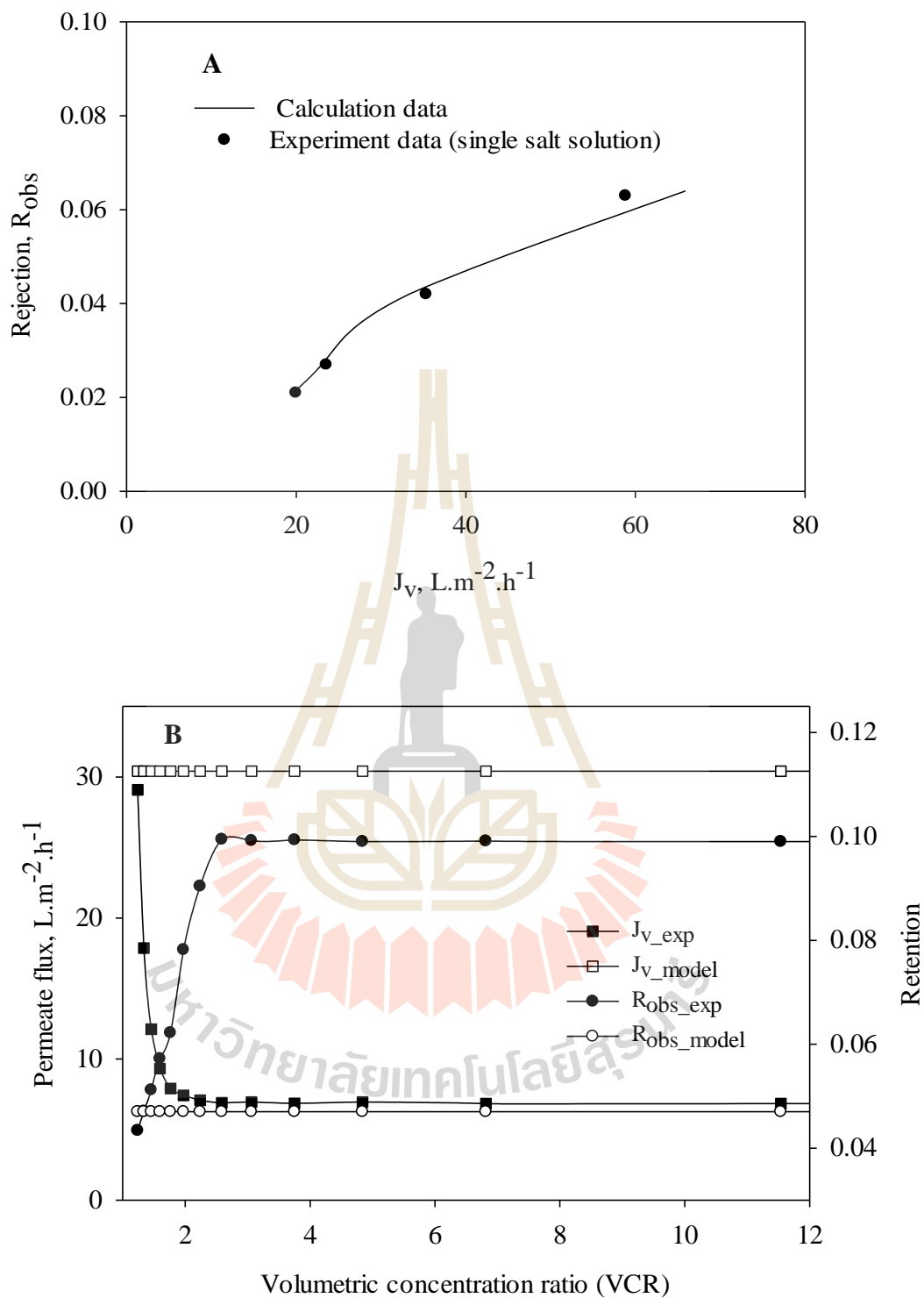


Figure 4.5 Experimental and modeling results for permeate flux as the function of lactate rejection of model solution (A) and permeate flux plus lactate rejection as function of volumetric concentration ratio (B). $T = 30\text{ }^{\circ}\text{C}$, $TMP = 10.3\text{ bar}$.

4.1.4 The performance of nanofiltration experiment

As explained earlier, the advantage of NF was performed not only in the high rejection of multivalent and macromolecules but also in the large concentration of sodium lactate which was the target compound, could go through. The experimental data for rejections of various components were determined and shown in Fig. 4.6. As expected, the rejection of multivalent compounds as Ca^{2+} , Fe^{2+} , PO_4^{3-} , Mg^{2+} , SO_4^{2-} , Mn^{2+} were observed with higher rejection values about 0.147, 0.18, 0.258; 0.314, 0.468, 0.63, respectively when comparing to the rejection of monovalent compounds such as Na^+ , K^+ , Cl^- (0.099, 0.096 and 0.063). The selectivity rejects of multivalent electrolytes mostly based on both size exclusion and electrostatic interaction in comparison to monovalent electrolytes (Wu et al., 2016). With the higher molecular weight as well as the higher ionic charge (more electrostatic) and higher ionic radius (more steric hindrance), multivalent electrolytes permeation was lower than monovalent electrolytes permeation (Pérez-González et al., 2015), demonstrating the higher rejection of multivalent electrolytes. Furthermore, the high rejection was found for the protein after nanofiltration. There are 95.86 % of protein was removed and remained only 0.103 g.L⁻¹ in permeate flux. The effective of nanofiltration for eliminating protein was shown mainly due to its small molecular weight cut off. As is illustrated by graph Fig.4.6B, one more important advantage of NF process was the performance. There was the high rejection of large bio-molecules, colloid and suspended particles in fermentation broth which were shown at the high decolouration effect. This step significantly facilitates further purification step since the higher temperature of further purification technique (evaporation, esterification, and distillation) could lead to form the darker color and reduce the purity of final product.

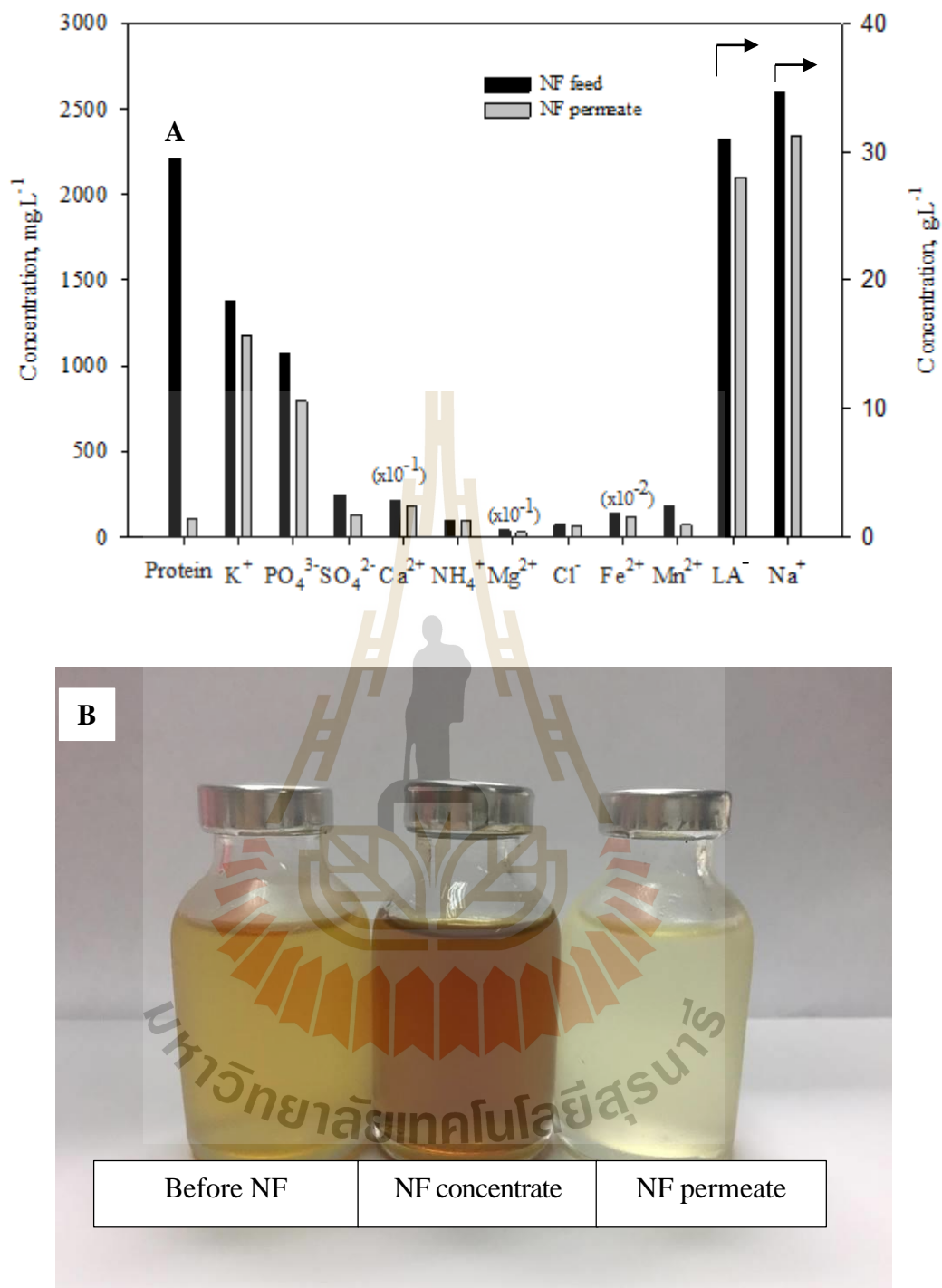


Figure 4.6 Histograms showing the compositions of the feed and the NF permeate solutions (A). Evidence of the decolouration induced by the NF process (B).

4.2 Kinetic analysis of ethyl lactate (ELA) production via pervaporation -assisted esterification technique: mathematical model

4.2.1 Preliminary kinetic study of esterification reaction in batch mode

In recent year, several researchers have done their work showing the basic characteristic of the batch esterification (Asthana et al., 2006; Delgado et al., 2007; Kasinathan et al., 2010; Khunnonkwao; et al., 2012). Effect of reaction temperature, initial ratio of alcohol and lactic acid, catalyst type and catalyst loading were indicated. It was shown that ethanol, a primary alcohol, which is non-toxic, a high environmentally friend and show a high conversion result of lactic ester, was a good indicator for esterification reaction (Benedict, 2003; Filachione & Costello, 1952; Wasewar et al., 2009). Sulfuric acid as a homogeneous catalyst was investigated for esterification reaction between lactic acid and ethanol by Dimilla (Dimilla, 1957). Moreover, acidification by H_2SO_4 was an important step in the recovery lactic acid. The lactic salt from fermentation broth reacts with H_2SO_4 to form free lactic acid while the excess H_2SO_4 was a catalyst for reaction. Panwana et al. studied the effect of sulfuric acid concentration on the ethyl lactate yield during esterification. It was found that the increase of catalyst concentration did not change much on the esterification yield despite the equilibrium point of reaction was reduced. The optimum H_2SO_4 concentration for lactic acid esterification was 1.5 % w/v concentration with the molar ratio of anhydrous ethanol to lactic acid was shown at 3:1 which is the ratio that was conducted for most reactions (Khunnonkwaoa et al., 2012).

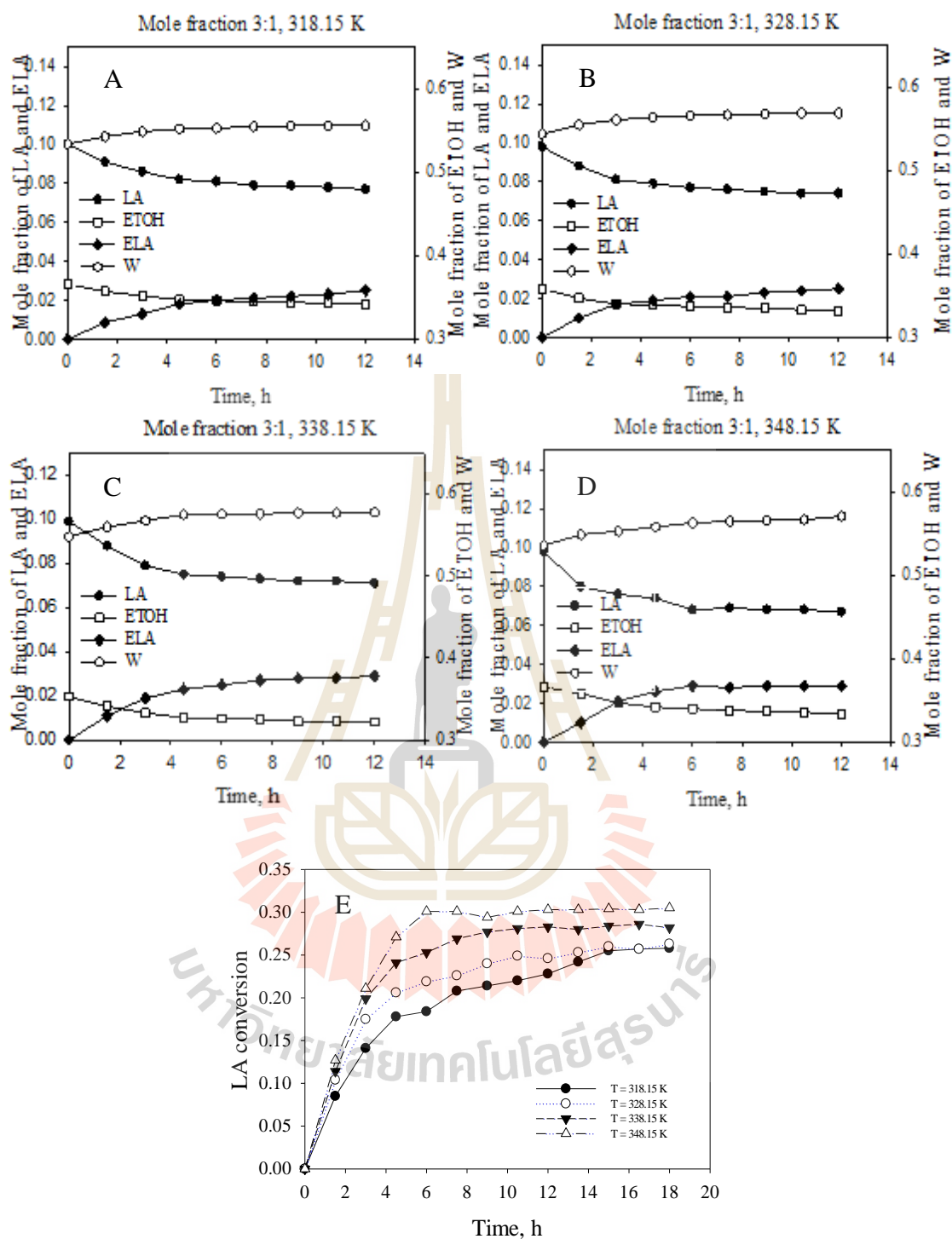


Figure 4.7 The concentration of lactic acid, ethanol, ethyl lactate and water from fermentation broth during esterification at A. 45 °C; B. 55 °C; C. 65 °C, D. 75 °C, (E). LA conversion of esterification reaction of the experiments with 1.5 wt% H₂SO₄, ratio of E:L is 3:1, W:L is 5:1 at 45 °C, 55 °C, 65 °C, and 75 °C.

The molar fractions of LA, ETOH, ELA, and water as the function of time were shown in Fig. 4.7. The mole fraction of ethyl lactate was increased dramatically during 5 – 6 hour of reaction (75 °C), 8 – 9 hour (65 °C), 13 – 14 hour (55 °C), 17 – 18 hour (45 °C) and kept constant value at the equilibrium value around 0.025 – 0.209. The quantity of ethyl lactate, as well as the conversion of lactic acid, increased with the raise of temperature. From the result in Fig. 4.7E, the conversion of lactic acid was presented as 0.258 (45 °C) after 18h, 0.263 (55 °C) after 15h, 0.282 (65 °C) after 7.5h and 0.305 (75 °C) after 18 hours. The explanation for this higher performance of ethyl lactate yield obtained in high temperature is the disproportionately increase in the number of high energy collisions as well as the rise of molecular energy levels at high temperature which causes the reaction to proceed faster (Aslam et al., 2000). Moreover, the rate constants for each temperature were calculated using NRTL model and the results were then collected in Table 4.2.

Table 4.2 Kinetic parameters of sodium lactate esterification with ethanol using 1.5 wt% of H₂SO₄ as catalyst.

Temperature, K	E:L and W:L	k, s ⁻¹	Ke	R ²
318.15	7:1 and 10.9:1	3.772 x 10 ⁻⁴	1.763	0.965
328.15	7:1 and 11:1	4.974 x 10 ⁻⁴	1.850	0.975
338.15	7:1 and 10.7:1	5.52 x 10 ⁻⁴	1.798	0.982
348.15	7:1 and 10.8:1	8.448 x 10 ⁻⁴	1.710	0.950
318.15	3.663:1 and 5.35:1	2.598 x 10 ⁻⁴	2.990	0.962
328.15	3.644:1 and 5.537:1	2.598 x 10 ⁻⁴	2.757	0.974

Table 4.2 (Continued).

Temperature, K	E:L and W:L	k, s ⁻¹	Ke	R ²
338.15	3.555:1 and 5.527:1	4.02 x 10 ⁻⁴	3.079	0.970
348.15	3.745:1 and 5.48:1	5.587 x 10 ⁻⁴	2.901	0.932

From the results in Table 4.2, the upward trend of reaction rate constant was found with the increase of reaction temperature but the equilibrium constants depend slightly on the variation of temperature. The temperature dependence of kinetic constant was fitted with the Arrhenius equation and shown in Fig. 4.8. From the slope of the Arrhenius equation, the activation energies were calculated and shown in Table 4.9.

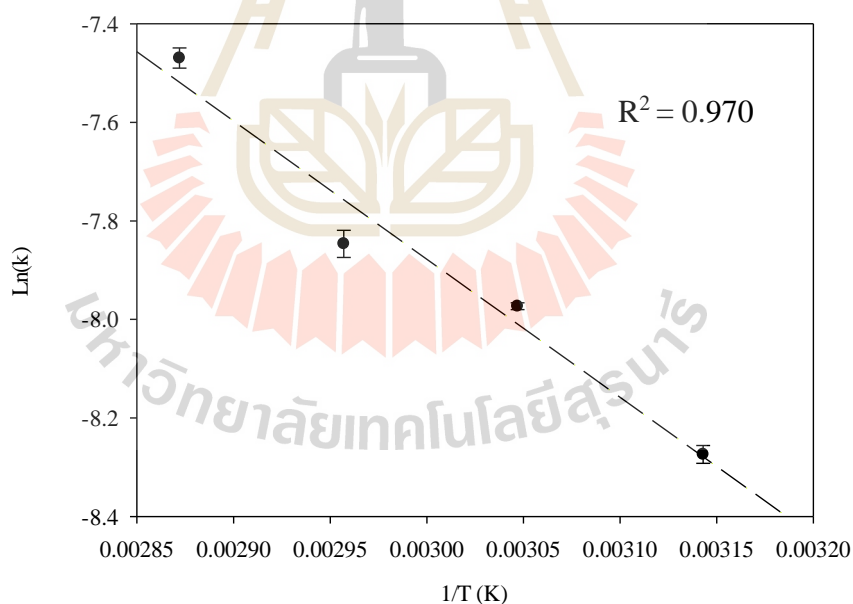


Figure 4.8 Arrhenius plot between $\ln(k)$ and $(1/T)$, K⁻¹ for esterification reaction of the experiments with 1.5 wt% H₂SO₄, ratio of E:L is 3:1, W:L is 5:1 at 45 °C, 55 °C, 65 °C, and 75 °C.

According to this linearity plot, the Arrhenius parameter of sodium lactate esterification that is necessary for simulation were evaluated, could be obtained and shown in the following table:

Table 4.3 The kinetic parameters of lactic acid, magnesium lactate, ammonium lactate and sodium lactate with ethanol.

System	Operation (Initial feed, T °C, catalyst wt%)	k (s ⁻¹)	k ₀ (s ⁻¹)	E _A (kJ.mol ⁻¹)	Reference
Lactic acid – Ethanol	E:L = 3:1 75 °C 0.5 wt% H ₂ SO ₄	9.68 x 10 ⁻³	-	-	(Dimilla, 1957)
Magnesium lactate – Ethanol (UNIQUAC)	E:L = 3:1, 75 °C, 0.17 wt% H ₂ SO ₄	7.262 x 10 ⁻⁴	3.739	1.012 x 10 ⁴	(Daengpradab, 2014)
Sodium lactate – Ethanol (NRTL)	E:L = 3:1, 75 °C, 1.5 %wt H ₂ SO ₄	5.587 x 10 ⁻⁴	1.274	2.248 x 10 ⁴	This study

It can be obtained from Table 4.3 is the rate of the reaction with sodium lactate was slower than the rate of lactic acid. The slow rate could be mainly due to the presence of sodium ions in the solution, thus the excess amount of sulfuric acid is necessary in order to compensate H^+/Na^+ ion exchange reaction for esterification of sodium lactate with ethanol. Furthermore, the existing of sodium sulfate in the solution would show the ionic force and the ionic strength of solution might effect to the activity coefficient and equilibrium constant of the reaction (Banat et al., 2002). The same effect of another ion, ammonium, and magnesium, to esterification was indicated in the studies of Kasinathan et al. and Boonpradad Daengpradad, respectively (Daengpradab, 2014; Kasinathan et al., 2010). However, with the excess sulfuric acid makes the sodium sulfate, which should be separated and then removed after esterification reaction. Despite the high solubility of sodium sulfate in water (21.5 g/100 g solution at 25 °C), which makes the elimination of sodium sulfate after esterification more difficult, the excess amount of ethanol was be used to insoluble Na_2SO_4 (solubility of Na_2SO_4 in ethanol is 0.095 g/ 100g solution at 25 °C). Therefore, Na_2SO_4 could be removed out of the system by using filtration.

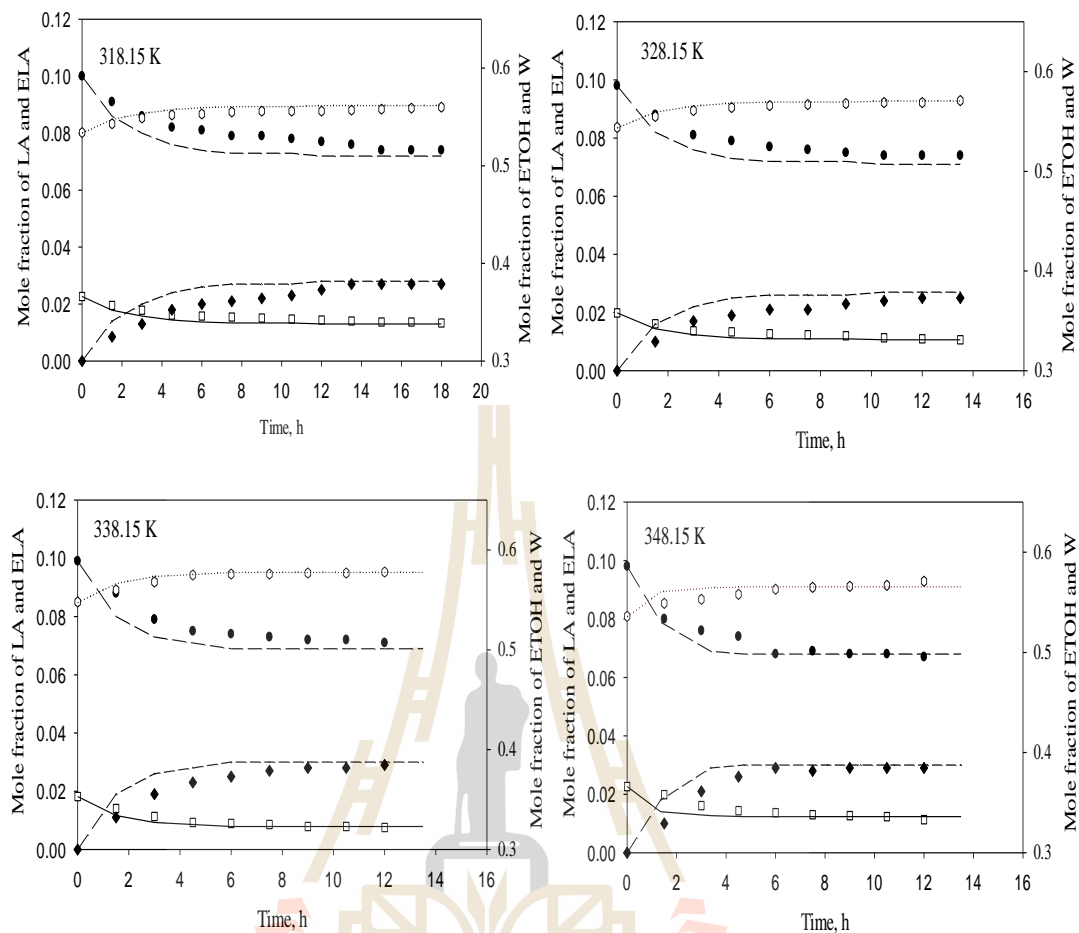


Figure 4.9 The comparison between experimental mole fraction profile and predicted mole fraction profile of lactic acid esterification of the experiments with 1.5wt% H_2SO_4 , ratio of E:L is 3:1, W:L is 5:1 at 45 °C, 55 °C, 65 °C and 75 °C (\bullet : LA, \square : ETOH, \blacklozenge : ELA, \circ : W, --- : LA model, — : ETOH model, - - - : ELA model, : W model).

As shown in Fig. 4.9, the good agreement between the experimental and prediction mole fraction profile of the esterification reaction. The average deviations between the calculated by using NRTL model and experimental for sodium lactate esterification were 9.383%; 8.618%; 8.135% and 7.087% at the four experiment temperature 45 °C, 55 °C, 65 °C and 75 °C, respectively. This deviation might be due

to the effect of the impurities in the sodium lactate solution and the sodium sulfate producing during the reaction (Daengpradab, 2014). Moreover, at the high concentration with the high temperature, lactic acid could undergo oligomerization to form a linear oligomer lactic acid, which was believed to adversely affect ethyl lactate yield in the reaction and caused higher deviation of prediction and experimental data (Vu et al., 2005).

4.2.2 The model for pervaporation-assisted esterification

4.2.2.1 Performance of pervaporation in quaternary mixture

During esterification reaction, water quantity was obviously changed by time. And with the different feed water mole fraction was correlated to the water performance through pervaporation. The portrait of total flux, the mole fraction of water on the feed side of the pervaporation module at the different temperature is shown in Fig. 4.10.

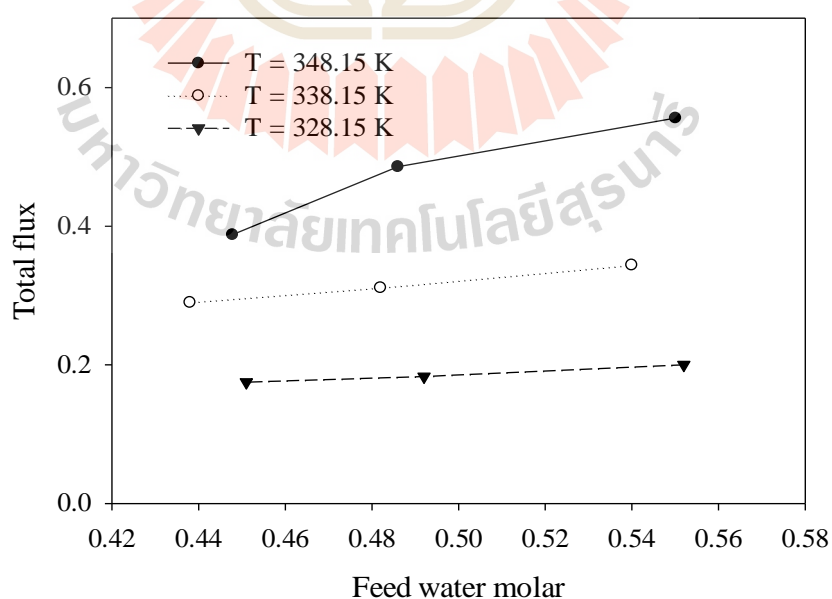


Figure 4.10 Influence of feed water mole fraction on total permeation flux, J_{tot} ($\text{kg}\cdot\text{m}^{-2}\cdot\text{h}^{-1}$) at various operating temperatures.

As the data are shown in this figure, the flux increased with the feed water composition and temperature. The higher mole fraction of water in feed, the higher the total permeate flux and water were obtained at the different temperature in the feed with the linear trend. These results consisted with the finding of Benedict and associates (Benedict, 2003) when they studied the effect of feed composition in the permeation characteristics for quaternary mixture present during the esterification of lactic acid with ethanol. This changing was probably due to the better driving force between the feed side and the permeate side. At the higher water concentration in feed, the greater number of water molecules were found in contact with the selective layer of the membrane. Therefore, more water molecules were absorbed into the membrane lead to the more water molecules passed through the membrane and the higher water permeation flux. Moreover, it could also be observed that dense Hybrid silica AR top layer membrane has a higher effective performance of water than the other components of the quaternary mixture because it's the smallest radius of gyration (0.615 \AA) comparing with ethanol (2.259 \AA), ethyl lactate (3.622 \AA) and lactic acid (3.298 \AA) (Pereira, 2009). Hence, the definition of selectivity of a quaternary mixture which represented the pervaporation working can be readily simplified to binary component mixtures, water, and remainder. The effect of temperature on the selectivity parameter of a mixture was illustrated in the graph below:

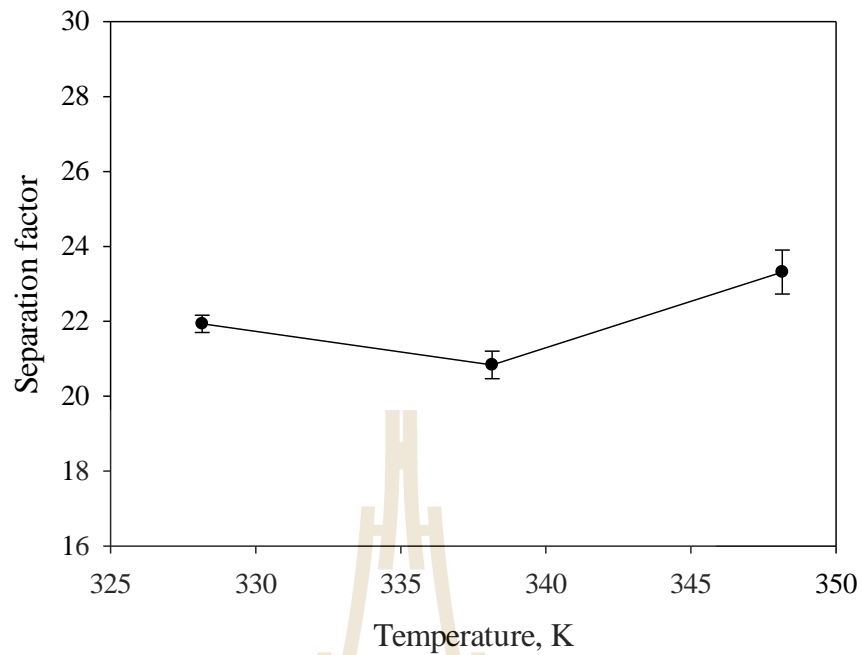


Figure 4.11 Influence of the temperature on the separation factor for the fermentation mixture at 55 °C, 65 °C and 75 °C.

At three various feed temperature experiments (55 °C, 65 °C and 75 °C), the high affect of temperature to the separation factor was indicated. It can be seen in Fig. 4.11 is the greatest value of separation factor during pervaporation was obtained at the highest temperature 75 °C at 22.937. The similar trend was also obtained in the study of Carla Sofia Marques Pereira et al. (Pereira, 2009).

4.2.2.2 Pervaporation parameter estimation

The design for pervaporation requires the knowledge of the permeance of each component as the function of temperature that can be calculated in the Eq. 2.29 (section 2.3.4) The information of permeance temperature dependence is related to the following graph:

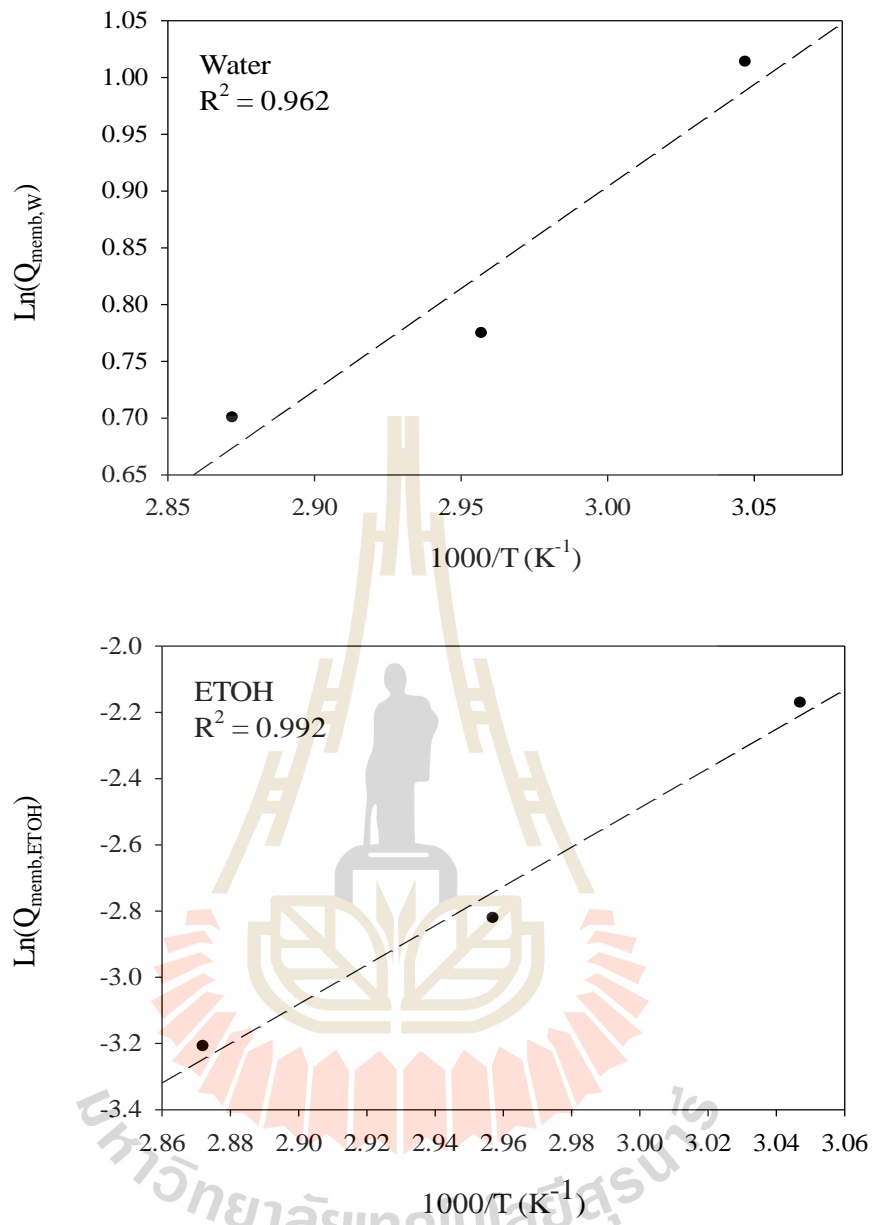


Figure 4.12 Temperature dependence of species permeances, $Q_{memb,w}$ and $Q_{memb,ETOH}$ ($\text{mol}\cdot\text{m}^{-2}\cdot\text{h}^{-1}\cdot\text{bar}^{-1}$) and linear fitting.

The intercept and slope of linear regression are represented the pre-exponential factor ($Q_{memb,0}$) and the activation energy of permeation, which is a combination of activation energy of diffusion and the heat of adsorption on the membrane (E_{perm}). These parameters were calculated following equation 2.25 and Fig.

4.12 are shown in Table 4.4. It can be seen from this table is, even though, the driving force of system rose due to temperature increases, the membrane permeability decreased as the negative values of the activation energies of permeation (Pereira, 2009). The deviation between values from parameter estimation modeling and experimental fluxes could be calculated using MRD (Eq 2.17) in which n is the number of pervaporation experiments.

Table 4.4 Pervaporation parameters (the pre-exponential factor and the activation energy).

Component	$Q_{memb,0}$ (mol.h ⁻¹ .m ⁻² .bar ⁻¹)	E_{perm} (J.mol ⁻¹)	R ²
Water	0.013	-1.423 x 10 ⁴	0.911
Ethanol	1.891 x 10 ⁻¹⁰	-5.482 x 10 ⁴	0.961

The total permeation fluxes calculated by using parameter in Table 4.4 as a function of the experimental fluxes data had been plotted in Fig. 4.13 with a good agreement.

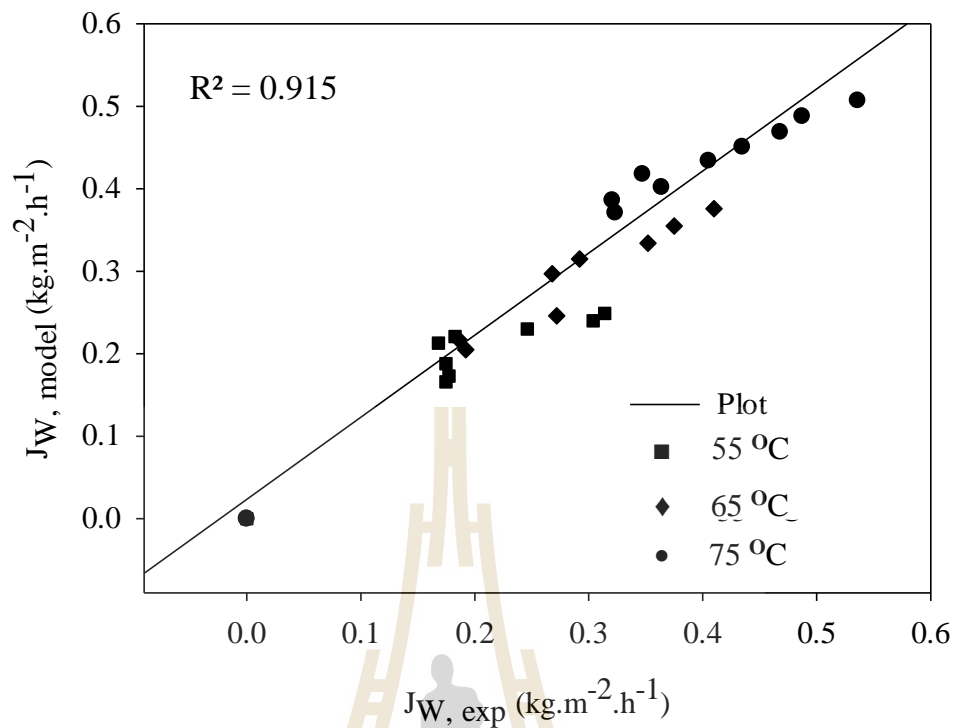


Figure 4.13 Calculated total permeation flux versus experimental total permeation flux at different temperature 55 °C; 65 °C; 75 °C.

4.2.2.3 The performance of pervaporation-assisted esterification.

Because the extent of esterification is thermodynamically limited and the slow reaction rate of reaction, removal of reaction products is required to achieve complete conversion. To overcome such thermodynamic limitations, reactive distillation (RD) or pervaporation, evaporation can be implemented as a scalable industrial process to continuously remove either water or ester from the reactive media as it is formed (Londono, 2010). Since pervaporation is a modular membrane process, it can easily be coupled with processes such as esterification (Gitis & Rothenberg, 2016).

The advantage of pervaporation membrane to the esterification reaction was shown through the value of lactic acid conversion in Fig. 4.14 and Fig. 4.15.

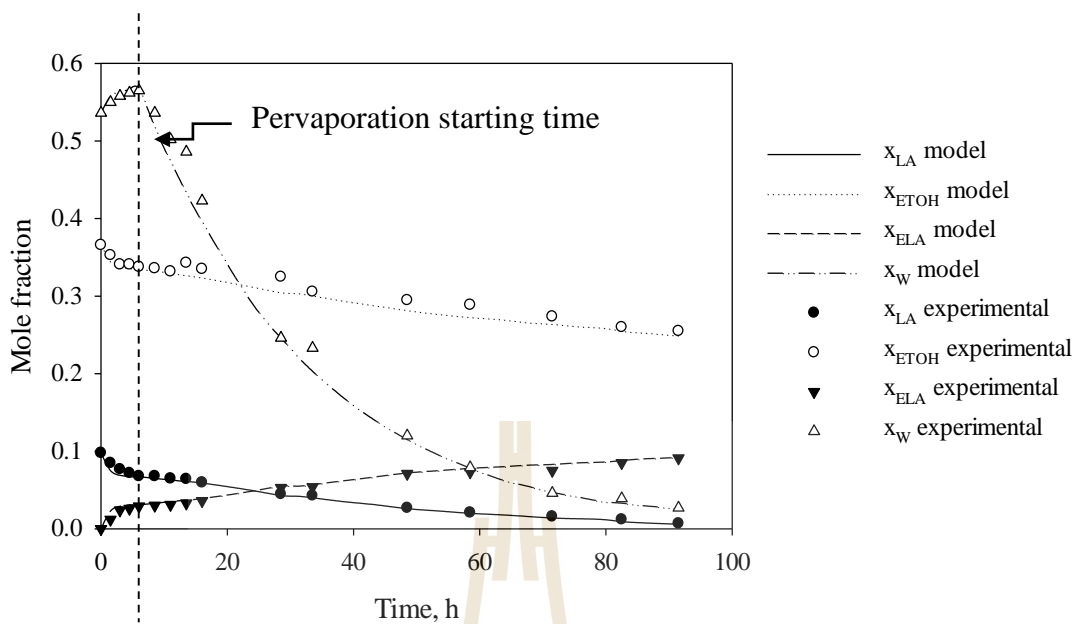


Figure 4.14 Mole fraction of lactic acid, ethyl lactate, ethyl lactate, and water as the function of time obtained from experimental data and the model data by using pervaporation-assisted esterification at 75 °C, $A/V = 23.8 \text{ m}^{-1}$.

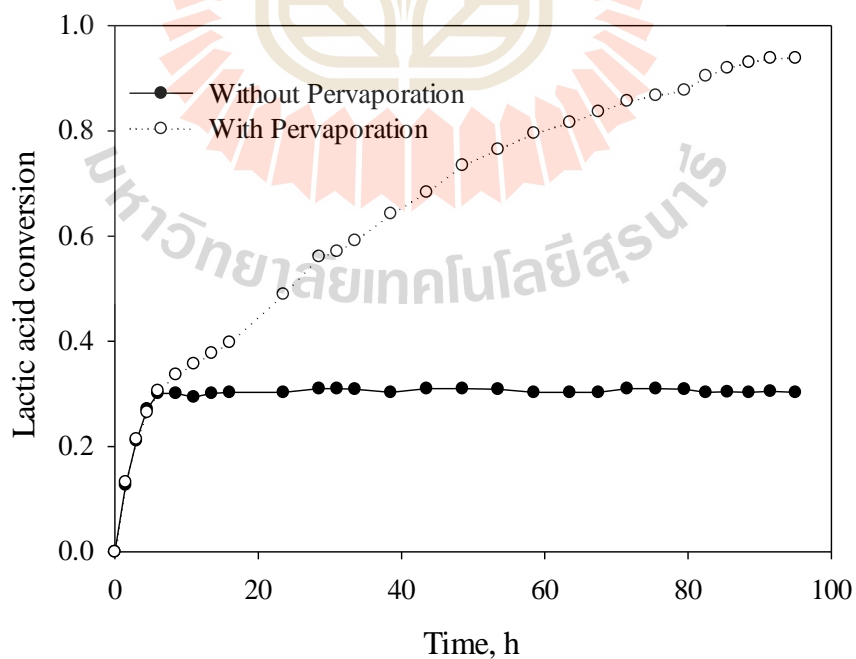


Figure 4.15 Lactic acid conversion profile for esterification reaction with and without pervaporation at 75 °C, E:L = 7:1, W:L = 5.5:1, $A/V = 23.8 \text{ m}^{-1}$.

As can be observed in these figures, the yield of ethyl lactate was significantly intensified due to the pervaporation module. In this process, hydrophilic membrane permitted the selective permeation of water from the mixture, so mostly water was removed and led to increase the reaction rate. 94.96% of water was separated out of the system led to the higher lactic acid conversion (0.928) comparing to conversion of lactic acid (0.306) in the batch esterification at 75°C after 92h. The improvement of ethyl lactate yield was obtained according to the disappeared of the reverse reaction by removal of the product (water) as soon as it was formed. As a result, it drove the position of the equilibrium to the ester side and the conversion of the thermally limited esterification reaction is enhanced (Jing et al., 2009; Jyoti et al., 2015).

The generalized parameter of water F_w , a coupling factor, and measures how the permeation of one component affects the conversion of the reaction was also defined by using Eq. 16. For water the F_w was $4.25 > 0$, this result confirmed that the reaction conversion would be enhanced by pervaporative removal of water component. It is obvious that the use of a water selective Hybrid Silica AR membrane $\alpha\text{-Al}_2\text{O}_3$ will be advantageous to the esterification reaction because of the preferential removal of water from the reaction mixture (Zou et al., 2010).

According to the experimental profile, the kinetic parameters of esterification and modeling of pervaporation, mole fraction profile of each component (LA, ETOH, ELA, and water) in the mixture was obtained. The good agreement between the profile determined by the model equation and experimental data was observed in Fig. 4.14. The average deviations between the calculated by using NRTL model and experimental were confirmed using the mean relative deviation (MRD) with small error (4.624%).

Finally, the value in Table 4.16 was shown the summarization the performance parameters of different types of membranes for several systems using polymer and ceramic membrane obtained in the pervaporation studies of research articles as well as in this study. The values of important parameters including permeation flux and selectivity of membrane in this study, $J_{tot} = 0.5 \text{ kg.m}^{-2}.\text{h}^{-1}$ and $\alpha = 22.937$ is presented. It was noted that the ceramic mono channel tube with dense Hybrid silica AR top layer examined in this study of dehydration in pervaporation membrane bioreactor showed a pretty good pervaporation performance when the results compared with those of published ones for these other system in various membrane module, although the pervaporation performance of the membrane for the fermentation broth separation in fermentation-pervaporation process was not as good as that for model solution separation.

Table 4.5 Comparison of membrane performance parameters of different pervaporation systems.

System	Material, type of membrane	Operation condition	Dehydration performance	Reference
Ethanol – water	Microporous silica, cylindrical membrane	40 – 70 °C, 0.667 – 3.333 kPa	$J_{tot} = 0.385 – 0.8$ $\text{kg.m}^{-2}.\text{h}^{-1}$, $\alpha = 10 – 500$	(Ong & Tan, 2016)
Fermentation broth	Polymethylsiloxane (PDMS), flat sheet	35 °C, 4 kPa	$J_{tot} = 0.35$ $\text{kg.m}^{-2}.\text{h}^{-1}$	(Fan et al., 2016)

Table 4.5 (Continued).

System	Material, type of membrane	Operation condition	Dehydration performance	Reference
Ethanol – water	Polysulfone (PS), hollow fiber	50 °C, 100 Pa	$J_{tot} = 0.265$ $\text{kg}\cdot\text{m}^{-2}\cdot\text{h}^{-1}$, $\alpha = 6.4$	(Guo et al., 2010)
Ethanol – water	Ceramic support (HybSi membrane), tubular	80 °C, 20 mmHg	$J_{tot} = 1.5 - 3.38$ $\text{kg}\cdot\text{m}^{-2}\cdot\text{h}^{-1}$, $\alpha = 120$	(Klinov et al., 2017)
Ethanol – water	Ceramic support (Silica), tubular	70 °C, 3.8 mmHg	$J_{tot} = 1.35$ $\text{kg}\cdot\text{m}^{-2}\cdot\text{h}^{-1}$, $\alpha = 200$	(Veen et al., 2001)
Fermentation broth (LA – ETOH – ELA – W)	Ceramic (Hybrod Silica AR membrane $\alpha\text{-Al}_2\text{O}_3$), tubular	75 °C, 10 mbar	$J_{tot} = 0.5$ $\text{kg}\cdot\text{m}^{-2}\cdot\text{h}^{-1}$, $\alpha = 22.779$	This study

4.3 Membrane-assisted purification of optically pure D-(-)-lactic acid from fermentation broth process

The flow diagram of purification process of D-(-)-lactic acid recovery from fermentation broth involves nanofiltration and pervaporation – assisted esterification of lactate salts in ethanol was shown in the following figure:

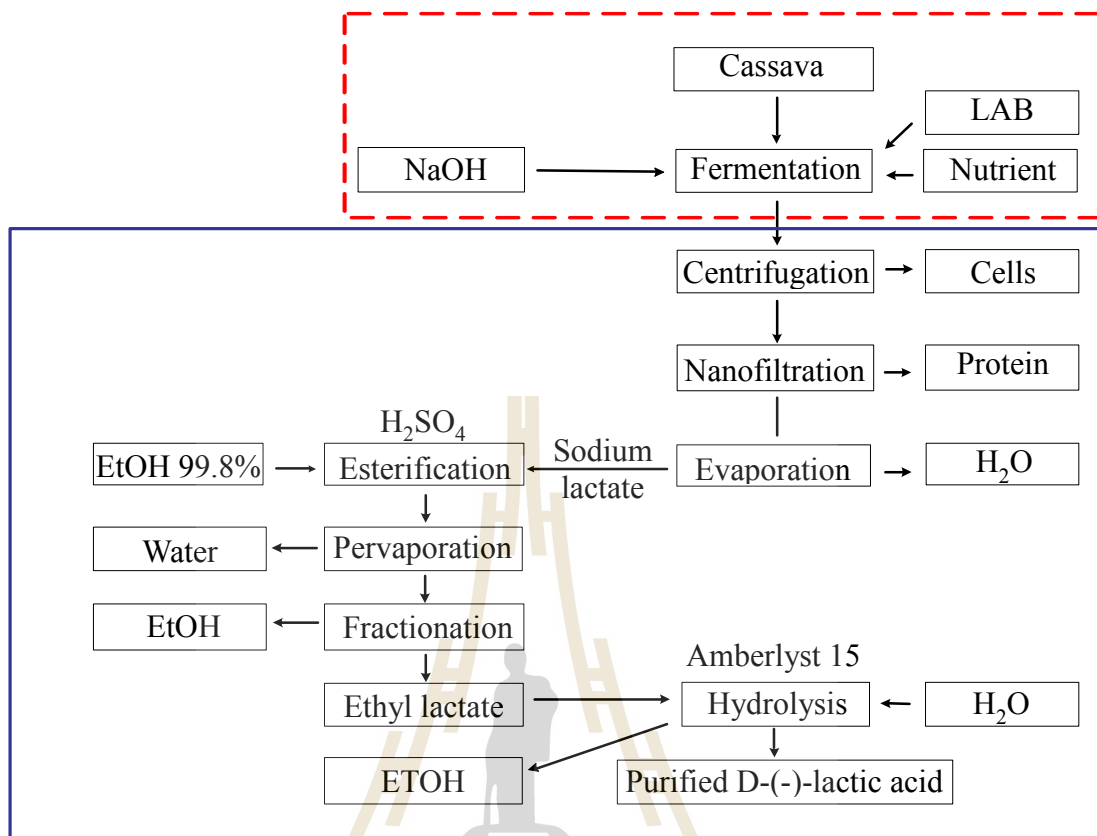
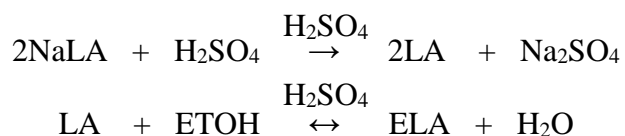


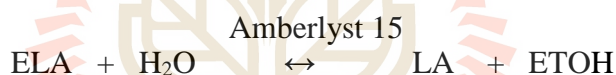
Figure 4.16 Process of lactic acid purification.

The fermentation broth was treated by centrifugation at 5000 rpm for 15 minutes at room temperature (Komesu et al., 2014) and then by nanofiltration (30 °C, 1.28 m.s⁻¹ and 10.3 bar) to separate cell biomass, protein and color compounds. Following the evaporation technique (65 °C, 1 mbar) to reduce the excess water, D-(-)-lactic acid broth (385 g.L⁻¹) was then purified from the clean broth by esterification in ethanol and 1.5 % w/w H₂SO₄ as a catalyst (75 °C, 1 mbar) with the reaction as follow:



During esterification process, pervaporation was used to remove water from the reactive media in order to overcome the thermodynamic limitation of esterification. Sodium sulfate that formed from the reaction was separated by filtration using filter Whatman 1 (Sigma Aldrich, Singapore) with pore size is 11 μm .

Because the high mole fraction of ethanol was obtained in the liquid phase after esterification and the ethanol/ethyl lactate binary mixture does not result in azeotrope formation, the excess of ethanol could be completely separated by conventional distillation. The condition of operation of distillation column was 70 – 90 $^{\circ}\text{C}$ at 250 mbar. After that, the pure of ethyl lactate was obtained by this distillation column at 60 $^{\circ}\text{C}$ and 20 mbar. The purified ethyl lactate was then subjected to hydrolysis with deionized water using 3 wt% Amberlyst 15 as a catalyst. The operating temperature was maintained at 110 $^{\circ}\text{C}$, and the initial molar ratio of water to ethyl lactate was 15:1. During the hydrolysis reaction, ethyl lactate reacted with water to produce lactic acid and ethanol as follow:



Two purification steps were employed. In the first step, ethanol generated from the reaction was removed by distillation (110 $^{\circ}\text{C}$ at atmosphere). In the last step, the excessive water was removed by vacuum evaporation (65 $^{\circ}\text{C}$, 1 mbar) to produce concentrated D-(-)-lactic acid.

The purity of final D-(-)-lactic acid of this study was shown in Table 4.5 and Fig. 4.18. The result showed that more than 95% D-(-)-lactic acid could obtain. The pure D-lactic acid could be obtained and be a good material for the production of poly(D-lactide) polymer.

Table 4.6 The summary characteristic of fermentation broth, nanofiltration permeate and final product.

Compound	Fermentation broth	NF permeate	D-(-)-LA product
Cell, g.L ⁻¹	2.754	0.017	-
Protein, , g.L ⁻¹	2.489	0.103	-
Glucose, , g.L ⁻¹	18.340	0.517	-
Na ⁺ , ppm	34.530	31.180	2.230
K ⁺ , ppm	2483	1175.360	Trace
NH ₄ ⁺ , ppm	159.230	96.140	2.290
Cl ⁻ , ppm	79.330	64.490	19.160
Ca ²⁺ , ppm	35.050	17.913	1.280
Mn ²⁺ , ppm	31.100	67.900	0.177
Mg ²⁺ , ppm	76.290	27.630	Trance
Fe ²⁺ , ppm	2.420	1.160	Trance
SO ₄ ²⁻ , ppm	454.240	131.020	1.580
PO ₄ ³⁻ , ppm	1909.120	791.070	Trance
pH	6.9	6.59	2.34
D-(-)-lactic acid, g.L ⁻¹	34	28	100

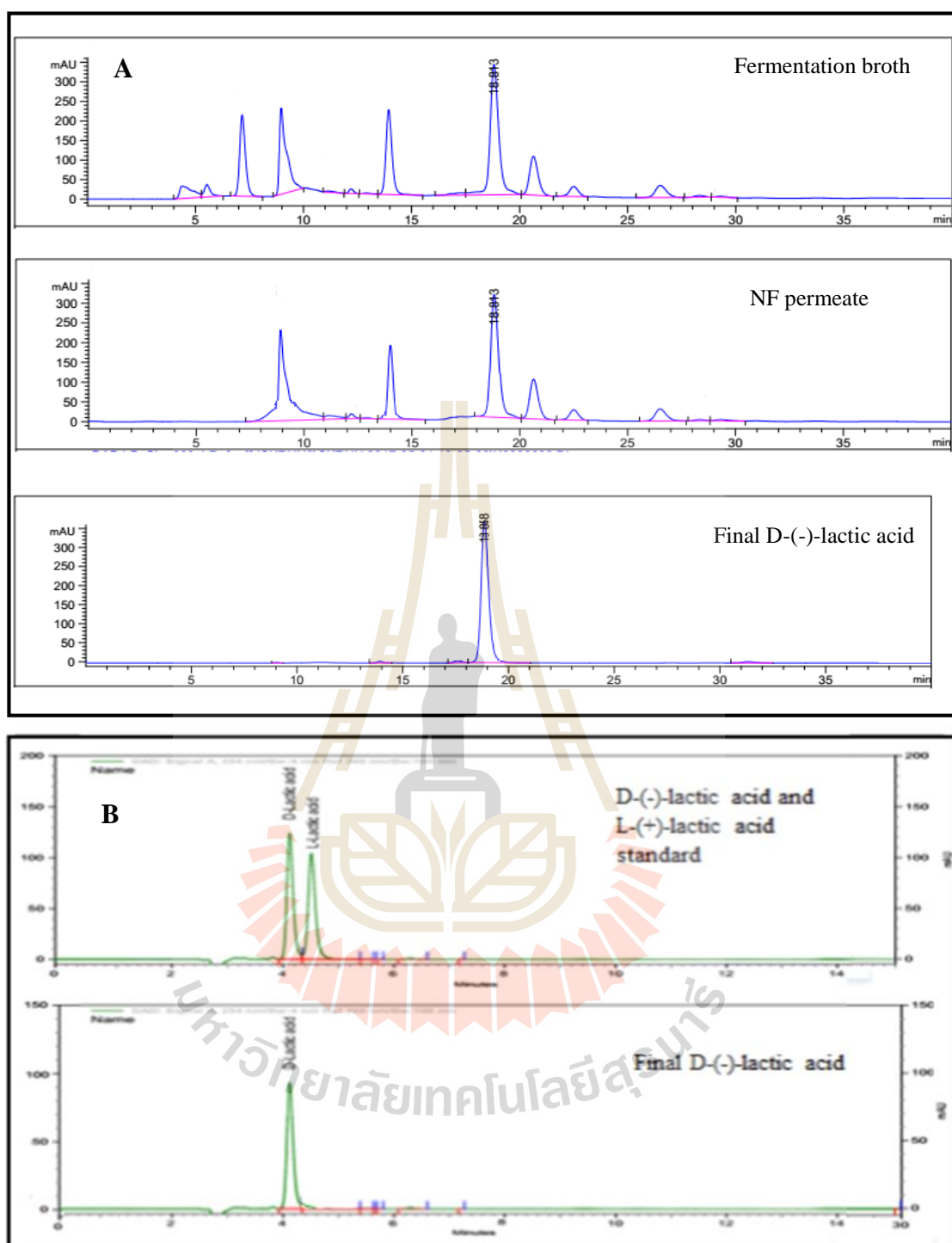


Figure 4.17 HPLC chromatograms of sample taken during purification processes of lactic acid and final D-(-)-lactic acid fermentation broth (A) and chiral separation of optical purity of purified D-(-)-lactic acid (B).

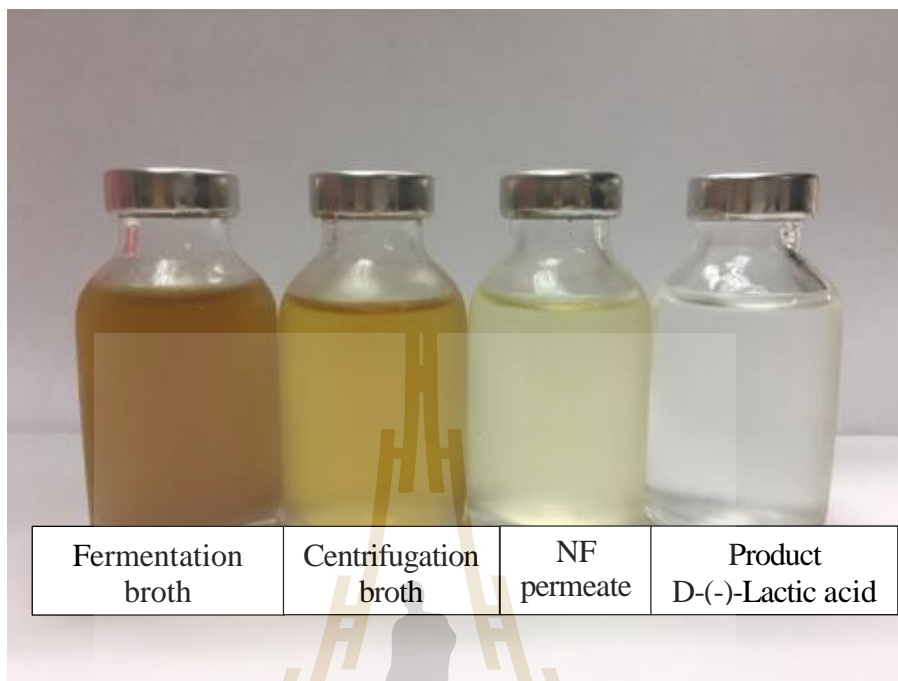


Figure 4.18 Image of samples taken during purification processes of lactic acid and final D-(-)-lactic acid.

CHAPTER V

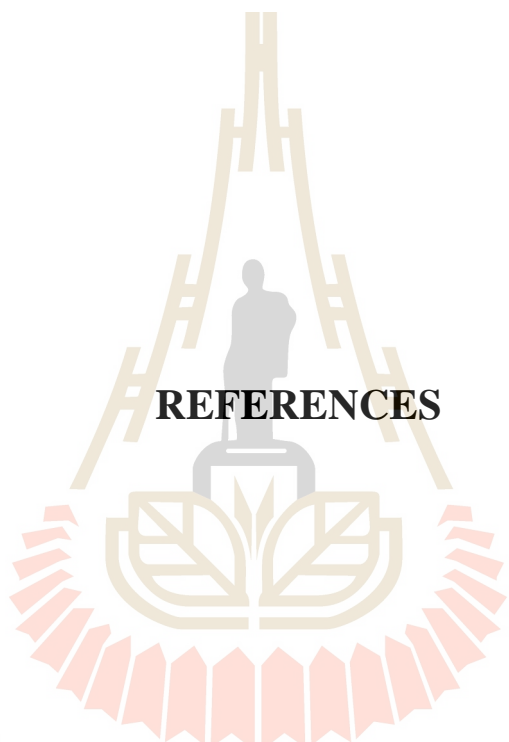
CONCLUSIONS

This study presented the data from the experiment and mathematical model for membrane-assisted purification of optical pure-D-(-)-lactic acid from fermentation broth. Spiral wound nanofiltration membrane and pervaporation-assisted esterification was employed for the purification D-(-)-lactic acid from fermentation broth successfully. D-(-)-lactic acid of more than 95% purity was produced. NF was indicated as a high potential pretreatment technique for the organic acid purification with the high eliminate rate of protein and macro color compounds but the low lactic acid rejection. The model parameters that have been studied are observed retention and lactate rejection, were estimated based on experimental data and using Spiegler–Kedem model. In this model, the reflection coefficient (σ) and the solute permeability (P_s) were obtained using the best-fit method for the prediction of the permeate flux and rejection of lactate. The result was showed that the rejections of lactate in fermentation broth were predicted with a good agreement with the experimental data (MRD = 5.169%).

Pervaporation-assisted esterification of lactic acid with ethanol in the presence of sodium salt and acid sulfuric as catalyst was also studied in this study. The experiment was performed with the Hybrid Silica AR membrane for the real mixture (sodium lactate, ethanol, ethyl lactate, water). The information of reaction kinetics and pervaporation performance of the membrane were investigated for the design of PVMR. The kinetic

including the activation energy and reaction rate constant for this reaction to obtain ethyl lactate at 75 °C, E:L = 3:1 and 1.5 %wt as catalyst were found at 1.274 (s⁻¹) and 2.248 x 10⁴ (J.mol⁻¹), respectively. The water flux at the permeate side of the pervaporation membrane was obtained by maintaining a high recirculation rate for the reactor and a low permeate pressure. The total and partial permeation fluxes changing trend were upward with the mole fraction of water in the feed side of pervaporation and the operating temperature. In contrast to the water performance, the other components had a high rejection during the system, separation factor was found at 22.779. Arrhenius dependence with temperature was also assumed for the total permeation flux. The performance of pervaporation was modeled through pre-exponential factor $Q_{\text{membW},0} = 0.013$ (mol.h⁻¹.m⁻².bar⁻¹), $Q_{\text{membETOH},0} = 1.891 \times 10^{-10}$ (mol.h⁻¹.m⁻².bar⁻¹) and the activation energy $E_{\text{permW}} = -1.4227 \times 10^4$ (J.mol⁻¹); $E_{\text{permETOH}} = -5.4816 \times 10^4$ (J.mol⁻¹) which were presented the good agreement with the experimental data (MRD = 4.624%). After fractionation, hydrolysis, and evaporation, high purity of D-(-)-lactic acid was produced.

The results obtained in this study maybe useful for the effort of the reducing the cost of D-(-)-lactic acid by presenting more available of D-(-)-lactic acid as monomer for PLA industry. Moreover, the proposed model of nanofiltration and pervaporation-assisted can be used for predicting the process behaviors, providing a useful tool in process design and optimization.



REFERENCES

มหาวิทยาลัยเทคโนโลยีสุรนารี

REFERENCES

- Ahmed, A.-A., & Lovitt, R. W. (2007). Fouling strategies and the cleaning system of NF membranes and factors affecting cleaning efficiency. **Journal of Membrane Science** 303(1-2): 4-28.
- Ahmed, F. N. (2013). **Modified Spiegler-Kedem Model to Predict the Rejection and Flux of Nanofiltration Processes at High NaCl Concentrations**. Masters of Applied Science, Department of Civil Engineering, University of Ottawa, Ottawa, Canada.
- Alsahy, Q. F., Albyati, T. M., & Zablouk, M. A. (2013). A study of the effect of operating conditions on reverse osmosis membrane performance with and without air sparging technique. **Chem. Eng. Comm** 200: 1-19.
- Aslam, M., Torrence, G. P., & Zey, E. G. (2000). **Esterification**. **Encyclopedia of Chemical Technology**. John Wiley & Sons, Inc.
- Asthana, N. S., Kolah, A. K., Vu, D. T., Lira, C. T., & Miller, D. J. (2006). A Kinetic Model for the Esterification of Lactic Acid and Its Oligomers. **Industrial & Engineering Chemistry Research** 45(15), 5251-5257.
- Banat, F., Al-Asheh, S., & Simandl, J. (2002). Effect of dissolved inorganic salts on the isothermal vapor–liquid equilibrium of the propionic acid–water mixture. **Chemical Engineering and Processing: Process Intensification** 41(9): 793-798.
- Benedict, D. J., Parulekar, S. J., & Tsai, S.-P. (2003). Esterification of Lactic Acid and Ethanol with/without Pervaporation. **Industrial & Engineering Chemistry Research** 42(11): 2282-2291.

- Bhanushali, D. S. (2002). **Solvent-resistant nanofiltration membranes: separation studies and modeling**. Doctor of Philosophy, College of Engineering, University of Kentucky, Lexington, Kentucky.
- Boonpan, A., Pivsa-art, S., Pongswat, S., Areesirisuk, A., & Sirisangsawang, P. (2013). Separation of D, L-Lactic Acid by Filtration Process. **Energy Procedia** 34: 898-904.
- Boontawan, P., Kanchanathawee, S., & Boontawan, A. (2011). Extractive fermentation of L-(+)-lactic acid by *Pediococcus pentosaceus* using electrodeionization (EDI) technique. **Biochemical Engineering Journal** 54(3): 192-199.
- Bouchoux, A., Balmann, H. R.-d., & Lutin, F. (2005). Nanofiltration of glucose and sodium lactate solutions: Variations of retention between single- and mixed-solute solutions. **Journal of Membrane Science** 258(1-2): 123-132.
- Carrère, H., & Blaszkow, F. (2001). Comparison of operating modes for clarifying lactic acid fermentation broths by batch cross-flow microfiltration. **Process Biochemistry** 36(8-9): 751-756.
- Chandrapala, J., Duke, M. C., Gray, S. R., Weeks, M., Palmer, M., & Vasiljevic, T. (2016). Nanofiltration and nanodiafiltration of acid whey as a function of pH and temperature. **Separation and Purification Technology** 160: 18-27.
- Chookietwattana, K. (2014). Lactic Acid Production from Simultaneous Saccharification and Fermentation of Cassava Starch by *Lactobacillus Plantarum* MSUL 903. **APCBEE Procedia** 8: 156-160.
- Chow, S. H.-H. (1962). **Purification of lactic acid**. Master of Science, Department of Chemical Engineering, Kansas state University, Manhattan, Kansas.

- Dach, H. (2008). **Comparison of nanofiltration and reverse osmosis processes for a selective desalination of brackish water feeds.** Doctor of philosophy, Department of Engineering Sciences, Universit'e d'Angers, Anger, France.
- Daengpradab, B. (2014). **Study of ethyl lactate production from fermentation-derived magnesium lactate by reactive distillation.** Master of Science, Department of Chemical Engineering, Suranaree University of Technology, Nakhon Ratchasima, Thailand.
- Delgado, P., Sanz, M. T., & Beltrán, S. (2007). Kinetic study for esterification of lactic acid with ethanol and hydrolysis of ethyl lactate using an ion-exchange resin catalyst. **Chemical Engineering Journal** 126(2-3): 111-118.
- Delgado, P., Sanz, M. T. S., Beltrán, S., & Núñez, L. A. (2010). Ethyl lactate production via esterification of lactic acid with ethanol combined with pervaporation. **Chemical Engineering Journal** 165(2): 693-700.
- Delgado, P., Sanzo, M. T., & Beltrán, S. (2008). Pervaporation study for different binary mixtures in the esterification system of lactic acid with ethanol. **Separation and Purification Technology** 64(1): 78-87.
- Dey, P., Linnanen, L., & Pal, P. (2012). Separation of lactic acid from fermentation broth by cross flow nanofiltration: Membrane characterization and transport modelling. **Desalination** 288: 47-57.
- Dimilla, R. A. T. a. E. (1957). Kinetics of the Ethyl Alcohol-Lactic Acid Reaction. **Industrial and Engineering Chemistry** 49: 847-855.
- Ericksson, P. (1988). Nanofiltration extends the range of membrane filtration. **Environ. Prog.** 7: 58-62.

- Fan, S., Xiao, Z., & Li, M. (2016). Energy efficient of ethanol recovery in pervaporation membrane bioreactor with mechanical vapor compression eliminating the cold traps. **Bioresource Technology** 211: 24-30.
- Filachione, E. M., & Costello, E. J. (1952). Lactic Esters by Reaction of Ammonium Lactate with Alcohols. **Industrial & Engineering Chemistry** 44(9): 2189-2191.
- Gao, J., Zhao, X. M., Zhou, L. Y., & Huang, Z. H. (2007). Investigation of Ethyl Lactate Reactive Distillation Process. **Chemical Engineering Research and Design** 85(4): 525-529.
- Ghaffar, T., Irshad, M., Anwar, Z., Aqil, T., Zulifqar, Z., Tariq, A., Kamran, M., Ehsan, N., & Mehmood, S. (2014). Recent trends in lactic acid biotechnology: A brief review on production to purification. **Journal of Radiation Research and Applied Sciences** 7(2): 222-229.
- Gitis, V., & Rothenberg, G. (2016). **Ceramic Membranes: New Opportunities and Practical Applications**. Weinheim: Wiley-VCH.
- Grand.View.Research. (2015). **Lactic Acid And Poly Lactic Acid (PLA) Market Analysis By Application (Packaging, Agriculture, Transport, Electronics, Textiles) And Segment Forecasts To 2020**. Report ID: 978-1-68038-126-9.
- Guo, J., Zhang, G., Wu, W., Ji, S., Qin, Z., & Liu, Z. (2010). Dynamically formed inner skin hollow fiber polydimethylsiloxane/polysulfone composite membrane for alcohol permselective pervaporation. **Chemical Engineering Journal** 158(3): 558-565.
- Guo, L., & Santschi, P. H. (2007). **Ultrafiltration and its Applications to Sampling and Characterisation of Aquatic Colloids**. **Environmental Colloids and Particles** (pp. 159-221). John Wiley & Sons, Ltd.

- Hama, S., Mizuno, S., Kihara, M., Tanaka, T., Ogino, C., Noda, H., & Kondo, A. (2015). Production of d-lactic acid from hardwood pulp by mechanical milling followed by simultaneous saccharification and fermentation using metabolically engineered *Lactobacillus plantarum*. **Bioresource Technology** 187: 167-172.
- Hidalgo, A. M., León, G., Gómez, M., Murcia, M. D., Gómez, E., & Gómez, J. L. (2013). Application of the Spiegler–Kedem–Kachalsky model to the removal of 4-chlorophenol by different nanofiltration membranes. **Desalination** 315: 70-75.
- Hilal, N., Al-Zoubi, H., Darwish, N. A., Mohamma, A. W., & Abu Arabi, M. (2004). A comprehensive review of nanofiltration membranes: Treatment, pretreatment, modelling, and atomic force microscopy. **Desalination** 170(3): 281-308.
- Jing, M., Minhua, Z., Lianyu, L., Xin, Y., Jing, C., & Zhongyi, J. (2009). Intensifying esterification reaction between lactic acid and ethanol by pervaporation dehydration using chitosan–TEOS hybrid membranes. **Chemical Engineering Journal** 155(3): 800-809.
- Jyoti, G., Keshav, A., & Anandkumar, J. (2015). Review on Pervaporation: Theory, Membrane Performance, and Application to Intensification of Esterification Reaction. **Journal of Engineering** 2015: 1-24.
- Karabelas, A. J., Kostoglou, M., Koutsou, C. P. (2015). Modeling of spiral wound membrane desalination modules and plants – review and research priorities. **Desalination** 356: 165-186.
- Kasinathan, P., Kwak, H., Lee, U., Hwang, D. W., Hwang, Y. K., & Chang, J.-S. (2010). Synthesis of ethyl lactate from ammonium lactate solution by coupling solvent extraction with esterification. **Separation and Purification Technology** 76(1): 1-7.

- Kedem, O., & Katchalsky, A. (1958). Thermodynamic analysis of the permeability of biological membranes to non-electrolytes. **Biochimica et Biophysica Acta** 27: 229-246.
- Kertes, A. S., & King, C. J. (1986). Extraction chemistry of fermentation product carboxylic acids. **Biotechnol Bioengineer** 28: 269-282.
- Khunnonkwao, P., Ariyawong, C., Lertsiriyothin, W., & Boontawan, A. (2012). Purification of D-(-)-Lactic Acid from Fermentation Broth Using Nanofiltration, Esterification, Distillation, and Hydrolysis Technique. **Advanced Materials Research** 550-553: 2945-2952.
- Khunnonkwao, P., Boontawan, P., Haltrich, D., Maischberger, T., & Boontawana, A. (2012). Purification of L-(+)-Lactic acid from pre-treated fermentation broth using vapor permeation-assisted esterification. **Process Biochemistry** 47(12): 1948-1956.
- Khunnonwao, P. (2010). **Purification of L-(+)-lactic acid from fermentation broth by pervaporation-assisted esterification technique**. Master of Science, Department of Biotechnology, Suranaree University of Technology, Nakhon Ratchasima, Thailand.
- Kim, J. H., Na, J.-G., Shim, H. J., & Chang, Y. K. (2012). Modeling of ammonium lactate recovery and impurity removal from simulated fermentation broth by nanofiltration. **Journal of Membrane Science** 396: 110-118.
- Klinov, A. V., Akberov, R. R., Fazlyev, A. R., & Farakhov, M. I. (2017). Experimental investigation and modeling through using the solution-diffusion concept of pervaporation dehydration of ethanol and isopropanol by ceramic membranes HybSi. **Journal of Membrane Science** 524: 321-333.

- Komesu, A., Figueroa, J. E. J., Rios, L. F., Martinez, P. F. M., Lunelli, B. H., Oliveira, J. A. R., Filho, R. M., & Maciel, M. R. W. (2015). Evaluation of Operational Parameters for Ethyl Lactate Production Using Reactive Distillation Process. **Chemical engineering transactions** 43: 1141-1146.
- Komesu, A., Martins, P. F., Lunelli, B. H., Oliveira, J., Maciel Filho, R., & Wolf Maciel, M. R. (2014). Evaluation of lactic acid purification from fermentation broth by hybrid short path evaporation using factorial experimental design. **Separation and Purification Technology** 136: 233-240.
- Košutić, K., Dolar, D., & Kunst, B. (2006). On experimental parameters characterizing the reverse osmosis and nanofiltration membranes' active layer. **Journal of Membrane Science** 282(1): 109-114.
- Labban, O., Liu, C., Chong, T. H., & Lienhard V, J. H. (2017). Fundamentals of low-pressure nanofiltration: Membrane characterization, modeling, and understanding the multi-ionic interactions in water softening. **Journal of Membrane Science** 521: 18-32.
- Li, L., Eom, H.-J., Park, J.-M., Seo, E., Ahn, J. E., Kim, T.-J., Kim, J. H., & Han, N. S. (2012). Characterization of the major dehydrogenase related to D-lactic acid synthesis in *Leuconostoc mesenteroides* subsp. *mesenteroides* ATCC 8293. **Enzyme and Microbial Technology** 51(5): 274-279.
- Litchfield, J. H. (2009). Lactic Acid, Microbially Produced. In M. Schaechter (Ed.), **Encyclopedia of Microbiology (Third Edition)**. Oxford: Academic Press.
- Londono, A. O. (2010). **Separation of succinic acid from fermentation broths and esterification by a reactive distillation method**. Doctor of Philosophy, Department of Chemical Engineering, Michigan State University, Michigan, United State.

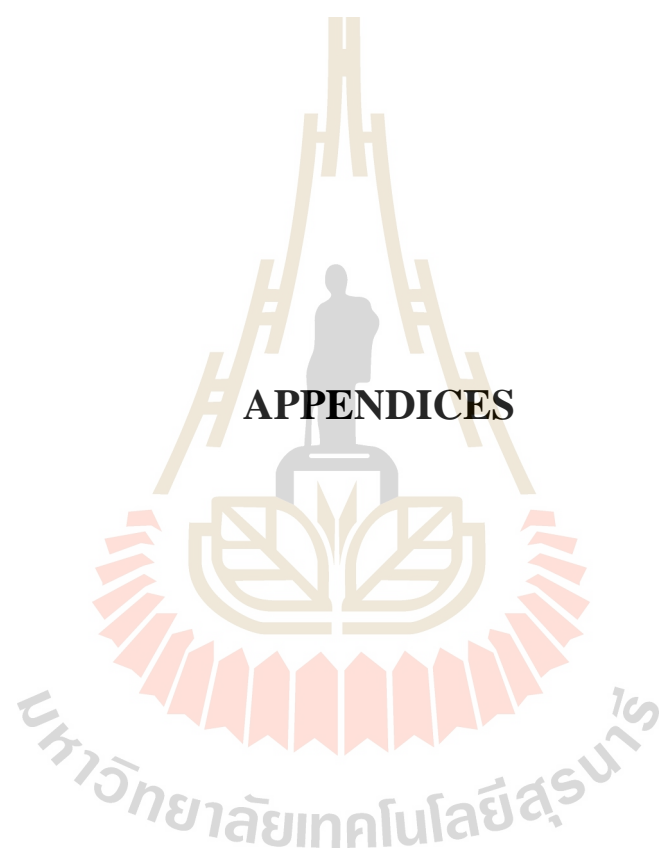
- Lopes, M. S., Jardini, A. L., & Filho, R. M. (2012). Poly (Lactic Acid) Production for Tissue Engineering Applications. **Procedia Engineering** 42:1402-1413.
- Lubsungneon, J., Srisuno, S., Rodtong, S., & Boontawan, A. (2014). Nanofiltration coupled with vapor permeation-assisted esterification as an effective purification step for fermentation-derived succinic acid. **Journal of Membrane Science** 459: 132-142.
- Ma, Y., Wang, J., & Tsuru, T. (2009). Pervaporation of water/ethanol mixtures through microporous silica membranes. **Separation and Purification Technology** 66(3): 479-485.
- Markovic, T., Vukosavljevic, P., Vladislavljevic, G., & Bukvic, B. (2006). Investigations of hydrodynamic permeability ceramic membranes for microfiltration. **Journal of Agricultural Sciences** 51(2): 151-164.
- Martinez, F. A. C., Balciunas, E. M., Salgado, J. M., González, J. M. D., Converti, A., & Oliveira, R. P. d. S. (2013). Lactic acid properties, applications and production: A review. **Trends in Food Science & Technology** 30(1): 70-83.
- Matheswaran, M., Kwon, T. O., Kim, J. W., & Moon, I. S. (2007). Factors affecting flux and water separation performance in air gap membrane distillation. **Journal of Industrial and Engineering Chemistry** 13(6): 965-970.
- Matsuda, H., Inaba, K., Sumida, H., Kurihara, K., Tochigi, K., & Ochi, K. (2016). Vapor-liquid equilibria of binary and ternary mixtures containing ethyl lactate and effect of ethyl lactate as entrainer. **Fluid Phase Equilibria** 420: 50-57.
- Narayanan, N., Koychoudhury, P. K., & Srivastava, A. (2004). L-(+)-lactic acid fermentation and its product polymerization. **Journal of Biotechnology** 7(2): 167-179.

- Oliveira, E. E. d. M., & Barbosa, C. C. R. (2013). Stability of a nanofiltration membrane after contact with a low-level liquid radioactive waste. **Química Nova** 36(9): 1434-1440.
- Ong, Y. T., & Tan, S. H. (2016). Pervaporation separation of a ternary azeotrope containing ethyl acetate, ethanol and water using a buckypaper supported ionic liquid membrane. **Chemical Engineering Research and Design** 109: 116-126.
- Pereira, C. S. M. (2009). **Process Intensification for the Green Solvent Ethyl Lactate Production based on Simulated Moving Bed and Pervaporation Membrane Reactors**. Doctor of Philosophy, Department of Chemical and Biological Engineering, University of Porto, Porto, Portugal.
- Pérez-González, A., Ibáñez, R., Gómez, P., Urriaga, A. M., Ortiz, I., & Irabien, J. A. (2015). Nanofiltration separation of polyvalent and monovalent anions in desalination brines. **Journal of Membrane Science** 473: 16-27.
- Pisarello, M. L., Dalla, C. B., Mendow, G., & Querini, C. A. (2010). Esterification with ethanol to produce biodiesel from high acidity raw materials: Kinetic studies and analysis of secondary reactions. **Fuel Processing Technology** 91(9): 1005-1014.
- Porter, M. C. (1990). **Handbook of industrial membrane technology**. Wesrwood, New Jersey, U.S.A.: Noyes Publications.
- Pramkaew, S. (2010). **Selection of lactic acid bacteria for D-lactic acid production from cassava starch**. Master of Science, Department of Microbiology, Suranaree University of Technology, Nakhon Ratchasima, Thailand.
- Rodrigues, A. E., & Minceva, M. (2005). Modelling and simulation in chemical engineering: Tools for process innovation. **Computers & Chemical Engineering** 29(6): 1167-1183.

- Roy, Y., Sharqawy, M. H., & Lienhard, J. H. (2015). Modeling of flat-sheet and spiral-wound nanofiltration configurations and its application in seawater nanofiltration. **Journal of Membrane Science** 493: 360-372.
- Schefflan, R. (2011). **Teach Yourself the Basics of Aspen Plus**. Hoboken, NJ: Wiley.
- Schwarzer, R. (2006). **Esterification of acetic acid with methanol: A Kinetic Study on Amberlyst 15**. Master of Science, Department of Chemical Engineering, University of Pretoria, Pretoria, South Africa.
- Spiegler, K. S., & Kedem, O. (1966). Thermodynamics of hyperfiltration (reverse osmosis): criteria for efficient membranes. **Desalination** 1(4): 311-326.
- Tsibranska, I. H., Tylkowski, B. (2013). Concentration of ethanolic extracts from *Sideritis* ssp. L. by nanofiltration: Comparison of dead-end and cross-flow modes. **Food and Bioproducts Processing** 91(2): 169-174.
- Tsuji, H. (2002). Autocatalytic hydrolysis of amorphous-made polylactides: effects of l-lactide content, tacticity, and enantiomeric polymer blending. **Polymer** 43(6): 1789-1796.
- Tsuji, H., & Fukui, I. (2003). Enhanced thermal stability of poly(lactide)s in the melt by enantiomeric polymer blending. **Polymer** 44(10): 2891-2896.
- Veen, H. M. v., Delft, Y. C. v., Engelen, C. W. R., & Pex, P. P. A. C. (2001). Dewatering of organics by pervaporation with silica membranes. **Separation and Purification Technology** 22-23: 361-366.
- Vela, M. C. V., Bergantiños-Rodríguez, E., Blanco, S. Á., & García, J. L. (2008). Influence of feed concentration on the accuracy of permeate flux decline prediction in ultrafiltration. **Desalination** 221(1): 383-389.

- Vijayakumar, J., Aravindan, R., & Viruthagiri, T. (2008). Recent Trends in the Production, Purification and Application of Lactic Acid. **Chemical and Biochemical Engineering Quarterly** 22(2): 245-264.
- Vu, D. T., Kolah, A. K., Asthana, N. S., Peereboom, L., Lira, C. T., & Miller, D. J. (2005). Oligomer distribution in concentrated lactic acid solutions. **Fluid Phase Equilibria** 236(1-2): 125-135.
- Wang, L., Zhao, B., Liu, B., Yang, C., Yu, B., Li, Q., Ma, C., Xu, P., & Ma, Y. (2010). Efficient production of L-lactic acid from cassava powder by *Lactobacillus rhamnosus*. **Bioresource Technology** 101(20): 7895-7901.
- Wang, X., Wang, G., Yu, X., Chen, H., Sun, Y., & Chen, G. (2017). Pretreatment of corn stover by solid acid for D-lactic acid fermentation. **Bioresource Technology** 239: 490-495.
- Wasewar, K., Patidar, S., & Agarwal, V. K. (2009). Esterification of lactic acid with ethanol in a pervaporation reactor: modeling and performance study. **Desalination** 243(1-3), 305-313.
- Wee, Y. J., Kim, J. N., & Ryu, H. W. (2006). Biotechnological Production of Lactic Acid and Its Recent Applications. **Food Technol. Biotechnol.** 44: 163-172.
- Wu, C., Liu, S., Wang, Z., Zhang, J., Wang, X., Lu, X., Jia, Y., Hung, W.-S., & Lee, K.-R. (2016). Nanofiltration membranes with dually charged composite layer exhibiting super-high multivalent-salt rejection. **Journal of Membrane Science** 517: 64-72.
- Xu, H., Teng, C., & Yu, M. (2006). Improvements of thermal property and crystallization behavior of PLLA based multiblock copolymer by forming stereocomplex with PDLA oligomer. **Polymer** 47(11): 3922-3928.

- Xuehui, L., & Lefu, W. (2001). Kinetic model for an esterification process coupled by pervaporation. **Journal of Membrane Science** 186(1): 19-24.
- Yamane, H., & Sasai, K. (2003). Effect of the addition of poly(D-lactic acid) on the thermal property of poly(L-lactic acid). **Polymer** 44(8): 2569-2575.
- Zhang, W., Na, S., Li, W., & Xing, W. (2015). Kinetic Modeling of Pervaporation Aided Esterification of Propionic Acid and Ethanol Using T-Type Zeolite Membrane. **Industrial & Engineering Chemistry Research** 54(18): 4940-4946.
- Zhang, Y. (2015). **Optically pure D-lactic acid biosynthesis from diverse renewable biomass: Microbial strain development and bioprocess analysis**. Doctor of philosophy, Department of Grain Science and Industry, Kansas State University, Manhattan, Kansas.
- Zou, Y., Tong, Z., Liu, K., & Feng, X. (2010). Modeling of Esterification in a Batch Reactor Coupled with Pervaporation for Production of n-Butyl Acetate. **Chinese Journal of Catalysis** 31(8): 999-1005.



APPENDICES

APPENDIX A

THERMODYNAMIC PROPERTIES

A.1 Available literature data

Table A.1 Basic properties of lactic acid, ethanol, ethyl lactate and water.

Properties	Lactic acid	Ethanol	Ethyl lactate	Water
Molecular weight – M (g.mol ⁻¹)	90.079	46.069	118.133	18.015
Density – ρ (g.cm ⁻³)	1.209	0.789	1.031	1.027
Melting temperature – T _f (K)	289.95 – 291.15	159.15	248.25	273.15
Boiling point – T _b (K)	395.15	351.45	426.15 – 427.15	373.15
Critical temperature – T _c (K)	616.00	516.25	588.00	647.13
Critical pressure – P _c (bar)	59.65	63.84	38.60	221.20
Critical volume – V _c (cm ³ .mol ⁻¹)	216.9	166.9	354.0	57.1

The data presented in this section are from Yaws (Pereira, 2009). In Table A.1, some physical and thermodynamic properties of lactic acid, ethanol, ethyl lactate and water are presented.

A.2 Density

The modified form of the Rackett equation was selected for correlation of saturated liquid density as a function of temperature.

$$\rho_L = AB^{-\left(1-\frac{T}{T_c}\right)^n} \quad (\text{A.1})$$

with ρ_L (g.cm^{-3}) and T (K).

Table A.2 Constants used for density calculation.

Constants	Lactic acid	Ethanol	Water	Ethyl lactate
A	0.39816	0.26570	0.34710	0.33372
B	0.26350	0.26395	0.27400	0.21190
n	0.28570	0.23670	0.28571	0.45530
T_{\min} (K)	291.15	159.05	273.16	247.15
T_{\max} (K)	T_c	T_c	T_c	T_c

A.3 Viscosity

The correlation for liquid viscosity as a function of temperature is given by Eq A.3.

$$\log_{10} \eta = A + \frac{B}{T} + CT + DT^2 \quad (\text{A.3})$$

with η_L (cP) and T (K)

Table A.3 Constants used for viscosity calculation.

Constants	Ethanol	Water	Ethyl lactate
A	-6.4406	-10.2158	-20.0105
B	1.1176×10^3	1.7925×10^3	3.2123×10^3
C	1.3721×10^{-2}	1.7730×10^{-2}	4.1891×10^{-2}
D	-1.5465×10^{-5}	-1.2631×10^{-5}	-3.2733×10^{-5}
T_{\min} (K)	240	273	247
T_{\max} (K)	T_c	643	T_c

APPENDIX B

**BINARY PARAMETERS OF THE RELATED
COMPONENTS FOR ACTIVITY COEFFICIENT
CALCULATION USING NRTL MODEL**

**B.1 Binary parameter of lactic acid, ethyl lactate, ethanol and water
for NRTL model**

The binary parameters of the related components for NRTL model that determined by using regression in Aspen Plus and prediction in Dortmund databank, were showed in the following table:

Table B2 The binary parameters of the related components for NRTL model.

i	j	a_{ij}	a_{ji}	b_{ij}	b_{ji}	α_{ij}
Water	ETOH	3.622	-0.922	-636.726	284.286	0.3
Water	LA	-0.177	0.933	-453.881	-359.426	0.3
Water	ELA	20.388	0.088	1119.54	-69.983	0.3
LA	ELA	0	0	286.729	-69.681	0.3
ETOH	LA	0	0	206.595	-96.724	0.3
ETOH	ELA	1.267	-2.729	-70.6461	722.939	0.3

B.2 Activity coefficient calculation

Applying the binary parameters for NRTL model from Appendix B1 to calculate The NRTL activity coefficient (γ) expression for a binary system is shown in Eq 2.10

$$a_{\text{NRTL}} := \begin{pmatrix} 0 & 0 & 0 & 0.933465 \\ 0 & 0 & 1.26706 & -0.9223 \\ 0 & -2.72893 & 0 & 0.0877516 \\ -0.177177 & 3.622 & 20.3877 & 0 \end{pmatrix}$$

$$b_{\text{NRTL}} := \begin{pmatrix} 0 & -96.724 & 286.729 & -359.426 \\ 206.595 & 0 & -70.6461 & 284.286 \\ -69.6814 & 722.939 & 0 & -69.9831 \\ -453.881 & -636.726 & 1119.54 & 0 \end{pmatrix} K \quad \alpha := \begin{pmatrix} 0 & 0.3 & 0.3 & 0.3 \\ 0.3 & 0 & 0.3 & 0.3 \\ 0.3 & 0.3 & 0 & 0.3 \\ 0.3 & 0.3 & 0.3 & 0 \end{pmatrix}$$

Calculating coefficient activity was shown as equations in Mathcad as follow:

$$\tau(T, i, j) := a_{\text{NRTL}_{i,j}} + \frac{b_{\text{NRTL}_{i,j}}}{T}$$

$$G(T, i, j) := e^{(-\alpha_{i,j} \cdot \tau(T, i, j))}$$

$$\gamma(T, x) := \text{for } i \in 1..n_{\text{comp}} \left[\begin{array}{l} \gamma_i \leftarrow \exp \left[\frac{\sum_{j=1}^{n_{\text{comp}}} (\tau(T, j, i) \cdot G(T, j, i) \cdot x_j)}{\sum_{k=1}^{n_{\text{comp}}} (G(T, k, i) \cdot x_k)} \right] \dots \\ + \sum_{j=1}^{n_{\text{comp}}} \left[\frac{x_j \cdot G(T, i, j)}{\sum_{k=1}^{n_{\text{comp}}} (G(T, k, j) \cdot x_k)} \cdot \left[\tau(T, i, j) \dots \right. \right. \\ \left. \left. + \frac{\sum_{m=1}^{n_{\text{comp}}} x_m \cdot \tau(T, m, j) \cdot G(T, m, j)}{\sum_{k=1}^{n_{\text{comp}}} (G(T, k, j) \cdot x_k)} \right] \right] \end{array} \right]$$

APPENDIX C

LACTATE PERFORMANCE IN NANOFILTRATION BY SPIELER AND KEDEM MODEL

The procedure for an integrated modeling approach based mainly upon the SK model and the CFSD model is illustrated in a flow diagram format as follow:

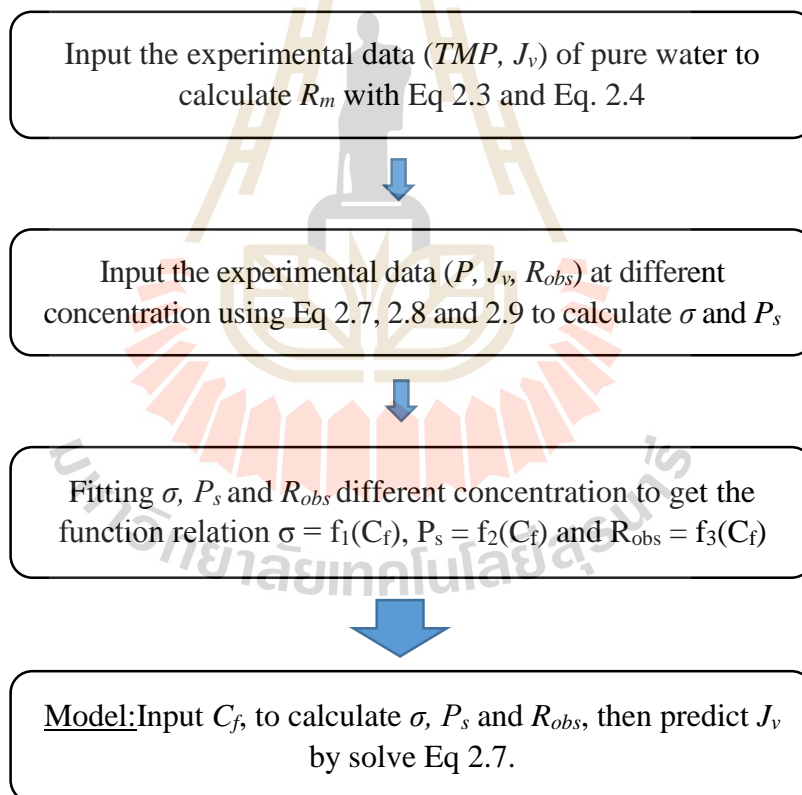


Figure C.1 Flow diagram of the integrated modeling approach proposed in this study.

APPENDIX D

KINETIC OF ESTERIFICATION AND

PERVAPORATION-ASSISTED ESTERIFICATION BY

NRTL MODEL IN MATHCAD

D.1 Kinetic of batch esterification

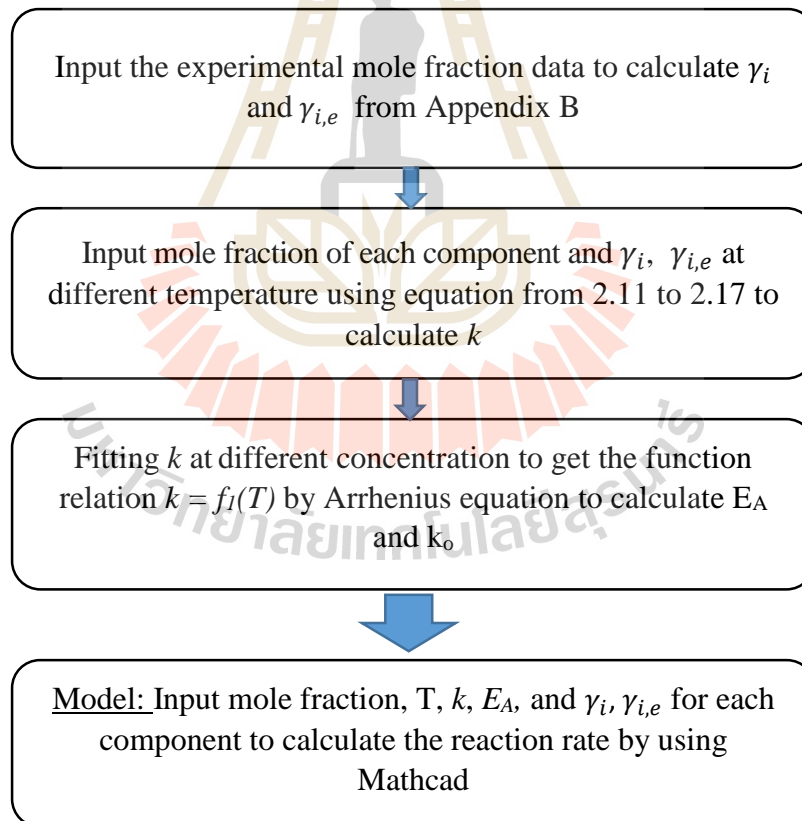


Figure D.1 Flow diagram of the batch esterification modeling approach proposed.

D.2 Saturation vapor pressure

The Antoine-type equation with extended term was selected for correlation of vapor pressure as a function of temperature:

$$\log_{10} P_{vp} = A + \frac{B}{T} + C \log_{10} T + DT + ET^2$$

with P_{vp} (mmHg) and T (K).

Table D.4 Constants used for vapor pressure calculation.

Constants	Lactic acid	Ethanol	Water	Ethyl lactate
A	-27.0836	23.8442	29.8605	32.0863
B	-3.9661×10^3	-2.8642×10^3	-3.1522×10^3	-2.9164×10^3
C	2.0233×10^1	-5.0474	-7.3037	-9.5666
D	-4.2176×10^{-2}	3.7448×10^{-11}	2.4247×10^{-9}	6.5114×10^{-3}
E	2.0310×10^{-5}	2.7361×10^{-7}	1.8090×10^{-6}	4.5645×10^{-13}
T _{min} (K)	291.15	159.05	273.16	247.15
T _{max} (K)	T _c	T _c	T _c	T _c

D.3 Kinetic of pervaporation-assisted esterification

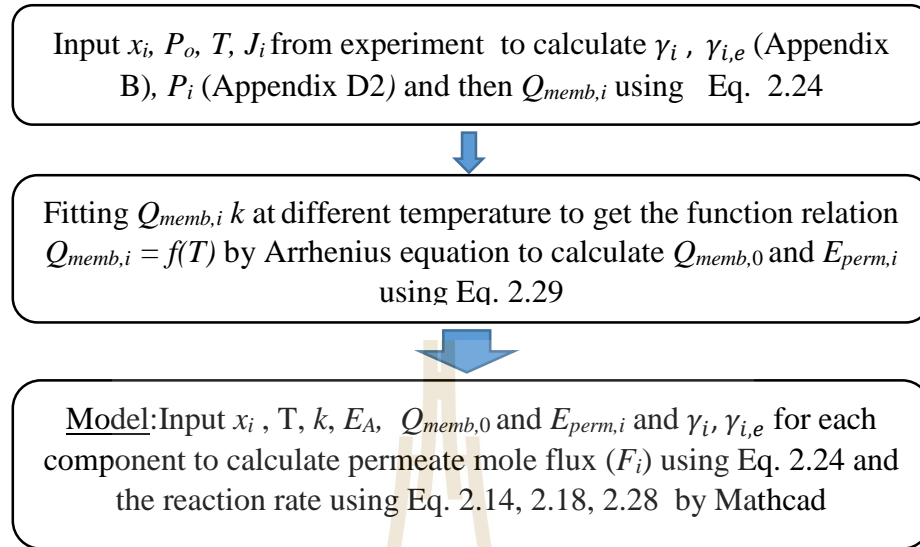


Figure D.2 Flow diagram of the pervaporation-assisted esterification modeling.

D.4 Mathcad formular for calculating the reaction rate of esterification and pevaporation-assisted membrane

$$r(T, x) := \begin{cases} \gamma_1 \leftarrow \gamma(T, x) \\ \text{for } i \in 1..n_{\text{comp}} \\ a_i \leftarrow x_i \cdot \gamma_{1,i} \\ k_{01} \cdot \exp\left(\frac{-E_{a1}}{R_{\text{gas}} \cdot T_1}\right) \cdot \left(\frac{a_{\text{LA}} \cdot a_{\text{EtOH}}}{K_{\text{eq1}}} \cdot \frac{a_{\text{EtLA}} \cdot a_{\text{W}}}{K_{\text{eq1}}} \right) \end{cases}$$

The reaction of batch esterification:

$$r_{\text{vec}}(t, x) := \begin{pmatrix} -r(T, x) \\ -r(T, x) \\ r(T, x) \\ r(T, x) \end{pmatrix} \cdot 1$$

The reaction of pervaporation-assisted esterification:

$${}^{\text{vec}} r_{\text{vec}2}(t, x) := \begin{pmatrix} -r(T, x) \\ -r(T, x) - F_{\text{EtOHcal}} \\ r(T, x) \\ r(T, x) - \text{cal } W_{2\text{cal}} \end{pmatrix} \cdot 1$$

BIOGRAPHY

Miss Trang Khanh Mai was born on November 27, 1990 in Thua Thien Hue, Vietnam. She earned her Bachelor's Degree in Food Science and Technology from College of Agriculture and Forestry in Hue University in 2013. After graduation, she has been employed under the position of laboratory technician by Hue Textile Garment Joint Stock company, Vietnam. In 2015, she continued her Master's degree in Biotechnology at School of Biotechnology, Institute of Agriculture Technology at Suranaree University of Technology (SUT), Nakhon Ratchasima, Thailand. During her study, she received financial support from Suranaree University of Technology. Her expertise includes the field of the downstream fermentation process and modeling process. Her research topic was the membrane-assisted purification of optically pure D-(-)-lactic acid from fermentation broth. During that time, she got the scholarship to study "Chemical process development" course at Technische Chemie, Carl von Ossietzky Universität Oldenburg, Germany.